A MULTIELECTRODE MICROCOMPARTMENT PLATFORM FOR SIGNAL TRANSDUCTION IN THE NERVOUS SYSTEM

A Dissertation
Presented to
The Academic Faculty

By

Venkata Surendra Kumar Ravula

In Partial Fulfillment
of the Requirements for the Degree
Doctor of Philosophy in the
School of Electrical and Computer Engineering

Georgia Institute of Technology
August 2006

A MULTIELECTRODE MICROCOMPARTMENT PLATFORM FOR SIGNAL TRANSDUCTION IN THE NERVOUS SYSTEM

Approved by:

Dr. A. Bruno Frazier, Advisor
School of Electrical and Computer Engineering
Georgia Institute of Technology

Dr. Mark Allen
School of Electrical and Computer Engineering
Georgia Institute of Technology

Dr. Robert Butera
School of Electrical and Computer Engineering
Georgia Institute of Technology

Dr. Jonathan D. Glass
Department of Neurology
Emory University

Dr. Paul Hasler
School of Electrical and Computer Engineering
Georgia Institute of Technology

Date Approved: June 20, 2006

To Mom and Dad

ACKNOWLEDGEMENTS

In simple words, I would like to thank my advisor, A. Bruno Frazier, who probably has wanted to (and maybe even has had reason to) take me less than seriously. He put up with me, and now look, six years later, I get a PhD out of the whole thing.

Half way into grad school, I met up with Jonathan Glass and he let me use his neurons and learn all about cell culture and neuropathology. Minsheng Wang and Seneshaw Asress in his lab helped me with the molecular biology of the nervous system.

Also, my fellow graduate students in the MIRL lab should tip their hats and take a bow for being laid-back and smart, at the same time. And of course everyone else at Georgia Tech and Emory who I bugged and tortured until I understood what they were talking about deserve my thanks.

TABLE OF CONTENTS

LIST OF TABLES AND GRAPHS

LIST OF FIGURES

SUMMARY

This dissertation presents the development of a multielectrode microcompartment platform for understanding signal transduction in the nervous system. The design and fabrication of the system and the characterization of the system for pharmacological and electrophysiological measurements of cultured neurons is presented in this work. The electrophysiological activity of cultured dorsal root ganglion (DRG) neurons and cortical neurons is shown on the MEA substrate. These recordings were measured and tied to the toxicological effects of the chemotherapeutic drug vincristine on DRGs.

Conventional electrophysiological recordings (via a patch micropipette) are made routinely to record action potentials and ion channel activity in neurons. Moreover, Campenot chambers (traditional compartmented culture systems) have been used for the last thirty years to study the selective application of drugs to neurons. Both of these techniques are useful and well established; however they have their limitations. For instance, Campenot chambers cannot be used very well for small processs-producing neurons, since the barriers are difficult to tranverse. Moreover, conventional patch recordings are labor-intensive, especially when more than one microelectrode needs to be positioned.

The developed system is composed of a two compartment divider, each compartment capable of housing axons or cell bodies. Underneath the divider, the substrate has 60 electrodes, arranged in several lines to accommodate several different neurite “tracks”. Neurons can be stimulated and their activity can be recorded in both of the compartments. The neurotoxin and chemotherapeutic drug vincristine was tested in the system on the DRGs. The drug caused length-dependent axonal degeneration in the

DRGs when applied locally. Moreover, electrophysiological activity in both compartments showed that only the activity in the axonal compartment was affected, leading us to believe that the mechanism behind the degeneration is localized to the distal axon.

CHAPTER 1

INTRODUCTION

1.1 Thesis Objectives and Motivation

The objective of this work is to design, fabricate, and test an integrated compartmented neuronal culture system that takes advantage of microsystems technology to create features that are several hundred microns or less in dimension. The two improvements to traditional compartmented cultures made through this work lie in the integration of electrodes into these systems and in the reduction of the size of intercompartmental barriers. Also, we will use the system to test a hypothesis on the effects of the neurotoxin vincristine. The following chapters give the motivation for and detailed methodology of how the work was undertaken.

More specifically, the aims of this work are as follows:

Aim 1. Design and microfabrication of the Campenot chamber system

Subaim 1.1. Design and fabrication of the chemical patterning mold.

Subaim 1.2. Design and fabrication of the compartment divider.

Subaim 1.3. Design and fabrication of the MEA substrate.

Aim 2. Characterization of the microfabricated Campenot chamber system

Subaim 2.1. Characterization of leakage in system

Subaim 2.2. Characterization of neurite patterning

Subaim 2.2. Characterization of the MEA substrate

Aim 3. Integration of microelectrode studies into the microfabricated Campenot chamber system.

Subaim 3.1. Examination of vincristine neurotoxicity

Subaim 3.2. Examination of electrophysiology with vincristine

1.2 Introduction to Micromachining Technology

Microelectronics technology has created a vast new playground in the world of objects that are on the order of 1μm [1-50]. The application of conventional microelectronics technology and associated emerging technologies to fields as disparate as physics and biology has produced devices that have integrated functionality and are collectively known as microelectromechanical systems (MEMS). MEMS technology has allowed researchers to manipulate biological particles, sense the environment, and actuate other parts.

The novelty of MEMS comes from the fact that it allows researchers to build things that have been impossible or very expensive with other techniques. MEMS brings much of its technology from the integrated circuit industry. The most important aspect of MEMS technology lies in its ability to miniaturize objects. By using the techniques of the semiconductor revolution, engineers can produce systems that are orders of magnitude smaller than the devices that exist in our everyday lives. Moreover, the use of photolithographic techniques makes producing thousands of copies of a single device easy. Finally, the ability to integrate multiple levels of functionality makes MEMS devices more functional than simple microelectronics [7].

Traditionally, MEMS have been fabricated with silicon since the majority of ICs made today use silicon technology. There are two main MEMS fabrication techniques that are based on silicon: bulk silicon micromachining and polysilicon surface micromachining. Bulk silicon micromachining is a type of micromachining that uses a

silicon wafer as the building material for the device. Silicon wafers made for the IC industry are single crystals of silicon cut on specific crystal planes. Certain chemicals etch different silicon crystal planes at different rates. This characteristic of silicon is used to etch holes into the substrate that follow specific crystal planes. This technique, known as anisotropic wet etching, can be used to make many features important to the bulk micromachining industry. Surface micromachining is a technique that resembles those used for the IC industry much more than bulk micromachining techniques. In polysilicon surface micromachining, many layers of polysilicon and silicon dioxide are deposited by chemical vapor deposition. Each layer is photolithographically patterned and plasma etched before the next layer is deposited. When the resulting stack of films is dipped in hydrofluoric acid, the silicon dioxide is chemically etched away, and this process leaves behind multi-layered structures of polysilicon [7].

An offshoot of MEMS fabrication strategies is soft lithography, in which a single silicon micromachined master, potentially fabricated by one of the two techniques discussed above, is used to micromold a liquid prepolymer (e.g., PDMS, PMMA) into useful structures. This technique is particularly relevant to the work in this project. Soft lithography is particularly attractive because one master can produce thousands and even millions of molds. With this technique, the prepolymer of the elastomer is poured over the master, cured, and peeled off. It has become popular for many reasons, including the ease with which these devices can be manufactured and the biocompatibility of the materials involved [51-65].

1.3 BioMEMS

Biological MEMS (or BioMEMS) has become the term of choice for applications of MEMs devices to problems in biology and medicine. BioMEMS is an area as varied as any in the engineering sciences. The key to the advantages associated with many of these devices lies in the leveraging of features that are unique to MEMS (such as the small features or the integration of microelectronics), and any of the techniques mentioned in the previous section as well as a host of others that are not mentioned can be used to fabricate devices that are grouped into this section [6, 66].

One useful designation is the differentiation of BioMEMS devices that are for in vitro applications and those that are for in vivo applications. A variety of implantable electronic devices are based upon or use MEMS technology, including sensors, immunoisolation capsules, and drug delivery microchips. Biosensors have been created to monitor pH, analytes, and pressure in the blood, tissue, and body fluids, but stable sensors for long-term implantation are difficult to find. Even those materials generally considered to be biocompatible produce some sort of toxic response. So, finding more biocompatible materials is one problem in moving this technology forward [6, 67-75]. Also, immunoisolation capsules are used for implantation of cells that perform some function in vivo [76-79]. For instance, microfabricated silicon capsules offer the advantages of reproducible small features and greater mechanical strength compared to the traditionally used polymer-based capsules. Finally, microfabricated drug delivery systems are useful for a number of applications involving the precise delivery of a drug in vivo. For instance, silicon microparticles are small silicon reservoirs that can be filled with a drug to be delivered in vivo [80, 81]. These devices would have a dissolvable cap

that would allow controlled release of the drug when delivered intravenously. Also, arrays of these reservoirs could be fabricated so that different drug doses can be incorporated into each reservoir and sealed with an electrochemically dissolvable gold membrane [82-84].

Some of the in vivo applications of BioMEMS that involve neurons include in vivo neural probes and retinal prostheses. There have been several versions of the in vivo neural probe that has been fabricated. The most work in this area has been done at the University of Mighican [85-101]. The "Michigan Probes" consists of a 1024-site 128-channel neuroelectronic interface that has integrated circuitry for processing recorded data. In addition to the probe shanks and the electronics, the Michigan probes also incorporate sensors for microfluidics and channels for drug delivery. The basic process for fabricating the Michigan probes is a silicon MEMS process that involves the deposition of several layers of conductors and dielectrics and a final etch step that releases the probes. An alternative to the Michigan probes is the Utah electrode array, which is a batch fabricated two dimensional depth array formed using silicon posts created by sawing and etch-back [102-110]. The individual posts are insulated with parylene and tipped with iridium. Each post is isolated from neighboring electrodes using a mote of glass surrounding the electrode at its base. Also, Jack Judy at UCLA has used similar features to fabricate a silicon multielectrode probe for deep brain stimulation [111, 112]. It is targeted for use in stimulating the deep portions of the brain like the thalamus, which is located more than 2cm below the cortex in rodents. The motivation for microfabricating such a structure is to provide a probe narrow enough to cause the least amount of damage. Meanwhile, the MEMS-based retinal implant is a very

ambitious project that involves the creation of a chip that would be able to restore vision to patients with macular degeneration and retinitis pigmentosa. The entire system consists of the MEMS implant and electronics for telemetry. Several approaches have been developed; most notably, the approach adopted by Sandia National Labs is one in which the electrodes are mounted on flexible springs so that they can be used to stimulate appropriate areas of the retinal surface [113-124].

Some of the in vitro applications include multielectrode arrays (MEAs), patch clamp devices, and other lab-on-a-chip applications. Multielectrode arrays (MEAs) have become popular over the last decade as a means of studying the electrophysiology of networks of neurons cultured in vitro. MEAs are used to culture a wide variety of neurons of the central and peripheral nervous systems. Researchers use them to culture neuronal cells to form a long-term, two way interface between the cultured networks and a computer. They are also used to study distributed network dynamics and neural plasticity using both recording and stimulation. Others have cultured individual DRG neurons and attempted at optimizing the neuron-electrode interface [125-141]. Others such as Lee have used micromachining technology to be able to perform sophisticated biological techniques on a chip. His lateral patch clamp, for instance, allows for high throughput, parallel analysis of ion currents in an excitable cell [142].

1.4 Campenot chambers

Our model system is the compartmented culture invented by Robert Campenot in 1976 [143-172]. The compartmented culture system provides all the basic requirements for complicated studies on neurons that combine electrical stimulation with biochemical

exposure. The compartmented culture was initially designed as a system to study the formation and maintenance of neuronal projections. Axons originating from neurons plated in a proximal compartment grow across a silicone grease barrier and enter into a separate fluid environment within a distal compartment (see Figure 1). The key to the construction of compartmented cultures is the application of silicone grease to a Teflon divider and then seating the divider into a culture dish with a collagen-coated substratum. With the conventional system, the grease barriers that neurons must traverse are large (~500μm) and, therefore, difficult to penetrate, especially for the small process-producing neurons of the central nervous system. To reduce these barriers, Ivins et al formed a thin barrier (150μm) with a glass coverslip seated with silicone grease [173]. However, these devices were time consuming to build and culture viability was low. Recently, microfabrication techniques have been used to build a novel Campenot chamber device. However, this device does not provide the full functionality of the traditional system. This system uses a hydrostatic pressure differential to allow the fluid in one compartment to "leak" into an adjacent compartment. The intention was to apply biochemicals to the "non-leaky" compartment, thereby allowing fluidic compartmentalization of one side of the cultured neurons. This design does not allow for tests in which the neurons in both compartments (both the extensions and the somas) could be isolated with a drug environment [174].

As part of this work, we build devices that would take advantage of the ability of MST to pattern small features that could guide neurons, provide fluidic isolation, and pattern electrodes [175-181]. Our compartmented culture systems will allow for complicated studies in which different parts of a neuronal culture could be biochemically

activated in coordination with the activation of arrays of lithographically defined microelectrodes. In addition, these systems will possess the traditional benefits of

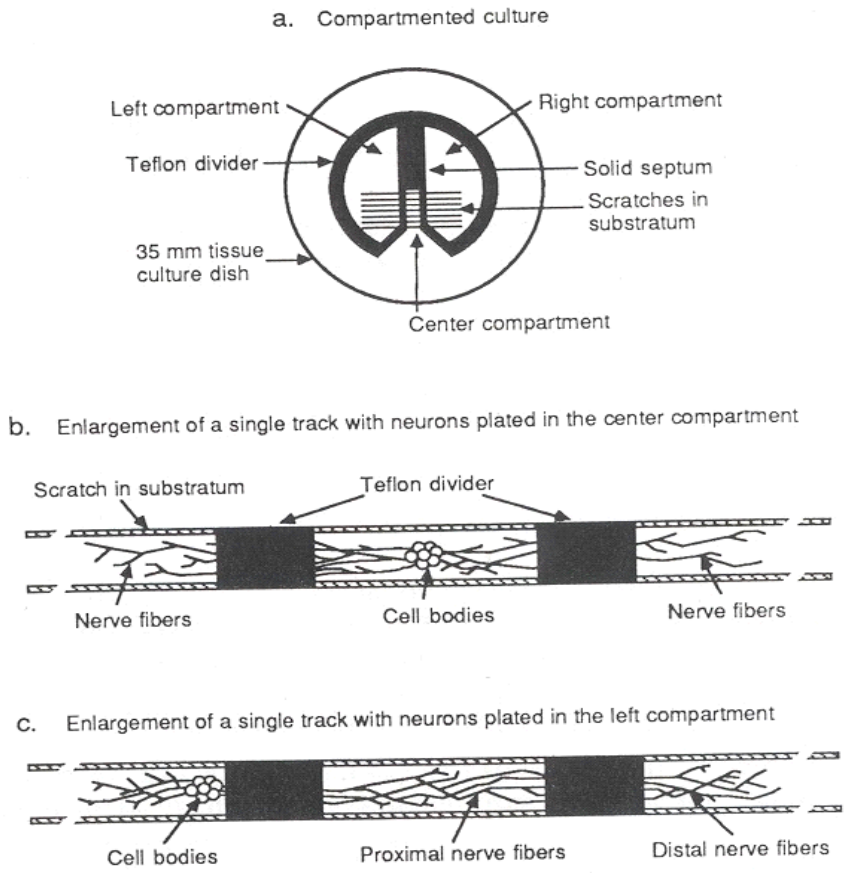

Figure 1.1. Traditional compartmented culture system (from [145]).

miniaturization: less reagent use and batch processing capability.

Campenot chambers are currently used for many applications, all of which center around the effects of compartmentalizing biochemicals on cultured neurons [144, 182-186]. However, to our knowledge, B. Campenot and P. Nelson's groups are the only ones to have used compartmented cultures with electrical stimulation and recording as part of their experiments [185, 187]. A problem for making electrophysiological measurements in traditional chambers is the difficulty of positioning conventional

microelectrode pipettes at desired locations within the chamber. We hope to remove this burden with a pre-patterned substrate that will create a structured arrangement of neurons interfacing with many electrodes. Moreover, we believe that the ability to stimulate and record from neuronal cultures as they are being exposed to drugs in real-time offers a novel and useful technique to understand the spatiotemporal consequences of the pharmacological agents on the culture.

1.5 Introduction to Neurons

Neurons are unique among cells in that they have such asymmetrical morphology. During development, neurons become assembled into functional networks by growing out axons and dendrites which connect to other neurons through synapses. The outgrowth of neurons moves forward by the action of growth cones --specialized structures at the tip of growing neurites. The cell body, or soma, is a 15-25μm diameter area of the cell that houses the nucleus. Neurons also have neurites, which are extensions that emerge from the cell bodies during the growth process. Neurites can grow to several millimeters in length and develop into two functionally different species: axons which function in sending signals to other cells and dendrites which function in receiving signals from other cells.

Neurons can also be characterized by the number and types of processes that they possess. Bipolar neurons like retinal cells and olfactory epithelium cells have two processes extending from the cell body. Pseudounipolar cells like dorsal root ganglion (DRGs) cells have two axons. Here, one axon extends centrally toward the spinal cord and the other axon extends towards the skin or muscle. Finally, multipolar neurons (see

Figure 1.2) like motor neurons, pyramidal neurons, and Purkinje cells have many processes extending from the cell body, but only one of these is the axon [188].

These structural differences result in functional differences between different parts of a neuron. Little is understood about the spatiotemporal distribution of various neuronal components, including organelles, ion channels, and ions. The introduction of chemical species into a system that allows the investigation of these components would prove useful for understanding basic cellular physiology and in answering questions that can be posed from the applied sciences in medicine in biology.

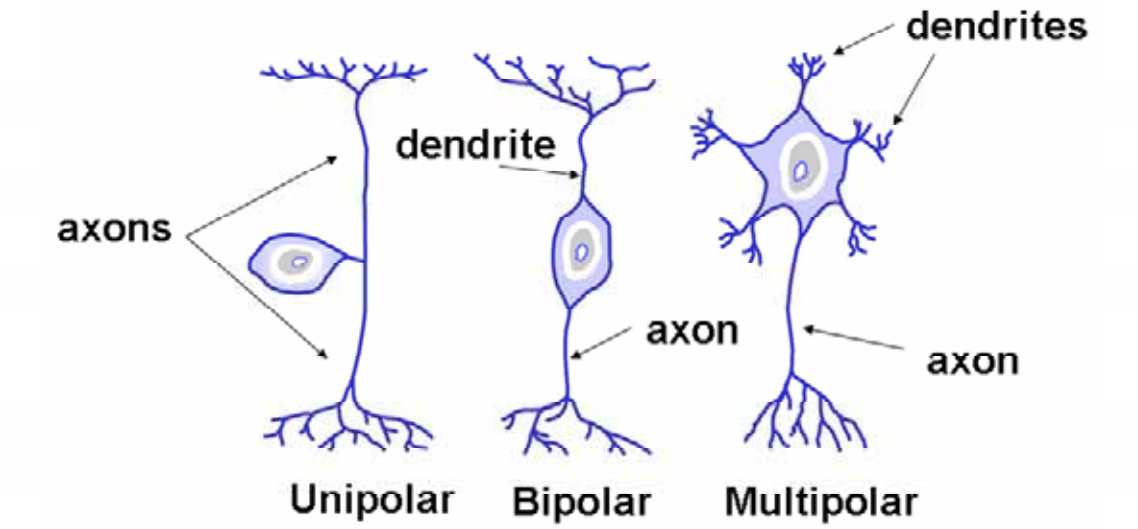

Figure 1.2. Different types of neuron morphologies.

The primary function of neurons is to provide electrical signaling between different regions of an organism. Action potentials are generated by ion channels, which consist of protein complexes that allow a chemical gradient to be established between the extracellular and intracellular environments. The primary ion channels involved in spikes are voltage-gated in that they are opened/closed by a change in the voltage potential across the membrane. There are also ligand-gated channels which are controlled by the binding of special chemicals (neurotransmitters) released from one cell and captured by another [189].

Action potentials, the electrical signals in neurons, are usually initiated at axon hillocks, points that have a low threshold for firing. Once initiated, the action potential moves along the cell membrane down the axon to the next cells. This backflow of information has a role in the strengthening and weakening of the synaptic connections between neurons and thus may play a role in learning, memory, and computation [190].

Dorsal root ganglia (DRG) neurons were chosen as the biological test vehicle for this compartmented culture system. This was done for several reasons. DRGs are neurons of the peripheral nervous system and grow extensions that are several millimeters in length. They are bipolar neurons that have two axons, one that connects to the central nervous system and the other that connects to receptors in areas like skin and muscle. Since they grow such long extensions in a relatively short period of time, we thought that they would allow us to move forward with culture experiments quickly. Moreover, they have relatively large cell bodies and we imagined that this would aid us in making optical measurements. Moreover, we chose DRGs because they have been characterized in compartmented cultures thoroughly. In addition to studies involving

drugs applied selectively to neurons, their electrophysiological activity has been studied in Campenot chambers by R.D. Fields and P. Nelson's group at the NIH. Moreover, DRGs form synapses with receptors in muscle tissue and with spinal cord neurons, making them a good model to study how activity changes as they pass electrophysiological information to other cells.

1.5.1 Ectopic Firing in Neurons

In many dysfunctions of the nervous system, the electrophysiological health of the neuron is implicated [191-206]. For instance, in many diseases in vivo the underlying culprit for the dysfunction is loss of the ability to conduct action potentials. In epilepsy, a rapid firing pattern is initiated that precedes the abnormal loss of consciousness. In ALS, a characteristic withering away of the neuromuscular junctions results in loss of function in various muscles of the body [207]. In Guillain-Barre syndrome and multiple sclerosis, demyelination and inflammation both contribute to the neurological deficits. In both of these cases, the conduction deficits attributable to demyelination are well known. Conduction deficits attributable to demyelination are well known, but it is becoming clear that factors such as nitric oxide, endocaine, cytokines, and antiganglioside antibodies also play significant roles. Other factors impairing impulse transmission include nodal widening, glutamate toxicity, and disturbances of both the blood-brain barrier and synaptic transmission [208]. Also, peripheral neuropathy is a major late complication of diabetes mellitus. Changes in polyol pathway flux, oxidative stress, non-enzymatic protein glycation, endothelial dysfunction leading to reduced nerve blood flow, disturbed

calcium homeostasis and deficits in neurotrophic factors probably all contribute to the clinical and neurophysiological findings in the diabetic patient with neuropathy [207].

Also, ectopic hyperexcitability in physically injured PNS neurons has been implicated in the feeling of pain. In recent years, some direct evidence of PNS ectopia has been obtained by percutaneous microneurographic recording from single nerve fibers in conscious humans. For example, Nystrom and Hagbarth showed ongoing discharge in the peroneal nerve in a lower extremity amputee. The patient had ongoing phantom foot pain that was augmented by percussion of the neuroma. In a related study, dysesthesias referred to the foot were triggered by straight-leg lifting in a patient with radicular pain related to surgery for disk herniation. This activity also caused ectopic bursts in the sural nerve. Also, changes in the degree of pain were caused by the injection of test substances at the areas where the pain was being felt. For instance, in animal studies, injection of adrenaline or K^+ channel blockers into an injured PNS neuron evokes pain, while the injection of Na^+ channel blockers (e.g., lidocaine) suppresses it [209].

As suggested above, ectopic hyperexcitability in severed DRGs is reflected in abnormal sensitivity to a broad range of depolarizing stimuli. For example, depolarization with elevated concentrations of extracellular K^+ evokes accelerated discharge, as does the application of the K^+ channel blockers tetraethylammonium (TEA) and 4-aminopyridine (4-AP). Another potential source of chemical excitation at nerve injury sites is the neurotransmitter/neuromodulator contents of neighboring axons. Temperature also has an interesting effect. In myelinated PNS neurons with some injury associated with them, the rate of spontaneous discharge increases with temperature while decreasing the temperature suppresses firing. On the other hand, most unmyelinated

axons work in reverse; their firing is lowered by warming and excited by cooling. Metabolic stimuli are also efficacious in producing a change in the electrophysiology of neurons. Ischemia and hypoxia, for example, cause very high firing frequencies followed by no activity in PNS neurons [209].

In addition to physical and metabolic stimuli, many substances found in the body are known to cause ectopic discharge in neurons. Examples are the catecholamines adrenaline and noradrenaline, which both promote and inhibit ectopic activity. Ectopic firing also may be aroused by many different inflammatory mediators, including bradykinin, histamine, serotonin, and certain eicosanoids. *In vivo*, these compounds are released by mast cells, macrophages, Schwann cells, and other cells at the injury site [209].

1.5.2 Distal Axonal Degeneration

Our devices will be applied towards the study of a phenotype found in many neurodegenerative diseases called distal axonal degeneration (DAD), a gradual degenerative condition that starts in the distal axon and proceeds proximally toward the cell body. Ever since the seminal paper of John Cavanagh tried to systematically group neuropathies exhibiting DAD, researchers have posited many theories on the underlying mechanisms behind this phenotype and have sought to use toxic chemical probes to mimic in vitro the phenotype of human diseases exhibiting DAD [210-213]. Figure 1.3 summarizes the most important of these theories. Cavanaugh initially thought that the dying back of axons in toxic neuropathies resulted from the toxin impairing the anabolic machinery of the neuronal perikaryon. Because protein synthesis does not occur in the

axon, it was believed that the reduced amounts of synthesized materials exported from the diseased neuronal perikaryon would fail to meet the metabolic needs of the axon. This would cause the distal portion of the axon to receive an inadequate supply of materials and thus undergo degeneration. However, several studies have disputed this claim. For instance, the pattern of nerve fiber change observed in experimental hexacarbon neuropathy demonstrated that PNS fiber diameter can be more important than axon length in determining vulnerability. Also, in this neuropathy, giant axonal swellings develop in nerve terminals only after swellings have appeared more proximally in the supporting nerve fiber. These observations persuaded Cavanaugh to abandon his long held view that dying-back disease followed neuronal perikaryon dysfunction and prompted him to consider the idea that these toxins might be acting directly on the nerve fiber through the impairment of axonal transport. To support this idea, Mendell and collaborators, for example, demonstrated that the rate of downflow in the proximal portion of sciatic nerves is impaired progressively during the course of the disease [214]. Moreover, Griffin et al showed that similar giant axonal swellings in proximal axons following *β, β'*-iminodipropionitrile (IDPN) intoxication resulted from a selective blockade of neurofilament proteins known to move along in a slow phase of axonal transport [215]. Meanwhile, Spencer and Schaumberg took this idea one step futher and suggested that the predisposing event causing degeneration was toxin-induced blockage of pathways synthesizing chemical energy within the fiber and the resulting reduction in the amount of energy available to drive energy-requiring functions. The phenotype occurs first in the distal axon because the intraaxonal enzymes responsible for energy synthesis are supplied by axonal transport from the distant neuronal perikaryon [213].

More recently, Glass has shown that when applying the neurotoxin vincristine to DRG neurons in compartmented cultures, only the distal axon in susceptible to the drug in causing DAD, and neither the cell bodies or the axons in the adjacent compartments are affected [216-218].

By spatially dividing the neuron in our system into two different drug compartments and monitoring the electrophysiological health of the neuron in both, we hope to understand how the entire cell responds and resolve a basic physiological question that results from our work with vincristine in compartmented cultures. Is the observed morphology telling us the entire story of vincristine-induced DAD, leading us to believe that the distal axon dies on its own due to physiological mechanisms that are locally initiated, or is its death preordained by subtle physiological signals from the soma

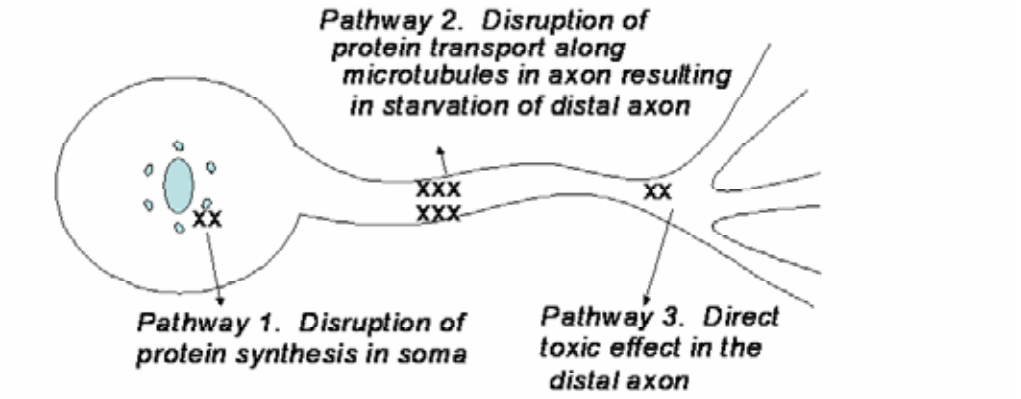

Figure 1.3. Potential metabolic pathways of neurotoxicant-induced distal axonal degeneration.

as observed by changes in its normal spike activity which later cause the observed phenotype? More specifically, if the soma changes its electrophysiological activity before any morphological change observed at the distal axon, one could argue that this change initiates the timing and progression of DAD and would support the involvement of an underlying metabolic pathway that involves the soma. Alternately, if the electrophysiological response deficit and eventual disappearance is confined to only the axonal compartment, one could argue that a metabolic pathway localized to the distal axon is the pathological substrate. By understanding the answers to these questions through the electrophysiological experiments possible with our system, we will be better able to target pharmacological interventions on the neuron for treating disorders exhibiting this phenotype.

1.6. References

[1] A. A. Berlin and K. J. Gabriel, "Distributed MEMs: new challenges for computation," *IEEE Computational Science and Engineering*, vol. 4, pp. 12-16, 1997.

[2] S. Chowdhury, M. Ahmadi, and W. C. Miller, "Microelectromechanical systems and system-on-chip connectivity," *IEEE Circuits and Systems Magazine*, vol. 2, pp. 4-28, 2002.

[3] S. Chowdhury, M. Ahmadi, and W. C. Miller, "Design of a MEMs acoustical beamforming sensor microarray," *IEEE Sensors Journal*, vol. 2, pp. 617-27, 2002.

[4] P. B. Chu, S.-S. Lee, and S. Park, "MEMs: the path to large optical crossconnects," *IEEE Communications Magazine*, vol. 40, pp. 80-87, 2002.

[5] P. D. Dobbelaere, K. Falta, S. Gloeckner, and S. Patra, "Digital MEMs for optical switching," *IEEE Communications Magazine*, vol. 40, pp. 88-95, 2002.

[6] A. C. R. Grayson, R. S. Shawgo, A. M. Johnson, N. T. Flynn, L. Yawen, M. J. Cima, and R. Langer, "A BioMEMs review: MEMs technology for physiologically integrated devices," *Proceedings of the IEEE*, vol. 92, pp. 6-21, 2004.

[7] D. A. Koester, K. W. Markus, and M. D. Walters, "MEMs: small machines for the microelectronics age," *Computer*, vol. 29, pp. 93-94, 1996.

[8] S. Lucyszyn, "Review of radio frequency microelectromechanical systems technology," *IEE Proceedings of Science, Measurements, and Technology*, vol. 151, pp. 93-103, 2004.

[9] K. W. Markus, "Developing infrastructure to mass-produce MEMs," *IEEE Computational Science and Engineering*, vol. 4, pp. 49-54, 1997.

[10] K. W. Markus and K. J. Gabriel, "MEMs: the systems function revolution," *Computer*, vol. 32, pp. 25-31, 1999.

[11] R. Osiander, S. L. Firebaugh, J. L. Champion, D. Farrar, and M. A. G. Darrin, "Microelectromechanical devices for satellite thermal control," *IEEE Sensors Journal*, vol. 4, pp. 525-531, 2004.

[12] E. Peeters, "Challenges in commercializing MEMs," *IEEE Computational Science and Engineering*, vol. 4, pp. 44-48, 1997.

[13] G. M. Rebeiz, G. L. Tan, and J. S. Hayden, "RF MEMs phase shifters: design and applications," *IEEE Microwave Magazine*, vol. 3, pp. 72-81, 2002.

[14] K. J. Rebello, "Applications of MEMs in surgery," *Proceedings of the IEEE*, vol. 92, pp. 43-55, 2004.

[15] M. Sadiku, "MEMs," *IEEE Potentials*, vol. 21, pp. 4-5, 2002.

[16] Y. Tze-Wei, K. L. E. Law, and A. Goldenberg, "MEMs optical switches," *IEEE Communications Magazine*, vol. 39, pp. 158-63, 2001.

[17] C. Wang, G. Jia, L. H. Taherabadi, and M. J. Madou, "A novel method for the fabrication of high-aspect ratio C-MEMs structures," *Journal of Microelectromechanical Systems*, vol. 14, pp. 348-358, 2005.

[18] C. B. O'Neal, A. P. Malshe, S. B. Singh, W. D. Brown, and W. P. Eaton, "Challenges in the packaging of MEMS," presented at International Symposium on Advanced Packaging Materials: Processes, Properties, and Interfaces, 1999.

[19] R. R. Mansour, M. Bakri-Kassem, M. Daneshmand, and N. Messiha, "RF MEMS devices," presented at International Conference on MEMS, NANO, and Smart Systems, 2003.
[20] K. Persson and K. Boustedt, "Fundamental requirements on MEMS packaging and reliability," presented at International Symposium on Advanced Packaging Materials, 2002.
[21] R. L. Bratter, "Commercial success in the MEMS marketplace," presented at IEEE/LEOS International Conference on Optical MEMS, 2000.
[22] B. Wang, "Considerations for MEMS packaging," presented at Conference on High Density Microsystem Design and Packaging and Component Failure Analysis, 2004.
[23] R. J. Pryputniewicz, T. F. Marinis, J. W. Soucy, and C. Furlong, "Development of packaging for MEMS inertial sensors," presented at Position Location and Navigation Symposium, 2004.
[24] K. F. Harsh, W. Zhang, V. M. Bright, and Y. C. Lee, "Flip-chip assembly for Si-based RF MEMS," presented at IEEE International Conference on Microelectromechanical Systems, 1999.
[25] M. C. Wu, P. R. Patterson, D. Hah, M.-C. M. Lee, S. Huang, and J.-C. Tsai, "Advanced MEMS for photonics," presented at Device Research Conference, 2002.
[26] B. Schoenlinner, A. Abbaspour-Tamijani, L. C. Kempel, and G. M. Rebeiz, "Switchable low-loss RF MEMS Ka-band frequency-selective surface," *IEEE Transactions on Microwave Theory and Techniques*, vol. 52, pp. 2474-2481, 2004.
[27] S. E. Lyshevski, "Distributed control of MEMS-based smart flight surfaces," presented at American Control Conference, 2001.
[28] E. R. Brown, "RF MEMS for digitally-controlled front-end components," presented at IEEE International Conference on Innovative Systems in Silicon, 1997.
[29] G. M. Rebeiz, "Phase-noise analysis of MEMS-based circuits and phase shifters," *IEEE Transactions on Microwave Theory and Techniques*, vol. 50, pp. 1316-1323, 2002.
[30] H. Miyajima, K. Murakami, and M. Katashiro, "MEMS optical scanners for microscopes," *IEEE Journal of Selected Topics in Quantum Electronics*, vol. 10, pp. 514-527, 2004.
[31] S. D. Robinson, "MEMS technology-micromachines enabling the "all optical network"," presented at Electronic Components and Technology Conference, 2001.
[32] R. M. LaFollette, J. N. Harb, and P. Humble, "Microfabricated secondary batteries for remote, autonomous electronic devices," presented at Annual Battery Conference on Applications and Advances, 2001.
[33] T. K. Tang, "MEMS for space applications," presented at IEEE International SOI Conference, 1999.
[34] K. Varian and D. Walton, "A 2-bit RF MEMS phase shifter in a thick-film BGA ceramic package," *IEEE Microwave and Wireless Components Letters*, vol. 12, pp. 321-323, 2002.

[35] M. Daneshmand, R. R. Mansour, and N. Sarkar, "RF MEMS waveguide switch," presented at IEEE MTT-S International Microwave Symposium Digest, 2004.
[36] L. E. Felton, N. Hablutzel, W. A. Webster, and K. P. Harney, "Chip scale packaging of a MEMS accelerometer," presented at Electronic Components and Technology Conference, 2004.
[37] E. Novak, F. Pasop, and T. Browne, "Production metrology for MEMS characterization," presented at Symposium on Design, Test, Integration and Packaging of MEMS/MOEMS, 2003.
[38] F. Sarvar, D. A. Hutt, and D. C. Whalley, "Application of adhesives in MEMS and MOEMS assembly: a review," presented at IEEE International Conference on Polymers and Adhesives in Microelectronics and Photonics, 2002.
[39] G. Shen, T. H. Cheng, S. K. Bose, L. Chao, and T. Y. Chai, "Architectural design for multistage 2-D MEMS optical switches," *Journal of Lighwave Technology*, vol. 20, pp. 178-187, 2002.
[40] A. P. D. Silva and H. G. Hughes, "The package integration of RF-MEMS switch and control IC for wireless applications," *IEEE Transactions on Advanced Packaging*, vol. 26, pp. 255-260, 2003.
[41] J. Qing, Y. Shi, W. Li, Z. Lai, Z. Zhu, and P. Xin, "Ka-band distributed MEMS phase shifters on silicon using AlSi suspended membrane," *Journal of Microelectromechanical Systems*, vol. 13, pp. 542-549, 2004.
[42] K. Kawano, T. Mori, M. Kuroda, and M. M. Tentzeris, "Numerical modeling of MEMS structures involving motion effected by the coupling of Maxwell's and mechanical equations," presented at IEEE International Symposium on Antennas and Propagation, 2004.
[43] S. M. Taleie, J. Zhang, and S. Kiaei, "Nonlinearlity and power consumption analysis of a low-IF MEMS receiver architecture," presented at Symposium on Circuits and Systems, 2004.
[44] R. Tian-Ling, "Novel MEMS devices for information systems," presented at Radio Science Conference, 2004.
[45] E. Jung, M. Wiemer, E. Farber, and R. Aschenbrenner, "Novel MEMS CSP to bridge the gap between development and manufacturing," presented at Electronic Components and Technology, 2004.
[46] M. Moraja and M. Amiotti, "Getters films at wafer level for wafer to wafer bonded MEMS," presented at Design, Test, Integration, and Packaging of MEMS/MOEMS, 2003.
[47] T. G. Brown, "Harsh military environments and microelectromechanical (MEMS) devices," presented at Sensors, 2003.
[48] S. E. Lyshevski, "MEMS smart variable-geometry flexible flight control surfaces: distributed control and high-fidelity modeling," presented at IEEE Conference on Decision and Control, 2003.
[49] S. Simion, "Modeling and design aspects of the MEMS switch," presented at Semiconductor Conference, 2003.
[50] M. J. Little, "Compliant MEMS and their use in optical components," presented at Optical Fiber Communication Conference, 2002.
[51] Y. Xia and G. M. Whitesides, "Soft Lithography," *Annual Review of Materials Science*, vol. 28, pp. 153-84, 1998.

[52] J. K. S. Poon, H. Yanyi, G. T. Paloczi, and A. Yariv, "Soft lithography replica molding of critically coupled polymer microring resonators," *IEEE Photonics Technology Letters*, vol. 16, pp. 2496-2498, 2004.
[53] D. A. Chang-Yen, R. K. Eich, and B. K. Gale, "A monolithic PDMS waveguide system fabricated using soft-lithography techniques," *Journal of Lightwave Technology*, vol. 23, pp. 2088-2093, 2005.
[54] G. M. Whitesides, "Unconventional methods and unconventional materials for microfabrication," presented at Solid State Sensors and Actuators, 1997.
[55] M. Knight and J. House, "Design and fabrication of a peristaltic micropump," presented at Symposium on Design, Test, Integration and Packaging of MEMS/MOEMS, 2003.
[56] J. A. Rogers, M. Meier, and A. Dodabalapur, "Distributed feedback lasers produced using soft lithography," presented at Device Research Conference Digest, 1998.
[57] C. P. Steinert, N. Schmitt, E. Deier, M. Daub, B. deHeij, and R. Zengerle, "A novel fabrication method for hybrid, microfluidic devices," presented at IEEE International Conference on Microelectromechanical Systems, 2005.
[58] H. Shah, D. Smith, J. Ballato, S. Foulger, P. Deguzman, and G. Nordin, "Direct generation of optical diffractive elements in perfluorocyclobutane (PFCB) polymers by soft lithography," *IEEE Photonics Technology Letters*, vol. 12, pp. 1650-1652, 2000.
[59] C. M. Nelson, E. Lim, and C. S. Chen, "Two to tango: micropatterned substrates to control cell-cell interactions," presented at EMBS/BMES Conference, 2002.
[60] P. F. Xiao, N. Y. He, Q. G. He, Z. C. Liu, and Z. H. Lu, "Soft lithography for oligonucleotide arrays fabrication," presented at EMBS Conference, 2001.
[61] G. M. Whitesides, "The bio/materials interface," presented at 1st Annual International Conference on Microtechnologies in Medicine and Biology, 2000.
[62] A. Perentos, G. Kostovski, and A. Mitchell, "Polymer long-period raised rib waveguide gratings using nano-imprint lithography," *IEEE Photonics Technology Letters*, vol. PP, pp. 1-3, 2005.
[63] B. G. Lee and A. Scherer, "Diffractive lens fabrication by replica molding," presented at Lasers and Electro-Optics, 2001.
[64] M. L. Adams, S. Quake, and A. Scherer, "On-chip absorption and fluorescence spectroscopy with polydimethylsiloxane (PDMS) microfluidic flow channels," presented at IEEE-EMB Special Topic Conference on Microtechnologies in Medicine and Biology, 2002.
[65] T. Pan, E. Kai, M. Stay, V. Barocas, and B. Ziaie, "A magnetically driven PDMS peristaltic micropump," presented at EMBS Conference, 2004.
[66] D. L. Polla, "BioMEMS applications in medicine," presented at Proceedings of the 2001 International Symposium on Micromechatronics and Human Science, 2001.
[67] R. F. Service, "Can sensors make a home in the body?" *Science*, vol. 297, pp. 962-963, 2002.
[68] P. U. Abel and T. v. Woedtke, "Biosensors for in vivo glucose measurement: Can we cross the experimental stage," *Biosensors and Bioelectronics*, vol. 17, pp. 1059-1070, 2002.

[69] D. A. Gough and J. C. Armour, "Development of the implantable glucose sensor: What are the prospects and whyis it taking so long?" *Diabetes*, vol. 44, pp. 1005-1009, 1995.
[70] M. E. Meyerhoff, "In vivo blood-gas and electrolyte sensors: progress and challenges," *Trends in Analytical Chemistry*, vol. 12, pp. 257-265, 1993.
[71] E. W. Kraegen and D. J. Chisholm, "Closure of the loop by glucose sensing-physiological and practical considerations," *Hormone Metabolism Research*, vol. 20, Supplement S, pp. 1-4, 1998.
[72] R. J. McNichols and G. L. Cote, "Optical glucose sensing in biological fluids: an overview," *Journal of Biomedical Optics*, vol. 5, pp. 5-16, 2000.
[73] B. Ziaie and K. Najafi, "An implantable microsystem for tonometric blood pressure measurement," *Biomedical Microdevices*, vol. 3, pp. 285-292, 2001.
[74] C. A. Grimes and D. Kouzoudis, "Thin-film magnetoelastic microsensors for remote query biomedical monitoring," vol. 2, pp. 51-60, 1999.
[75] D. A. Gough, "Issues related to in vitro operation of potentially implantable enzyme electrode glucose sensors," *Hormone Metabolism Research*, vol. 20, Supplement S, pp. 30-33, 1988.
[76] T. A. Desai, W. H. Chu, G. Rasi, P. Sinibaldi-Vallebona, P. Borboni, G. Beattie, A. Hayek, and M. Ferrari, "Implantation of microfabricated immunoisolating biocapsules," presented at Proceedings of the SPIE, Micro and Nanofabricated Electro-Optical-Mechanical Systems for Biomedical and Environmental Applications, 1998.
[77] T. A. Desai, W. H. Chu, G. Rasi, P. Sinbaldi-Vallebona, E. Guarino, and M. Ferrari, "Microfabricated biocapsules provide short-term immunoisolation of insulinoma xenografts," *Biomedical Microdevices*, vol. 1, pp. 131-138, 1999.
[78] T. A. Desai, D. Hansford, and M. Ferrari, "Characterization of micromachined silicon membranes for immunoisolation and bioseparation applications," *Journal of Membrane Science*, vol. 159, pp. 221-231, 1999.
[79] L. Leoni, A. Boiarski, and T. A. Desai, "Characterization of nanoporous membranes for immunoisolation: diffusion properties and tissue effects," *Biomedical Microdevices*, vol. 4, pp. 131-139, 2002.
[80] A. Ahmed, C. Bonner, and T. A. Desai, "Bioadhesive microdevices for drug delivery: a feasibility study," *Biomedical Microdevices*, vol. 3, pp. 89-95, 2001.
[81] F. J. Martin and C. Grove, "Microfabricated drug delivery systems: concepts to improve clinical benefit," *Biomedical Microdevices*, vol. 3, pp. 97-108, 2001.
[82] J. T. Santini, M. J. Cima, and R. Langer, "A controlled-release microchip," *Nature*, vol. 397, pp. 335-338, 1999.
[83] M. J. Cima, "Drug release from an implantable MEMs array," presented at ACS Prospectives Furture Directions of Drug Delivery Technologies: Molecular Design, Cellular Response, and Nanotechnology Conference, Boston, MA, 2002.
[84] Y. Li, R. S. Shawgo, R. Langer, and M. J. Cima, "Electrochemical disintegration of gold membranes on a MEMS device for drug delivery," presented at Fall Materials Research Society Meeting, Boston, MA, 2002.
[85] K. Wise, D. Anderson, J. Hetke, D. Kipke, and K. Najafi, "Wireless implantable microsystems: high density electronic interfaces to the nervous system," *Proceedings of the IEEE*, vol. 92, pp. 76-97, 2004.

[86] K. Najafi, "Micropackaging technologies for integrated microsystems: applications to MEMS and MOEMS," presented at SPIE Micromachining and Microfabrication Symposium, San Jose, CA, 2003.
[87] K. Najafi, J. Ji, and K. D. Wise, "Scaling limitations of silicon multichannel recording probes," *IEEE Transactions on Biomedical Engineering*, vol. 37, pp. 1-11, 1990.
[88] B. H. Stark and K. Najafi, "An ultra-thin hermetic package utilizing electroplated gold," presented at Transducers, 2001.
[89] T. Akin, K. Najafi, and R. M. Bradley, "A wireless implantable multichannel digital neural recording system for micromachined sieve electrode," *IEEE Journal on Solid-State Circuits*, pp. 109-118, 1998.
[90] M. Ghovanloo, K. Beach, K. D. Wise, and K. Najafi, "A BiCMOS wireless interface chip for micromachined stimulating microprobes," presented at Proceedings of the IEEE-EMBS Special Topic Conference on Microtechnologies in Medicine and Biology, 2002.
[91] M. Ghovanloo and K. Najafi, "A fully-digital frequency-shift-keying demodulator chip for wireless biomedical implants," presented at Proceedings of the IEEE Southwest Symposium on Mixed-Signal Design, 2003.
[92] M. Ghovanloo, K. D. Wise, and K. Najafi, "Toward a button-sized 1024-site wireless cortical microstimulating array," presented at Proceedings of the 1st International IEEE/EMBS Conference on Neural Engineering, 2003.
[93] P. Mohensi and K. Najafi, "A wireless FM microsystem for biomedical neural recording applications," presented at Proceedings of the Southwest Symposium on Mixed-Signal Design, 2003.
[94] H. Yu and K. Najafi, "Low-power interface circuits for bio-implantable microsystems," presented at IEEE Solid-State Circuits Conference, San Francisco, CA, 2003.
[95] K. D. Wise, J. B. Angell, and A. Starr, "An integrated circuit approach to extracellular microelectrodes," presented at Digest of the 8th International Conference on Engineering in Medicine and Biology, 1969.
[96] K. D. Wise and J. B. Angell, "A low-capacitance multielectrode probe for use in extracellular neurophysiology," *IEEE Transactions in Biomedical Engineering*, vol. BME-22, pp. 212-219, 1975.
[97] K. Najafi and J. F. Hetke, "Strength characterization of silicon microprobes in neurophysiological tissues," *IEEE Transactions on Biomedical Engineering*, vol. 37, pp. 474-481, 1990.
[98] J. F. Hetke, J. L. Lund, K. Najafi, K. D. Wise, and D. J. Anderson, "Silicon ribbon cables for chronically implantable microelectrode arrays," *IEEE Transactions in Biomedical Engineering*, vol. 41, pp. 314-21, 1994.
[99] K. L. Drake, K. D. Wise, J. Farraye, D. J. Anderson, and S. L. BeMent, "Performance of planar multisite microprobes in recording extracellular single-unit intracortical activity," *IEEE Transactions in Biomedical Engineering*, vol. 35, pp. 719-32, 1988.
[100] B. Ziaie, J. V. Arx, and K. Najafi, "A microfabricated planar high-current IrOx stimulating microelectrode," presented at Proceedings of the IEEE Engineering Medicine and Biology Conference, 1996.

[101] D. J. Anderson, K. Najafi, S. J. Tanghe, D. A. Evans, K. L. Levy, J. F. Hetke, X. L. Xue, J. J. Zappia, and K. D. Wise, "Batch-fabricated thin-film electrodes for stimulation of the central auditory system," *IEEE Transactions in Biomedical Engineering*, vol. 36, pp. 693-704, 1989.
[102] P. K. Campbell, K. E. Jones, R. J. Huber, K. W. Horch, and R. A. Normann, "A silicon-based, three dimensional neural interface: manufacturing processes for an intracortical electrode array," *IEEE Transactions on Biomedical Engineering*, vol. 38, pp. 758-768, 1991.
[103] P. J. Rousche and R. A. Normann, "Chronic intracortical microstimulation (ICMS) of cat sensory cortex using the Utah intracortical electrode array," *IEEE Transactions on Rehabilitation Engineering*, vol. 7, pp. 56-68, 1999.
[104] K. E. Jones, P. K. Campbell, and R. A. Normann, "A glass/silicon composite intracortical electrode array," *Annals of Biomedical Engineering*, vol. 20, pp. 423-37, 1992.
[105] R. A. Normann, "Microfabricated electrode arrays for restoring lost sensory and motor functions," presented at Digest of the IEEE International Conference on Solid-State Sensors, Actuators, and Microsystems, 2003.
[106] A. Banner and R. A. Normann, "A multielectrode array for intrafascicular recording and stimulation in sciatic nerve of cats," *Brain Research Bulletin*, vol. 51, pp. 293-306, 2000.
[107] P. K. Campbell, R. A. Normann, K. W. Horch, and S. S. Stensaas, "A chronic intracortical electrode array: preliminary results," *Journal of Biomedical Materials Research*, vol. 23, pp. 245-59, 1989.
[108] C. T. Nordhausen, E. M. Maynard, and R. A. Normann, "Single-unit recording capabilities of a 100 microelectrode array," *Brain Research*, vol. 726, pp. 129-140, 1996.
[109] R. A. Normann, D. J. Warren, J. Ammermuller, E. Fernandez, and S. Guillory, "High-resolution spatio-temporal mapping of visual pathways using multi-electrode arrays," *Vision Research*, vol. 41, pp. 1261-1275, 2001.
[110] P. J. Rousche and R. A. Normann, "Chronic recording capability of the Utah intracortical electrode array in cat sensory cortex," *Journal of Neuroscience Methods*, vol. 82, pp. 1-15, 1998.
[111] P. S. Motta and J. W. Judy, "Multielectrode microprobes for deep-brain stimulation fabricated with a customizable 3-D electroplating process," *IEEE Transactions on Biomedical Engineering*, vol. 52, pp. 923-933, 2005.
[112] P. S. Motta and J. W. Judy, "Micromachined probes for deep-brain stimulation," presented at 2nd Annual International IEEE-EMB Special Topic Conference on Microtechnologies in Medicine and Biology, Madison, WI, 2002.
[113] M. Okandan, K. Wessendorf, T. Christenson, T. Lemn, R. Shul, M. Baker, C. James, R. Myers, and D. Stein, "MEMS conformal electrode array for retinal implant," presented at Transducers, Boston, 2003.
[114] T. Yagi, N. Ito, M. Watanabe, and Y. Uchikawa, "A computational study on an electrode array in a hybrid retinal implant," presented at IEEE International Joint Conference on Computational Intelligence, 1998.
[115] E. T. Kim, J. M. Seo, J. A. Zhou, H. Jung, and S. J. Kim, "A retinal implant technology based on flexible polymer electrode and optical/electrical

stimulation," presented at IEEE International Workshop on Biomedical Circuits and Systems, 2004.
[116] Y. Ito, T. Yagi, H. Kanda, S. Tanaka, M. Watanabe, and Y. Uchikawa, "Cultures of neurons on micro-electrode array in hybrid retinal implant," presented at IEEE International Conference on Systems, Man, and Cybernetics, 1999.
[117] T. Yagi, Y. Ito, H. Kanda, S. Tanaka, M. Watanabe, and Y. Uchikawa, "Hybrid retinal implant: fusion of engineering and neuroscience," presented at IEEE International Conference on Systems, Man, and Cybernetics, 1999.
[118] D. C. Rodger and Y. C. Tai, "Microelectronic packaging for retinal prostheses," *IEEE Engineering in Medicine and Biology Magazine*, vol. 24, pp. 52-57, 2005.
[119] W. Liu, W. Fink, M. Tarbell, and M. Sivaprakasam, "Image processing and interface for retinal visual prostheses," presented at IEEE International Symposium on Circuits and Systems, 2005.
[120] A. P. Chu, K. Morris, R. J. Greenberg, and D. M. Zhou, "Stimulus induced pH changes in retinal implants," presented at EMBS Conference, 2004.
[121] H. Kanda, T. Yagi, Y. Ito, S. Tanaka, M. Watanabe, and Y. Uchikawa, "Efficient stimulation inducing neural activity in retinal implant," presented at IEEE Conference on Systems, Man, and Cybernetics, 1999.
[122] D. Balya and B. Roska, "Neuromorphic algorithm for retinal implants," presented at IEEE EMBS Conference on Neural Engineering, 2005.
[123] A. Schmid, "Retinomorphic information processing for electrical epi-retinal vision implant stimulation," presented at IEEE Symposium on Bioinformatics and Bioengineering, 2004.
[124] W. Liu, "Retinal implant: bridging engineering and medicine," presented at International Electron Devices Meeting, 2002.
[125] J. Buitenweg, W. L. C. Rutten, E. Marani, S. K. L. Polman, and J. Ursum, "Extracellular detection of active membrane currents in the neuron-electrode interface," *Journal of Neuroscience Methods*, vol. 115, pp. 211-221, 2002.
[126] S. M. Potter, "Distributed processing in cultured neuronal networks," *Progress in Brain Research*, vol. 130, pp. 49-62, 2001.
[127] M. Han, G. Gholmieh, W. Soussou, T. W. Berger, and A. R. Tanguay, "Conformally-mapped multielectrode arrays for in-vitro stimulation and recording of hippocampal acute slices," presented at EMBS/BMES Conference, 2002.
[128] W. Rutten, J. M. Mouveroux, J. Buitenweg, C. Heida, T. Ruardij, E. Marani, and E. Lakke, "Neuroelectronic interfacing with cultured multielectrode arrays toward a cultured probe," *Proceedings of the IEEE*, vol. 89, pp. 1013-1029, 2001.
[129] I. Suzuki, Y. Sugio, H. Moriguchi, A. Hattori, K. Yasuda, and Y. Jimbo, "Pattern modification of a neuronal network for individual-cell-based electrophysiological measurement using photothermal etching of an agarose architecture with a multielectrode array," *IEE Proceedings-Nanobiotechnology*, vol. 151, pp. 116-121, 2004.
[130] K. J. James and R. A. Normann, "Low-stress silicon nitride for insulating multielectrode arrays," *EMBS Society Conference: New Opportunities for Biomedical Engineers*, vol. 2, pp. 836-837, 1994.

[131] J. J. Mastrototaro, H. Z. Massoud, T. C. Pilkington, and R. E. Ideker, "Rigid and flexible thin-film multielectrode arrays for transmural cardiac recording," *IEEE Transactions Biomedical Engineering*, vol. 39, pp. 271-279, 1992.
[132] J. Pine, "Studying mammalian neurons in vitro with multielectrode arrays," presented at EMBS Society Conference, 2003.
[133] R. A. Blum, J. D. Ross, C. M. Simon, E. A. Brown, R. R. Harrison, and S. P. DeWeerth, "A custom multielectrode array with integrated low-noise preamplifiers," presented at EMBS Conference, 2003.
[134] M. E. Ruaro, P. Bonifazi, and V. Torre, "Toward the neurocomputer: image processing and pattern recognition with neuronal cultures," *IEEE Transactions on Biomedical Engineering*, vol. 52, pp. 371-383, 2005.
[135] W. L. C. Rutten, H. J. v. Wier, and J. H. M. Put, "Sensitivity and selectivity of intraneural stimulation using a silicon electrode array," *IEEE Transactions Biomedical Engineering*, vol. 38, pp. 192-198, 1991.
[136] W. L. C. Rutten, J. P. A. Smit, T. A. Frieswijk, J. A. Bielen, A. L. H. Brouwer, J. R. Buitenweg, and C. Heida, "Neuro-electronic interfacing with multielectrode arrays," *Engineering in Medicine and Biology Magazine*, vol. 18, pp. 47-55, 1999.
[137] R. R. Harrison and C. Charles, "A low-power low-noise CMOS amplifier for neural recording applications," *IEEE Journal of Solid-State Circuits*, vol. 38, pp. 958-965, 2003.
[138] E. Claverol-Tinture, M. Ghirardi, F. Fiumara, X. Rosell, and J. Cabestany, "Multielectrode arrays with elastomeric microstructured overlays for extracellular recordings from patterned neurons," *Journal of Neural Engineering*, vol. 2, pp. L1-7, 2005.
[139] H. Oka, K. Shimono, R. Ogawa, H. Sugihara, and M. Taketani, "A new planar multielectrode array for extracellular recording: application to hippocampal acute slice," *Journal of Neuroscience Methods*, vol. 93, pp. 61-67, 1999.
[140] M. P. Maher, J. Pine, J. Wright, and Y. C. Tai, "The neurochip: a new multielectrode device for stimulating and recording from cultured neurons," *Journal of Neuroscience Methods*, vol. 87, pp. 45-56, 1999.
[141] U. Egert, B. Schlosshauer, S. Fennrich, W. Nisch, M. Fejtl, T. Knott, T. Muller, and H. Hammerle, "A novel organotypic long-term culture of the rat hippocampus on substrate-integrated multielectrode arrays," *Brain Research Protocols*, vol. 2, pp. 229-242, 1998.
[142] A. Lau, P. Hung, and L. P. Lee, "Raised lateral patch clamp array in open-access fluidic system," presented at Microtas, Boston, MA, 2005.
[143] R. B. Campenot, "Retraction and degeneration of sympathetic neurites in response to locally elevated potassium," *Brain Researcch*, vol. 399, pp. 357-363, 1986.
[144] R. B. Campenot, "Local control of neurite development by nerve growth factor," *Proceedings of the National Academy of Sciences USA*, vol. 74, pp. 4516-4519, 1977.
[145] R. B. Campenot, *Cell-Cell Interactions: A Practical Approach*, 1992.
[146] E. P. d. Chaves, M. Bussiere, B. MacInnis, D. E. Vance, R. B. Campenot, and J. E. Vance, "Ceramide inhibits axonal growth and nerve growth factor uptake without compromising the viability of sympathetic neurons," *Journal of Biological Chemistry*, vol. 276, pp. 36207-36214, 2001.

[147] E. P. d. Chaves, M. Bussiere, D. E. Vance, and R. B. Campenot, "Elevation of ceramide within distal neurites inhibits neurite growth in cultured rat sympathetic neurons," *Journal of Biological Chemistry*, vol. 272, pp. 3028-3035, 1997.
[148] R. B. Campenot, "Independent control of the local environment of somas and neurites," *Methods in Enzymology*, vol. 58, pp. 302-307, 1979.
[149] B. Karten, D. E. Vance, R. B. Campenot, and J. E. Vance, "Cholesterol accumulates in cell bodies, but is decreased in distal axons, of Niemann-Pick C1-deficient neurons," *Journal of Neurochemistry*, vol. 83, pp. 1154-1163, 2002.
[150] B. Karten, D. E. Vance, R. B. Campenot, and J. E. Vance, "Trafficking of cholesterol from cell bodies to distal axons in niemann pick C1-deficient neurons," *Journal of Biological Chemistry*, vol. 278, pp. 4168-4175, 2003.
[151] B. Karten, H. Hayashi, R. B. Campenot, D. E. Vance, and J. E. Vance, "Neuronal models for studying lipid metabolism and transport," *Methods*, vol. 36, pp. 117-128, 2005.
[152] B. L. MacInnis and R. B. Campenot, "Regulation of Wallerian degeneration and nerve growth factor withdrawal-induced pruning of axons of sympathetic neurons by the proteasome and the MEK/Erk pathway," *Molecular and Cellular Neuroscience*, vol. 28, pp. 430-439, 2005.
[153] J. Bertrand, M. J. Winton, N. Rodriguez-Hernandez, R. B. Campenot, and L. McKerracher, "Application of Rho antagonist to neuronal cell bodies promotes neurite growth in compartmented cultures and regeneration of retinal ganglion cell axons in the optic nerve of adult rats," *Journal of Neuroscience*, vol. 25, pp. 1113-21, 2005.
[154] B. Karten, H. Hayashi, G. A. Francis, R. B. Campenot, D. E. Vance, and J. E. Vance, "Generation and function of astroglial lipoproteins from neimann-pick type c1-deficient mice," *Biochemical Journal*, vol. 387, pt 3, pp. 779-88, 2005.
[155] H. Hayashi, B. Karten, D. E. Vance, R. B. Campenot, R. A. Maue, and J. E. Vance, "Methods for the study of lipid metabolism in neurons," *Analytical Biochemistry*, vol. 331, pp. 1-16, 2004.
[156] H. Hayashi, R. B. Campenot, D. E. Vance, and J. E. Vance, "Glial lipoproteins stimulate axon growth of central nervous system neurons in compartmented cultures," *Journal of Biological Chemistry*, vol. 279, pp. 14009-14015, 2004.
[157] R. B. Campenot and B. L. MacInnis, "Retrograde transport of neurotrophins: fact and function," *Journal of Neurobiology*, vol. 58, pp. 217-229, 2004.
[158] B. L. MacInnis, D. L. Senger, and R. B. Campenot, "Spatial requirements for trkA kinase activity in the support of neuronal survival and axon growth in rat sympathetic neurons," *Neuropharmacology*, vol. 45, pp. 995-1010, 2003.
[159] J. E. Vance, R. B. Campenot, and D. E. Vance, "The synthesis and transport of lipids for axonal growth and nerve regeneration," *Biochimica et Biophysica Acta*, vol. 1486, pp. 84-96, 2000.
[160] H. Eng, K. Lund, and R. B. Campenot, "Synthesis of beta-tubulin, actin, and other proteins in axons of sympathetic neurons in compartmented cultures," *Journal of Neuroscience*, vol. 19, pp. 1-9, 1999.
[161] K. Kimpinski, R. B. Campenot, and K. Mearow, "Effects of the neurotrophins nerve growth factor, neurotrophin-3, and brain-derived neurotrophic factor

(BDNF) on neurite growth from adult sensory neurons in compartmented cultures," *Journal of Neurobiology*, vol. 33, pp. 395-410, 1997.
[162] D. L. Senger and R. B. Campenot, "Rapid retrograde tyrosine phosphorylation of trkA and other proteins in rat sympathic neurons in compartmented cultures," *Journal of Cell Biology*, vol. 138, pp. 411-421, 1997.
[163] J. G. Toma, D. Rogers, D. L. Senger, R. B. Campenot, and F. D. Miller, "Spatial regulation of neuronal gene expression in response to nerve growth factor," *Developmental Biology*, vol. 184, pp. 1-9, 1997.
[164] B. Campenot, K. Lund, and D. L. Senger, "Delivery of newly synthesized tubulin to rapidly growing distal axons of sympathetic neurons in compartmented cultures," *Journal of Cell Biology*, vol. 135, pp. 701-9, 1996.
[165] E. P. d. Chaves, D. E. Vance, R. B. Campenot, and J. E. Vance, "Alkylphosphocholines inhibit choline uptake and phosphatidylcholine biosynthesis in rat sympathetic neurons and impair axonal extension," *Biochemical Journal*, vol. 312 (pt 2), pp. 411-417, 1995.
[166] J. E. Vance, E. P. d. Chaves, R. B. Campenot, and D. E. Vance, "Role of axons in membrane phospholipid synthesis in rat sympathetic neurons," *Neurobiology of Aging*, vol. 16, pp. 493-498, 1995.
[167] E. P. d. Chaves, D. E. Vance, R. B. Campenot, and J. E. Vance, "Axonal synthesis of phosphatidylcholine is required for normal axonal growth in rat sympathetic neurons," *Journal of Cell Biology*, vol. 128, pp. 913-918, 1995.
[168] R. B. Campenot, D. D. Draker, and D. L. Senger, "Evidence that protein kinase C activities involved in regulating neurite growth are localized to distal neurites," *Journal of Neurochemistry*, vol. 63, pp. 868-878, 1994.
[169] R. B. Campenot, "NGF and the local control of nerve terminal growth," *Journal of Neurobiology*, vol. 25, pp. 599-611, 1994.
[170] R. B. Campenot and D. D. Draker, "Growth of sympathetic nerve fibers in culture does not require extracellular calcium," *Neuron*, vol. 3, pp. 733-743, 1989.
[171] W. S. Sussdorf and R. B. Campenot, "Influence of the extracellular potassium environment on neurite growth in sensory neurons, spinal cord neurons and sympathetic neurons," *Brain Researcch*, vol. 390, pp. 43-52, 1986.
[172] R. B. Campenot, "Development of sympathetic neurons in compartmentalized cultures. II. local control of neurite survival by nerve growth factor," *Developmental Biology*, vol. 93, pp. 13-21, 1982.
[173] K. J. Ivins, E. T. N. Bui, and C. W. Cotman, "β-amyloid induces local neurite degeneration in cultured hippocampal neurons: evidence for neuritic apoptosis," *Neurobiology of Disease*, vol. 5, pp. 365-378, 1998.
[174] B. L. MacInnis and R. B. Campenot, "Retrograde support of neuronal survival without retrograde transport of nerve growth factor," *Science*, vol. 295, pp. 1536-9, 2002.
[175] S. N. Bhatia, M. L. Yarmush, and M. Toner, "Controlling cell interactions by micropatterning in cocultures: hepatocytes and 3T3 fibroblasts," *Journal of Biomedical Materials Research*, vol. 34, pp. 189-199, 1997.
[176] J. M. Corey, B. C. Wheeler, and G. J. Brewer, "Compliance of hippocampal neurons to patterned substrate networks," *Journal of Neuroscience Research*, vol. 30, pp. 300-07, 1991.

[177] J. M. Corey, B. C. Wheeler, and G. J. Brewer, "Micrometer resolution silane-based patterning of hippocampal neurons: critical variables in photoresist and laser ablation processes for substrate fabrication," *IEEE Transactions on Biomedical Engineering*, vol. 43, pp. 944-955, 1996.
[178] R. S. Kane, S. Takayama, E. Ostuni, D. E. Ingber, and G. M. Whitesides, "Patterning proteins and cells using soft lithography," *Biomaterials*, vol. 20, pp. 2363-2376, 1999.
[179] S. K. Mohanty, S. K. Ravula, K. L. Engisch, and A. B. Frazier, "A microsystem using dielectrophoresis and electrical impedance spectroscopy for cell manipulation and analysis," presented at Transducers, Boston, 2003.
[180] D. A. Stenger, J. H. Georger, C. S. Dulcey, J. J. Hickman, A. S. Rudolph, T. B. Nielson, S. M. McCort, and J. M. Calvert, "Coplanar molecular assemblies of amino- and perfluorinated growth," *Journal of the American Chemical Society*, vol. 114, pp. 8435-8442, 1992.
[181] D. A. Stenger, J. J. Hickman, K. E. Bateman, M. S. Ravenscroft, W. Ma, J. J. Pancrazio, K. Shaffer, A. E. Schaffner, D. H. Cribbs, and C. W. Cotman, "Microlithographic determination of axonal/dendritic polarity in cultured hippocampal neurons," *Journal of neuroscience Methods*, vol. 82, pp. 167-173, 1998.
[182] S. Klostermann and F. Bonhoeffer, "Investigations of signaling pathways in axon growth and guidance," *Perspectives on Developmental Neurobiology*, vol. 4, pp. 237-252, 1996.
[183] A. Riccio, B. A. Pierchala, C. L. Ciarallo, and D. D. Ginty, "An NGF-TrkA-mediated retrograde signal to transcription factor CREB in sympathetic neurons," *Science*, vol. 277, pp. 1097-1100, 1997.
[184] D. R. Ure and R. B. Campenot, "Retrograde transport and steady-state distribution of ^{125}I-nerve growth factor in rat sympathetic neurons in compartmented cultures," *The Journal of Neuroscience*, vol. 17, pp. 1282-1290, 1997.
[185] P. Walicke, R. Campenot, and P. Patterson, "Determination of transmitter function by neuronal activity," *Proceedings of the National Academy of Sciences USA*, vol. 74, pp. 5767-5771, 1977.
[186] F. L. Watson, H. M. Heerssen, D. B. Moheban, M. Z. Lin, C. M. Sauvageot, A. Bhattacharyya, S. L. Pomeroy, and R. A. Segal, "Rapid nuclear responses to target-derived neurotrophins require retrograde transport of ligand-receptor complex," *The Journal of Neuroscience*, vol. 19, pp. 7889-7900, 1999.
[187] R. D. Fields, C. Yu, and P. G. Nelson, "Calcium, network activity, and the role of NMDA channels in synaptic plasticity *in vitro*," *Journal of Neuroscience*, vol. 11, pp. 134-46, 1991.
[188] E. R. Kandel, J. H. Schwartz, and T. M. Jessell, *Principles of neural science*, 4th ed. New York: McGraw-Hill Health Professions Division, 2000.
[189] T. D. Albright, T. M. Jessell, E. R. Kandel, and M. I. Posner, "Neural science: a century of progress and the mysteries that remain," *Neuron*, vol. 25, pp. S1-55, 2000.
[190] N. Spruston, Y. Schiller, G. Stuart, and B. Sakmann, "Activity-dependent action potential invasion and calcium influx in to hippocampal Ca1 dendrites," *Science*, vol. 268, pp. 297-300, 1995.

[191] M. A. Rogawski and W. Loscher, "The neurobiology of antiepileptic drugs for the treatment of nonepileptic conditions," *Nature Medicine*, vol. 10, pp. 685-692, 2004.
[192] W. Loscher and D. Schmidt, "New horizons in the development of antiepileptic drugs," *Epilepsy Research*, vol. 50, pp. 3-16, 2002.
[193] S. D. Silberstein, "Shared mechanisms and comorbidities in neurologic and psychiatric disorders," *Headache*, vol. 41, pp. S11-S17, 2001.
[194] M. A. Rogawski and W. Loscher, "The neurobiology of antiepileptic drugs," *Nature Reviews Neuroscience*, vol. 5, pp. 553-564, 2004.
[195] M. Pappagallo, "Newer antiepileptic drugs: possible uses in the treatment of neuropathic pain and migraine," *Clinical Therapeutics*, vol. 25, pp. 2506-2538, 2003.
[196] L. A. Gabel and J. J. Loturco, "Electrophysiological and morphological characterization of neurons with neocortical ectopias," *Journal of Neurophysiology*, vol. 85, pp. 495-505, 2001.
[197] C. Sarantopoulos, B. McCallum, W. M. Kwok, and Q. Hogan, "Gabapentin decreases membrane calcium currents in injured as well as in control mammalian primary afferent neurons," *Regional Anesthesia and Pain Medicine*, vol. 27, pp. 47-57, 2002.
[198] S. Arnold, B. Hyman, G. V. Hoesen, and A. Damasio, "Some cytoarchitectural abnormalities of the entorhinal cortex in schizophrenia," *Archives of General Psychiatry*, vol. 48, pp. 625-632, 1991.
[199] S. Balogh, G. Sherman, L. Hyde, and V. Denenberg, "Effects of neocortical ectopias upon the acquisition and retention of a non-spatial reference memory task in BXSB mice," *Developmental Brain Research*, vol. 111, pp. 291-293, 1998.
[200] G. Boehm, G. Sherman, B. Hoplight, L. Hyde, N. Waters, D. Bradway, A. Galaburda, and V. Denenberg, "Learning and memory in the autoimmune BXSB mouse: effects of neocortical ectopias and environmental enrichment," *Brain Research*, vol. 726, pp. 11-22, 1996.
[201] V. Caviness, P. Evrard, and G. Lyon, "Radial neuronal assemblies, ectopia, and necrosis of developing cortex: a case analysis," *Acta Neuropathologica*, vol. 41, pp. 67-72, 1978.
[202] M. Clark, G. Sherman, H. Bimonte, and R. Fitch, "Perceptual auditory gap detection deficits in male BXSB mice with cerebrocortical ectopias," *Neuroreport*, vol. 11, pp. 693-696, 2000.
[203] D. Spencer, K. Humphries, D. Mathis, and H. Lal, "Behavioral impairments related to cognitive dysfunction in the autoimmune New Zealand black mice," *Behavioral Neuroscience*, vol. 100, pp. 353-358, 1986.
[204] D. Prince and K. Jacobs, "Inhibitory function in two models of chronic epileptogenesis," *Epilepsy Research*, vol. 32, pp. 83-92, 1998.
[205] D. Prince, K. Jacobs, P. Salin, S. Hoffman, and I. Parada, "Chronic focal neocortical epileptogenesis: does disinhibition play a role?" *Canadian Journal of Physiology and Pharmacology*, vol. 75, pp. 500-507, 1997.

[206] H. Luhmann and K. Raabe, "Characterization of neuronal migration disorders in neocortical structures. I. Expression of epileptiform activity in an animal model," *Epilepsy Research*, vol. 26, pp. 67-74, 1996.
[207] M. S. Wang, Y. Wu, D. Culver, and J. D. Glass, "Pathogenesis of axonal degeneration: parallels between Wallerian degeneration and vincristine neuropathy," *Journal of Neuropathology and Experimental Neurology*, vol. 59, pp. 599-606, 2000.
[208] K. J. Smith, R. Kapoor, and P. A. Felts, "Demyelination: the role of reactive oxygen and nitrogen species," *Brain Pathology*, vol. 9, pp. 69-92, 1999.
[209] M. Devor, *Abnormal excitability in injured axons*. New York: Oxford University Press, 1995.
[210] J. B. Cavanagh, "The dying back process: a common denominator in many naturally occurring and toxic neuropathies," *Archives of Pathology and Laboratory Medicine*, vol. 103, pp. 659-64, 1979.
[211] J. B. Cavanagh and M. F. Gysbers, ""Dying back" above a nerve ligature produced by acrylamide," *Acta Neuropathologica*, vol. 51, pp. 169-177, 1980.
[212] M. S. Miller, M. J. Miller, T. F. Burks, and I. G. Sipes, "Altered retrograde axonal transport of nerve growth factor after single and repeated doses of acrylamide in the rat," *Toxicology and Applied Pharmacology*, vol. 69, pp. 96-101, 1983.
[213] P. S. Spencer, M. I. Sabri, H. H. Schaumburg, and C. L. Moore, "Does a defect of energy metabolism in the nerve fiber underlie axonal degeneration in polyneuropathies?" *Annals of Neurology*, vol. 5, pp. 501-07, 1978.
[214] J. R. Mendell, A. Sahenk, and K. Saida, "Alterations of fast axoplasmic transport in experimental methyl *n*-butyl ketone neuropathy," *Brain Research*, vol. 133, pp. 107-118, 1977.
[215] J. W. Griffin, P. N. Hoffman, and A. W. Clark, "Slow axonal transport: selective blockade by β, β'-iminodipropionitrile administration," *Science*, vol. 202, pp. 633-35, 1978.
[216] J. Glass, M. Wang, D. Culver, and Q. Wang, "Pathogenesis of toxin-induced dying-back neuropathy: the axon is the target," presented at Annals of Neurology Abstracts, 2002.
[217] Z. Sahenk, S. T. Brady, and J. R. Mendell, "Studies on the pathogenesis of vincristine-induced neuropathy," *Muscle Nerve*, vol. 10, pp. 80-84, 1987.
[218] L. S. Green, J. A. Donoso, I. E. Heller-Bettinger, and F. E. Samson, "Axonal transport disturbances in vincristine-induced peripheral neuropathy," *Annals of Neurology*, vol. 1, pp. 255-62, 1977.

CHAPTER 2

DESIGN AND FABRICATION METHODOLOGY

2.1. Chapter Outline

The compartmented culture system was developed using microfabrication tools. This chapter outlines the strategies employed and the results of these strategies. In general, microfluidics technology was used to create a chemical pattern and a compartment divider. Microelectronics technology was used to create the MEA.

A schematic of the complete compartmented culture system is shown in Figure 2.1. The final system integrates the microfluidic divider with a collagen patterned MEA substrate. Neurons plated in one compartment grow extensions into adjacent compartments across the microfluidic barrier, and microelectrodes interface with the neurons in each compartment. The initial sections (sections 2.2-2.4) introduce the background information on the fabrication strategies employed in building the device. Sections 2.5-2.10 describe the strategies for the design and fabrication of the microfluidic compartment divider component of the system. Next, sections 2.11 and 2.12 describe the strategies for designing and fabricating the collagen patterning mold. Finally, sections 2.13 and 2.14 describe the strategy for the design and fabrication of the multilelectrode array (MEA). Taken together, these three components form the entire system.

2.2. Background and Previous Work for Microfluidic Compartmentalization

Microfluidics has become an enabling technology in a wide variety of disciplines. Microfluidics is the study of fluids through micrometer size features. The ability to make networks of interconnecting channels is what lies at the heart of microfluidics. The

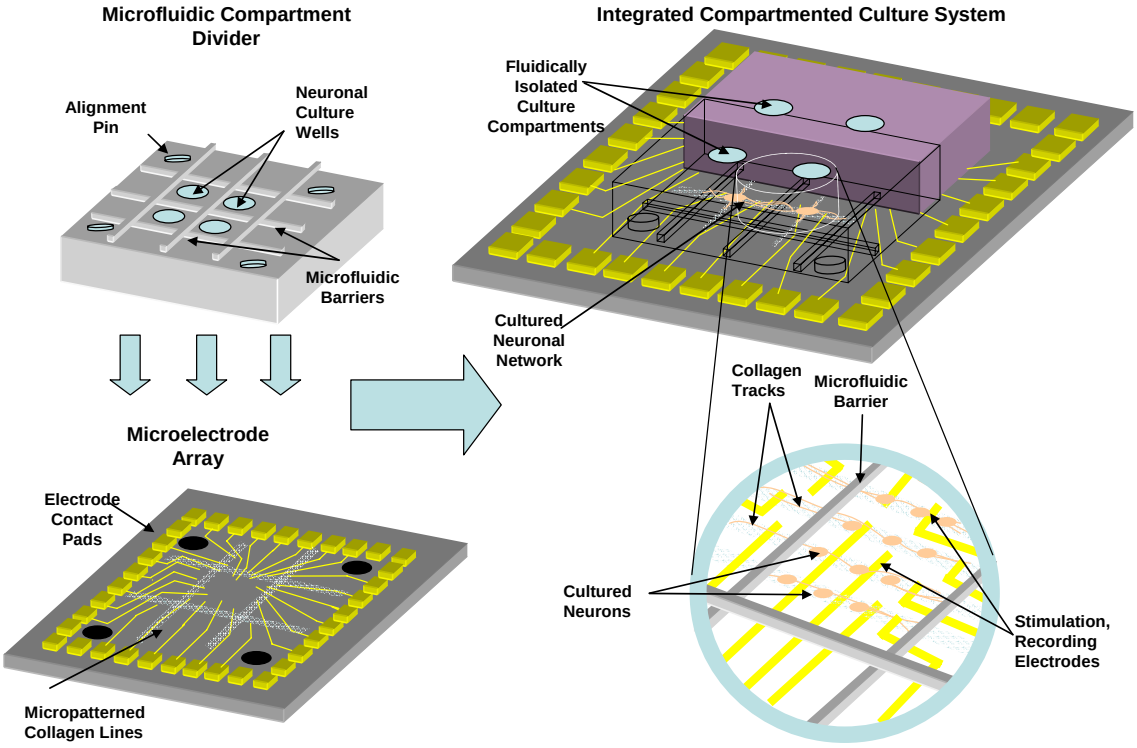

Figure 2.1. Schematic of integrated compartmented culture system, with microfluidic barriers and microelectrode array interfacing with cultured neurons. The multicompartment divider is aligned to and seated on the microelectrode array. Neurons are then plated in one or more of the compartments, after which they grow into adjacent compartments. Stimulation and recording electrodes on the microelectrode array interface with somal bundles and their processes in all of the compartments, allowing for complicated studies in which both neuronal pharmacology and electrophysiology can be simultaneously studied.

enabling technologies came first from the world of MEMS, where the use of photolithographic processes to obtain micrometer features in silicon and other substrates was well established. Silicon has traditionally been the material of choice for creating these channels; however, other materials like glass and quartz have also been used [1].

More recently, microchannels have been created by replication in polydimethylsiloxane (PDMS). PDMS is a polymer which is becoming increasingly popular for microfluidic applications, because the structures made in this material are inexpensive, easy to handle, and rapidly fabricated by replica molding. When cured, PDMS faithfully replicates nanometer size features on a master. Microchannels are easily formed in PDMS if the master has a raised network of ridges to serve as a microfluidic network. Moreover, PDMS is optically transparent in the UV and visible light range. Since PDMS is gas permeable, bubbles created inside channels by electrolysis of water or from other sources may be dissipated through the material. Masters made in silicon can also be used to imprint or hot-emboss channels in hard plastic materials like polymethylmethacrylate (PMMA) at temperatures close to the softening point of the plastic or at elevated pressures [2]. In addition to the micromolding of PDMS channels from a master, other technologies like laser ablation have also been used to fabricate polymer microchannels. This technique involves directing laser pulses at the plastic surface in defined regions, which causes degradation of the plastic at those spots as a consequence of a combination of photochemical and photothermal degradation processes [1].

2.3. Background and Previous Work for Chemical Patterning

Chemically patterned surfaces are useful for many experimental research projects that involve cell-substrate or cell-cell interactions. Patterned culture surfaces provide researchers with a way to study these cellular activities under controlled conditions. The simplest way to pattern a culture surface is to coat it uniformly with a material and then define its geometry using masking techniques. Letourneau et al deposited a thin layer of palladium to promote cell attachment and directed growth [3]. Moreover, irradiation through a mask has been used to create patterns of denatured materials that inhibit attachment and outgrowth [4]. Also, laser ablation of substrates was used by Corey et al to fabricate high resolution grid patterns of poly-d-lysine by exposing surfaces through a quartz mask [5].

Surface topography has also been manipulated to control neuronal growth. For example, Nelson et al used scratched grooves to guide axonal extensions and to create electrically active circuits of DRG cells [6]. Curtis and Clark investigated the impact of topological factors on cell growth, shape, orientation, and movement by anisotropic etching of silicon [7]. Britland et al used adhesive pathways and topographic channeling simultaneously to align DRG nerve cells in microfabricated channels [8].

Moreover, a number of researchers have applied micromachining and photolithographic techniques to chemically pattern cells on substrates. For example, Lom et al patterned conventional semiconductor industry photoresist to selectively define areas that allow amino and alkyl silanes [9]. This study proved that cells could be guided by both topographical and chemical cues. Using photoresist-based ways of chemically patterning a substrate, Bhatia et al studied the coculture of hepatocytes and 3T3

fibroblasts on chemically patterned substrates [10]. Here, borosilicate wafers were spin-coated with positive photoresist and exposed to ultraviolet light through a chromium mask. After patterning of the photoresist, aminoethylaminopropyltrimethoxysilane, glutaraldehyde, and a protein were bound to the surface of the wafer. Photoresist was then lifted off by sonication in acetone resulting in a glass/protein pattern. By taking advantage of the fact that one cell type adhered to the pattern in serum-free media and the other only in serum-containing media, the authors were able to establish a working coculture.

The most recent alternative method for creating surface patterns is elastomeric stamping in which a microstamp is created by polymerizing polydimethylsiloxane (PDMS) in a mold defined by patterned photoresist. PDMS stamps have been used to imprint a variety of materials, including proteins like polylysine and other materials like alkanethiols [11-13]. In these techniques, PDMS with surface topography is "inked" with a particular protein and brought into contact with a flat substrate. The adsorbed protein is then transferred to the substrate over time. In this way, complicated patterns in the stamp can be transferred to the substrate.

2.4. Background and Previous Work on Multielectrode Arrays

Multielectrode arrays (MEAs) have become useful for studying the properties of neurons in vitro. Several different types of neurons have been cultured on MEAs. These devices employ glass or silicon substrates, onto which electrode arrays made of gold, platinum, or indium tin oxide are fabricated. Neurons grow over the electrodes and this allows signals on the order of microvolts to be recorded between the neurons and the

electrodes. To prevent loss of the electrical signal between the neuron and the electrode, sufficient coupling needs to occur between the neuron and the substrate. Indeed, Buitenweg reported that sufficient coupling between the cell and the electrode occurs only when a neuron is located directly on top of the electrode [14].

The advantages of using extracellular electrode arrays for the study of neuronal network activity are many. Since the technique of extracellular recording is non-invasive and since it is possible to record from neurons over extended periods of time, neurons do not experience the damage that is normally associated with intracellular (patch or sharp electrode) recordings. Moreover, MEAs can be used to stimulate one or more cells in a network over long periods of time. More specifically, the dimensions and spacing of the extracellular microelectrodes make it possible to place a number of them under a single neuron so that the activity in the cell body, axon, and dendrite can be separately recorded. This creates the possibility of conducting complicated studies like the time progression of action potentials down the length of an axon. Finally, chemical or topographical patterning can be used to create a predetermined network of neurons that can be useful for certain experiments [15].

2.5. Design of the Compartment Divider Using Microchannel Flow

Several different compartment dividers were designed. All the designs were done using either AUTOCAD or Coreldraw, and the masks were printed using a high resolution photoplotter. The first designs envisioned the use of microchannels to squeeze silicone grease through them. The idea was to confine the grease by injecting it through the channel either before or after the culture of neurons. Two of the channel designs are

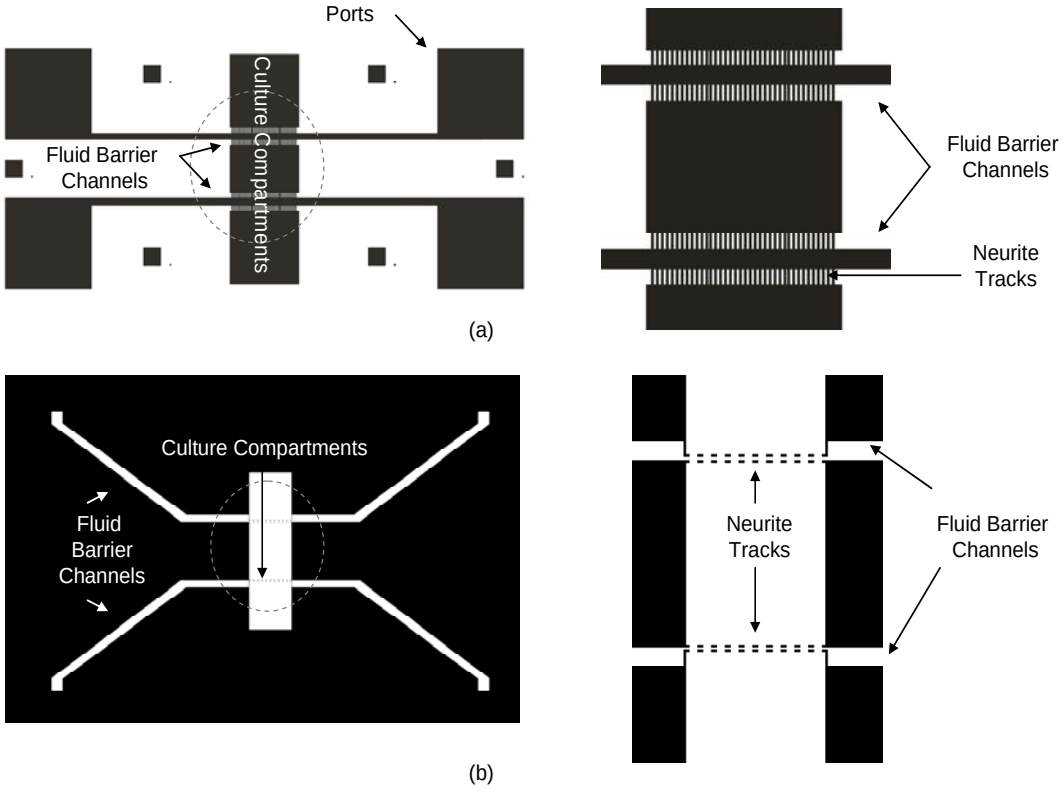

Figure 2.2. Two different mask designs of a three compartment microfluidic chamber. In both designs, the fluid barrier channels intersect the neurite tracks in the culture compartments. (a) Here, the two side culture compartments are 4mmX4mm and the center compartment is 2.5mmX4mm. The fluid barrier channels are 400µm wide and the neurite growth tracks are 50µm wide. (b) In the bottom design, the fluid barrier channels neck down to 100µm and the neurite tracks are 25µm wide. Figures on the right are zoomed-in views of the dashed circles on the left.

shown in Figure 2.2. To test the ability to slowly push or pull the grease (or other hydrophobic materials), we tested various designs in which we varied the size of the grease channels and the size of the neurite tracks that come perpendicular to them. The grease channels were varied in width from 100µm to 400µm while the neurite tracks were varied in width from 25µm to 100µm. We hoped that the greater resistance of the narrower neurite growth channels would prevent the grease from moving into them when moving through that area. The two side compartments were 4mmX4mm and the center compartment was 2.5mmX4mm. The sizes here were chosen such that they would hold an adequate amount of cell media (for culturing neurons) and so that the neurons initially plated in the center compartment would not have to traverse a great distance before they met the barrier. The long neck on the center compartment was included so that a reasonable amount of cell media could be placed into this reservoir, taking into account the possibility for some evaporation during the incubation process.

2.6. Fabrication of the Compartment Divider Using Microchannel Flow

With this fabrication strategy, we wanted to be able to align the electrodes to the grease barriers and the ports for plating neurons. Therefore, a process that involves the use of acetone-dissolvable photoresist was devised. The process flow is shown in Figure 2.3. After patterning a glass substrate (conventional borosilicate glass, 1mm thickness) with Ti/Au metal, AZ 4620 photoresist (Clariant Corp.) was patterned photolithographically to align the channel configuration with the electrodes. The process for using AZ 4620 is as follows. The resist was spun at 800rpm for 30s. Then it was baked for 20min at 95°C. The OAI optical aligner was used to expose the photoresist for

66s at 400mJ/cm^2, and it was developed using 400K developer (Clairiant Corp.) for 2-3min. The developer was diluted with 1 part developer for every 4 parts DI water.

The entire structure was placed in a Petri dish and PDMS (Sylgard 184, Dow

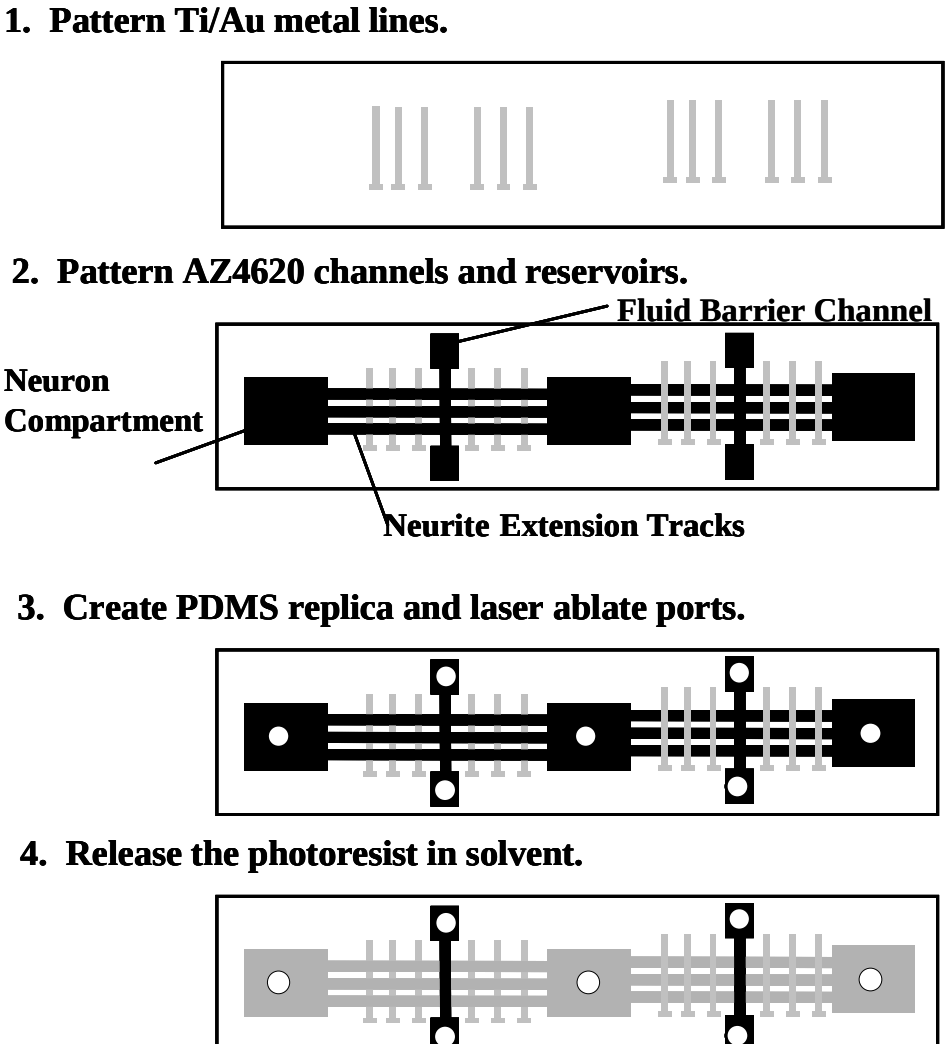

Figure 2.3. Process flow for fabrication of integrated compartmented culture system with fluid barrier channels.

Corning) was poured on top of the structure (30mL) and cured for 2hr at 100°C. Then ports were laser ablated with the CO_2 laser, and the photoresist was released by placing the entire structure in an acetone bath under ultrasonic agitation for several hours. After

acetone sonication, the structure was sonicated in isopropanol followed by DI water to remove all solvent residues. One of the problems encountered with this process was that when the structure was placed in acetone, the PDMS swelled due to absorption of the solvent, causing it to delaminate from the surface of the glass slide. We tried to minimize the amount of time it took to release the photoresist; however, it was difficult since the channels for delivering grease were so small (around 100μm). Causing enough solvent to move through the long grease channels proved difficult. Also, sometimes, some photoresist remained lodged in the channels, which would lead to later cytotoxicity problems. Several adhesion promoters for PDMS to glass were investigated but not implemented due to their known cytotoxicity. Also, ablating through the thick (3-4mm) PDMS samples that resulted from the molding process meant that there was significant damage and debris that was generated around the periphery of the ports. A modification to the above approach was to simply mold the PDMS divider and hand align/bond it to the substrate after fabrication. This approach, while adding the additional step of hand alignment, did allow us to avoid the problems associated with releasing the photoresist in the previous approach. After fabrication of the divider, it was "inked" with uncured PDMS and bonded to the glass slide by heat curing.

In the fabricated versions of these designs, we encountered several problems (see Figure 2.4). In many of these early designs, the microchannels intended for neurite outgrowth were perpendicular to the channel for grease delivery. We tried several methods of injecting the silicone grease into these channels. First, we connected a syringe pump to one of the ports with tubing and seated a plastic assembly. These devices usually failed when the grease entered the area where the main channel intersects

the channels perpendicular to it. The grease crept into the side channels and it became difficult to control its advance. We also tried different types of greases, with varying levels of viscosity. Most of these greases were from Dow Corning. The different greases we tried are Dow Corning high vacuum grease, Molykote bearing grease, and various mixtures of the high vacuum grease with different amounts of silicone oil. Pulling these substances in microchannels was feasible, but in all of these cases, the viscosity of the material meant that it would creep into the side channels. In addition, the grease was pulled through the channels at the output port rather than at the input port. This did not work because PDMS (due to its low Young's modulus) would bend to close the exit port.

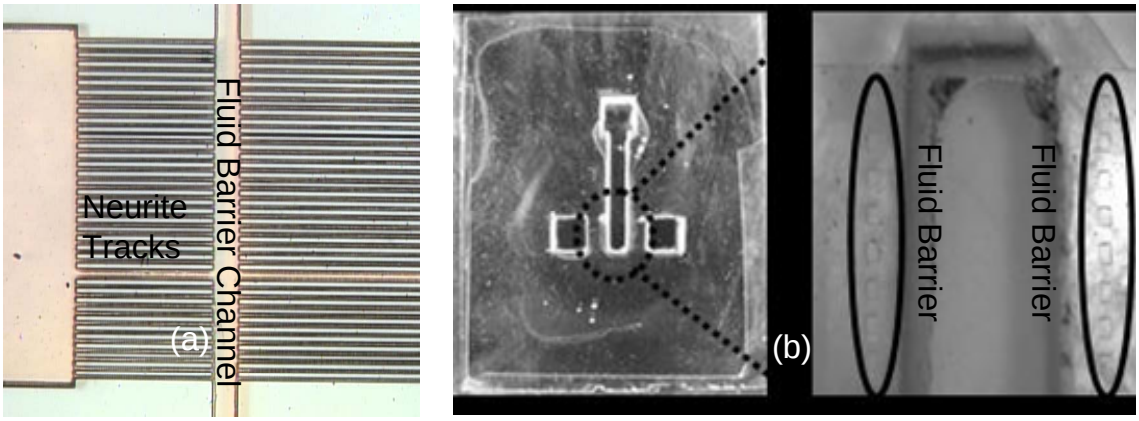

Figure 2.4. Fabricated compartment dividers in PDMS. (a) The fabricated version of the design shown in 2.2a. Neurite tracks are 50µm wide and grease channel perpendiular to it is 400µm wide. (b) Fabricated version of design shown in Figure 2.2b. Neurite tracks are 25µm wide and fluid barriers are 100µm wide.

2.7. Design of the Compartment Divider Using Microstenciling

Another strategy we employed was the use of a microstencil to pattern the silicone grease on the divider. The design of the photoresist master for micromolding a divider for stenciling was the same as in the previous section, except for the fact that no channels were included between compartments to act as fluid barriers or to serve as neurite growth tracks. For the stencil, normal Scotch tape or Shercon green tape was used to stencil

silicone grease onto the PDMS. In both cases the design consisted of an outline that went around the periphery of the culture compartments (see Figure 2.5). Spaces were included in the corners of the stencil to allow the stencil to be lifted off as one piece. The widths of the lines that were stenciled ranged from 200µm to 500µm with the CO_2 laser and 100µm to 150µm with the excimer laser.

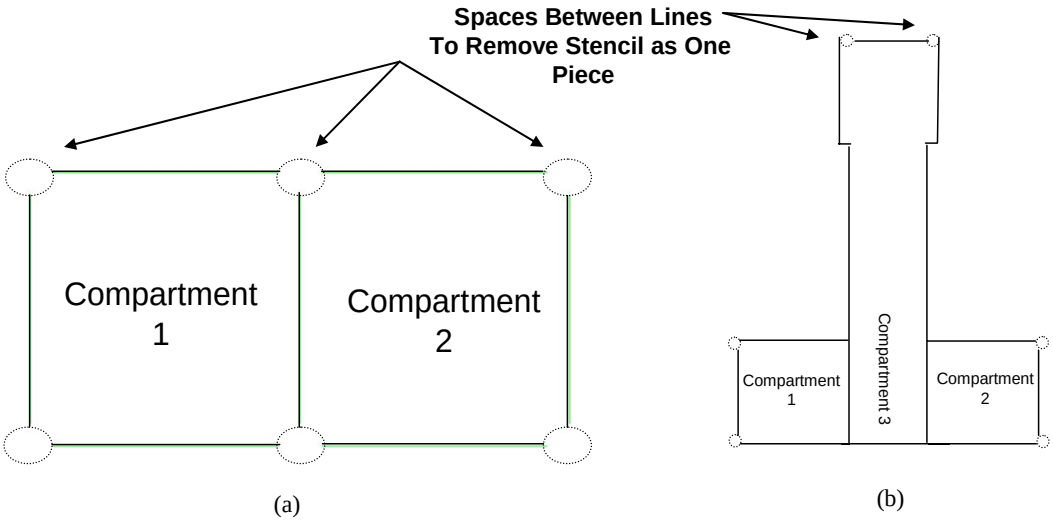

Figure 2.5. Patterns for microstenciling fluid barriers. (a) The stencil on the left is meant for a two compartment divider. (b) The compartment divider on the right was meant for a three compartment divider. The spaces in between the lines allow the stencil to be lifted off of the substrate as one piece.

2.8. Fabrication of the Compartment Divider Using Microstenciling

The fabrication strategy used with this technique is shown in Figure 2.6. Here, the PDMS mold was created by curing a 3inchX1inch block of PDMS (2-3mm thick) on a hot plate for 2hrs at 100°C. The tape was placed under a CO_2 or an excimer laser and ablated under low power and high velocity parameters. This was done so that the smallest amount of power would be applied to ablate fine lines in the tape. Then the tape is removed from the slab, leaving behind the stenciled grease pattern around the ports on

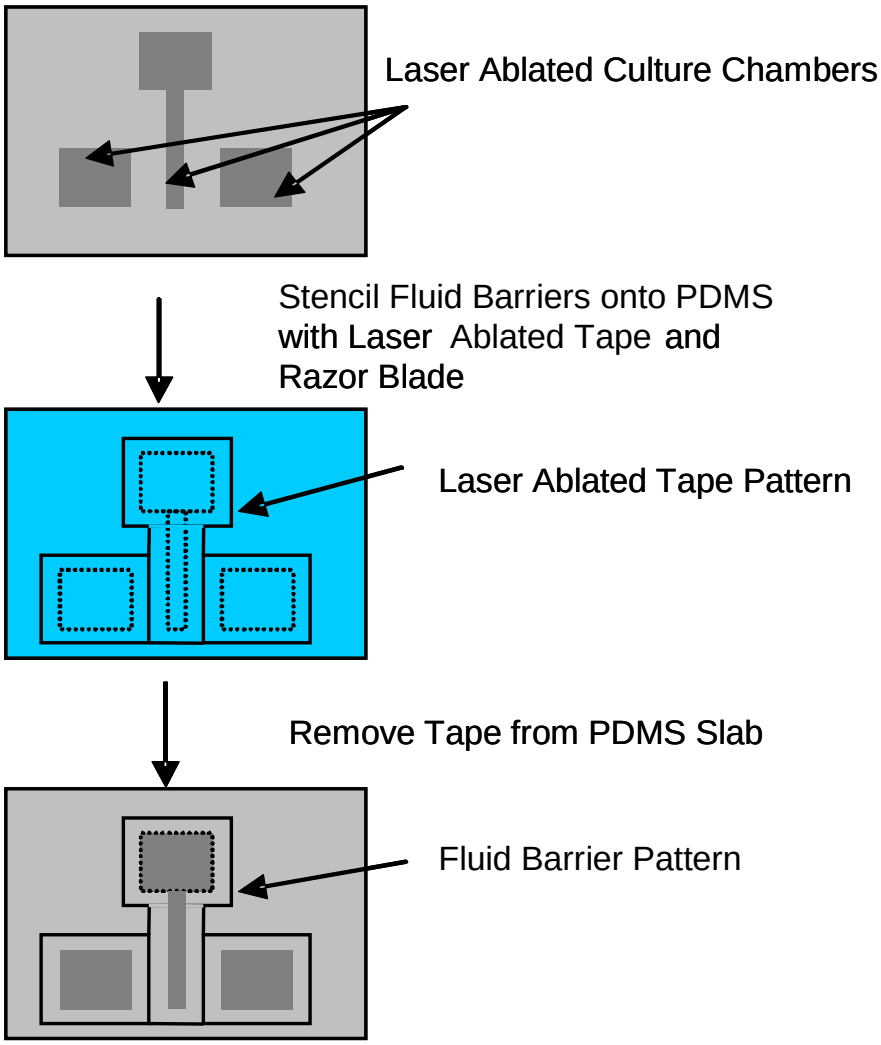

Figure 2.6. Process for stenciling fluid barriers onto a PDMS compartment divider.

the divider. Several problems were encountered when this technique was used. First, too much power caused the pattern to be much larger than intended on the stencil. While the CO_2 is good for high power applications, it is not good for producing fine features (<100μm). For this reason, we used the excimer laser. The laser was operated at a constant energy of 250mJ with 10 pulses/spot and 60 pulses/s. The excimer laser was used to cut an outline similar to the design used for the CO_2 laser. In both cases it was difficult to align the stencil to the PDMS compartment divider. A picture of stenciled grease barriers around the periphery of a single compartment is shown in Figure 2.7. In getting reproducible stenciled widths, it was important to align and seat the stencil properly around the compartment divider. A razor blade coated with Dow Corning silicone grease was used to brush it along the stencil. A second "raking" of the compartment divider was useful in removing grease from unnecessary areas and in lodging it firmly in the grooves of the stencil. The tape was then removed from the edge cleanly.

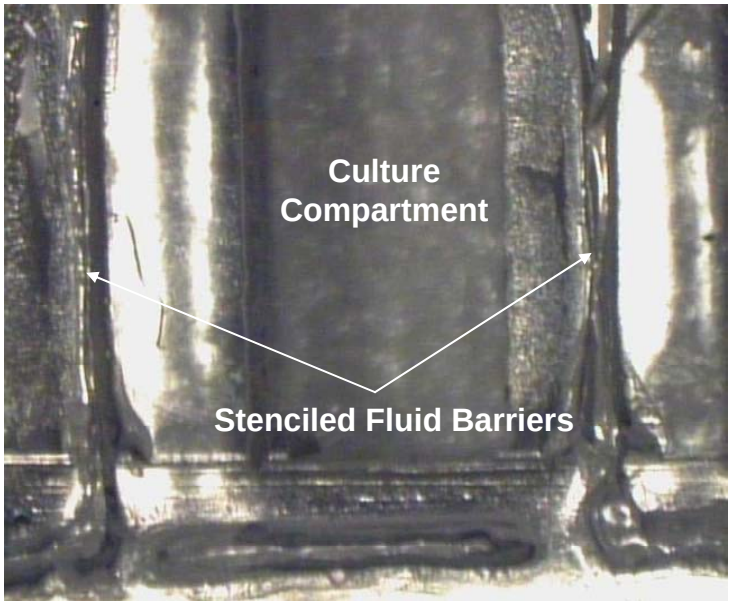

Figure 2.7. Stenciled fluid barriers on a compartment divider.

In an alternate approach, we tried placing a piece of tape directly on the compartment divider and laser ablating it directly. The advantage of this technique was to sidestep the issue of alignment that would come after creation of the stencil. However, it was very difficult to control the laser power parameters such that ablation stopped directly on top of the PDMS after it had gone through the adhesive. In almost all cases, the laser would ablate through part of the PDMS, causing damage to the divider. This was especially true for the CO_2 laser, which showed greater fluctuations in power delivered to the sample as it was ablating.

2.9. Design of the Compartment Divider Using Microstamping

In later designs, we tried experimenting with various ways of using the surface topography of the PDMS mold to micropattern silicone grease. In this way, alignment would take care of itself. In the initial designs, the mold itself was created using the AZ 4620 photoresist process described above. In the first of these designs, we had topography associated only with the area in between adjacent compartments. In later designs, the topography for stamping silicone grease was all the way around the compartment. Figure 2.8 shows the design of the final version of the divider that we created. This device was created from an SU-8 photoresist master. SU-8 was used because it can produce high aspect ratio features and because it is chemically durable after curing. The line widths for creating the compartment barriers in this picture are 300μm. Also, the culture compartments were 4mmX4mm. Smaller designs for the culture compartments did not work as well because they did not allow for an adequate amount of cell media to be contained in them.

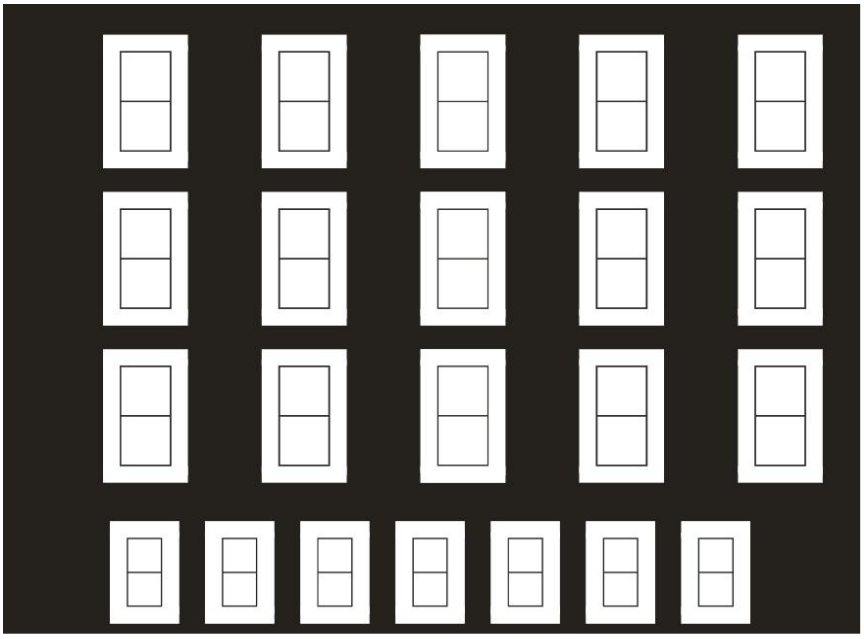

Figure 2.8. Mask design of a two compartment culture system assembled by stamping fluid barriers. Line widths for creating compartment barriers are 300μm. Only the larger designs at the top of the mask were used.

2.10. Fabrication of the Compartment Divider Using Microstamping

The fabrication strategy used with this technique is shown in Figure 2.9. Here, the PDMS divider would have raised and lowered portions created during the micromolding process. The laser ablated culture wells would be created around the topography. Grease would then be spread evenly on a glass slide using a razor blade and the divider would be brought into contact with it. It would be "stamped" only in those areas that were directly in contact with the glass slide. A slight amount of pressure was applied to the compartment divider as it was sitting on the grease-coated slide. Visual inspection under the glass slide verified the formation of contact between the slide and the divider. The divider was then removed from the slide with the use of forceps, leaving behind thin

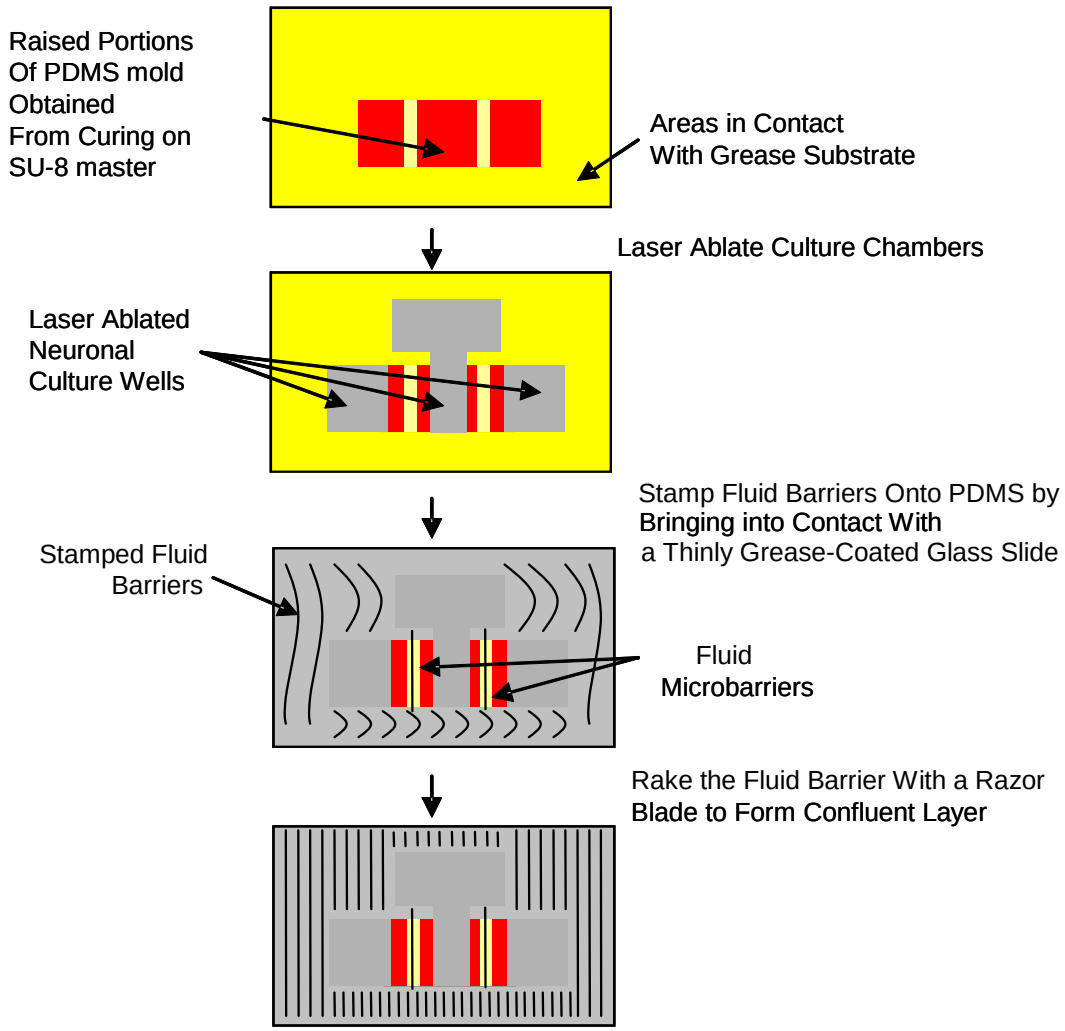

Figure 2.9. Process for stamping fluid barriers onto PDMS compartment divider.

silicone grease lines in those areas that were in contact with the slide. Figure 2.10 shows a fabricated divider with topography only at the barrier. Figure 2.10a shows silicone grease on the divider immediately after it has been removed from the slide. Figure 2.10b shows how the grease is evenly spread after lightly grazing the surface of the divider with a clean razor blade. Figure 2.10c is a zoomed-in view of a 100µm barrier coated with silicone grease.

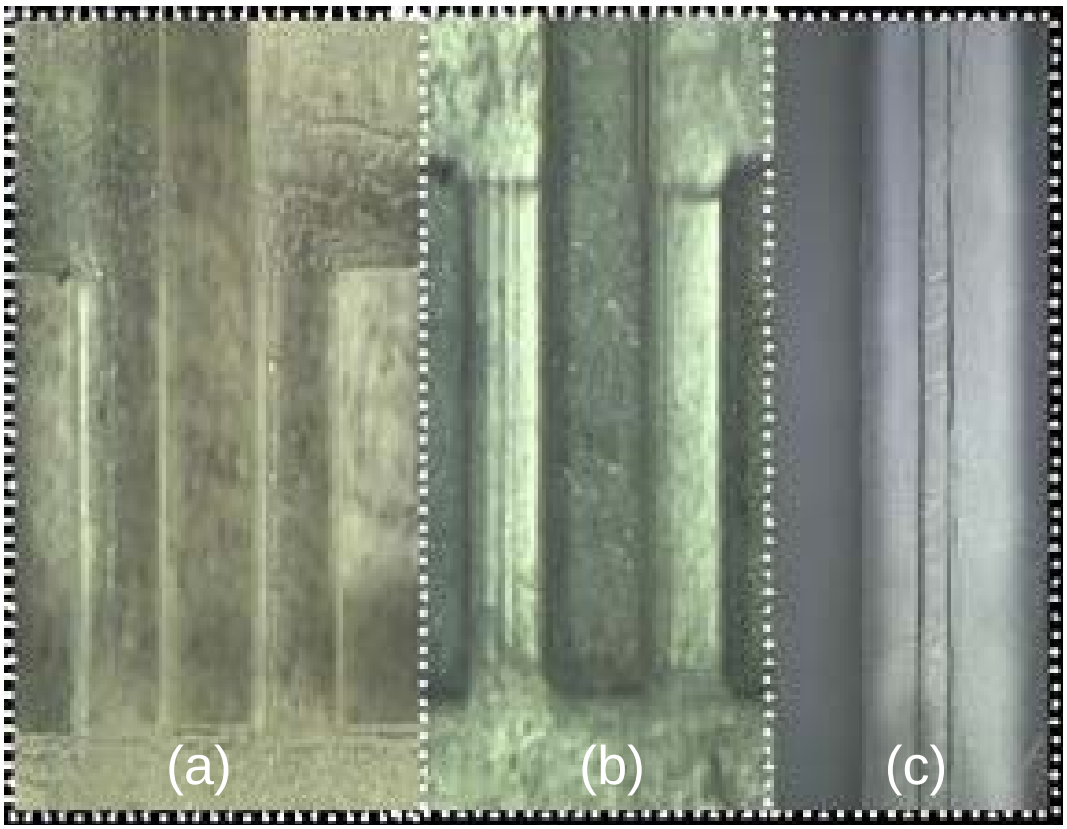

Figure 2.10. Stamped fluid barriers on a compartment divider with topography only between barriers. (a) PDMS divider right after stamping fluid barriers. (b) PDMS divider after raking the grease with a razor blade. (c) Zoomed-in view of one of the barriers.

As stated earlier, later designs used an SU 8 process that incorporated topography all the way around the PDMS divider. Here, SU 8 2100 was spun onto a 4in. Si wafer at 2100rpm for 30s on a spinner for a thickness of approximately 100µm. It was then

prebaked for 90min on a hotplate at 90°C. An OAI optical aligner was used to expose the photoresist with 400mJ/cm^2 of UV light. Finally, the photoresist was postbaked for 1 hour at 100°C. The wafer was developed using SU 8 photoresist developer (Microchem Corp.). The wafer was placed in the developer on a hotplate with a magnetic stirrer. A stirbar was rotated at 400rpm during the 20 minute develop process to fully remove all of the photoresist from the wafer. When the stirbar was not used, incomplete and uneven development resulted. Next, the finished master was seated in a Petri dish and PDMS (Sylgard 184 elastomer kit, 10:1 ratio of elastomer to curing agent) was poured onto the master for approximately 3mm thickness. The PDMS was cured on a hotplate for 1hr at 100°C. The mold was then peeled off of the master and ports were laser ablated in the PDMS using a CO_2 laser (see Figure 2.11). Debris was removed from the ablated area through ultrasonic agitation followed by a nitrogen blow dry. Patterning the divider shown in Figure 2.11 with silicone grease proceeded in a very straightforward manner. The divider was brought into contact with the glass slide as discussed earlier. Upon removing it with forceps, the periphery of the ports would be coated with silicone grease, creating a pattern that would completely enclose the ports when the divider was seated for later use in culture.

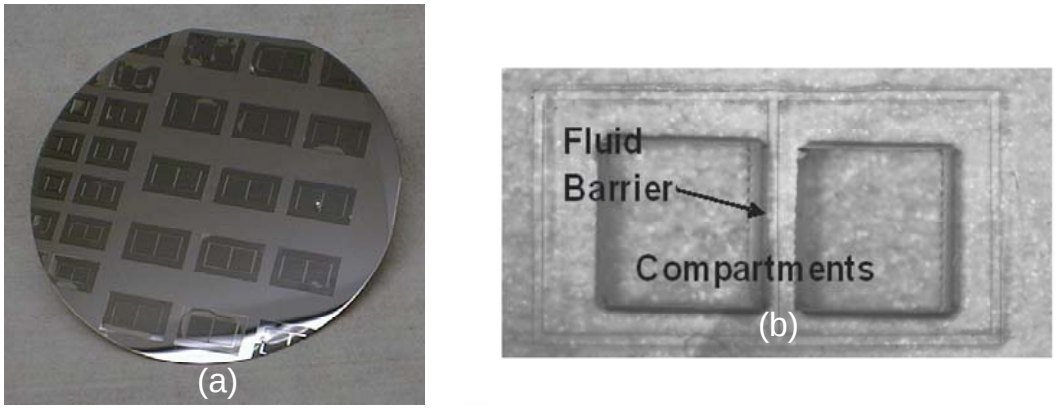

Figure 2.11. (a) Silicon master depicting microtopography for the compartment divider. The designs on the left are smaller versions of the ones on the right. (b) PDMS two-compartment divider. Ports are again laser ablated and are 4mmX4mm. The microtopography surrounding the ports is 200µm wide and 100µm high. This topography is used to micropattern fluid barriers and create a fluidic barrier that allows neurons to cross but does not allow drugs to pass through it. The collagen patterning mold is bonded to a glass substrate and liquid rat tail collagen is incubated in the channels and allowed to adsorb onto the substrate. It is then removed and the compartment divider is aligned to and assembled on top of the substrate.

2.11. Design of the Chemical Patterning Mold

Initially, the chemical patterning of the substrate was envisioned to be part of the process in making the compartment divider. The neurite tracks of the initial designs in which silicone grease was pushed through a microchannel would serve the dual purpose of selective patterning the surface with collagen. Here, collagen would be injected into the ports and channels prior to plating neurons. However, since we were not able to repeatably inject silicone grease into the microchannels of these early designs, we abandoned the associated approach for patterning collagen. Instead, we adopted an approach in which the collagen would be patterned separately, without the aid of the compartment divider. Figure 2.12 shows the design of the chemical patterning mold that was created. Here, the channels and spaces are 200µm wide and 10mm long. We selected these channels widths to match the widths of the growth tracks in traditional Campenot chambers.

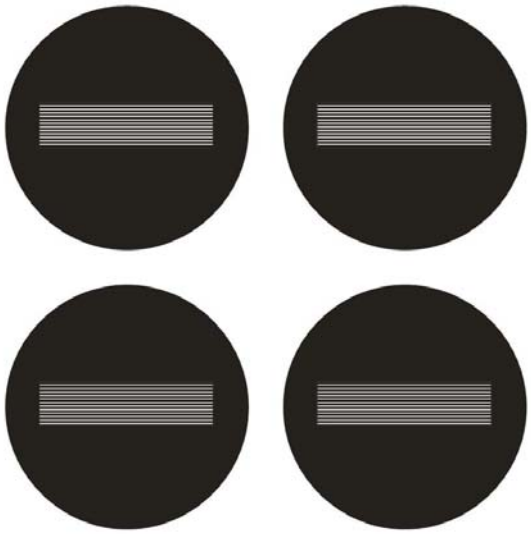

Figure 2.12. Mask design of the collagen patterning mold. Lines in the center of the four circles represent the channels for patterning collagen.

2.12. Fabrication of the Chemical Patterning Mold

It was created using the SU 8 process discussed above for creating the compartment divider. Channels were 200µm wide with 200µm spaces. The length of the channels was 20mm and the width of 10 adjacent channels was 4mm. A 3mm diameter port was ablated at one end of the mold to serve as the outlet port (this fits the tip of a conventional 5cc syringe from Becton Dickinson). The inlet port was 4mmX2mm to span the width of all the channels combined (see Figure 2.13).

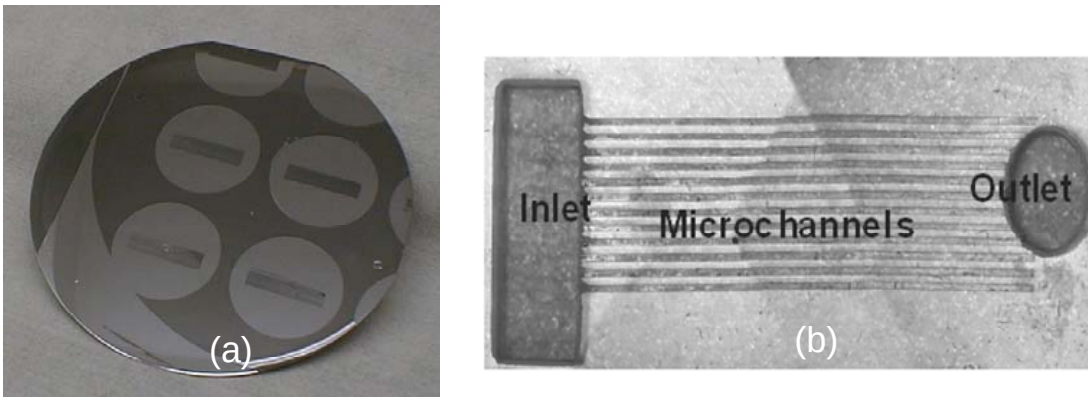

Figure 2.13. (a) Silicon master depicting four identical designs for creating the collagen patterning mold. (b) PDMS collagen patterning mold. Microchannels are 200µm wide and 20mm long. Inlet and outlet ports are laser ablated. The microchannels connecting the two ports serve to pattern the substrate with collagen.

Collagen could be patterned with this mold by injecting it through the channels and allowing it to dry inside. Also, the mold could be inked with collagen and the pattern could be stamped onto the glass slide. With the first technique, the inlet port was filled with collagen and it was drawn through the channels to the outlet port. An optimal incubation time was also developed, after which excess collagen was aspirated out of the channels. With the second technique, the mold was brought into contact with a thin layer

of collagen spread across a glass coverslip. Pressure was applied with a C-clamp to bring the mold into tight contact with the coverslip. After 10 minutes, the mold was removed from the C-clamp and seated on another sterile coverslip. Again, it was clamped to the coverslip for 10 minutes during which time the collagen adsorbed on the mold was allowed to adsorb onto the coverslip.

2.13. Design of the Multielectrode Array Substrate

Designs were created using AUTOCAD and transferred to a mask using a pattern generator. The designs for two fabricated MEAs are shown in Figures 2.14 and 2.15. The first MEA design includes three serpentine stimulation electrodes, one ground electrode, and 56 recording electrodes. This design was made so that most of the stimulation electrodes would be in one compartment and the recording electrodes would be in the adjacent one. In the second design (Figure 2.15), all of the electrodes are the same size. They are divided into four quandrants with a ground electrode in the center.

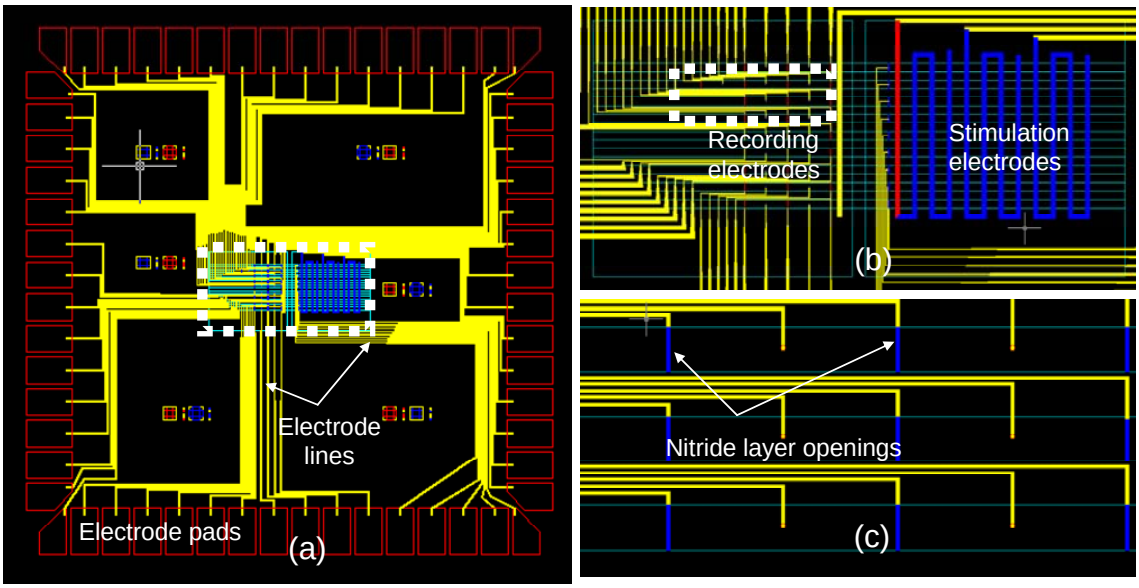

Figure 2.14. Mask design of MEA substrate in AUTOCAD. (a) Entire design of the substrate. The squares on the periphery are the electrode pads. lines starting at the pads are electrode lines. (b) Zoomed-in area of dashed square in a. Lines at the right are serpentine stimulation electrodes. (c) Zoomed-in area of dashed square in b.

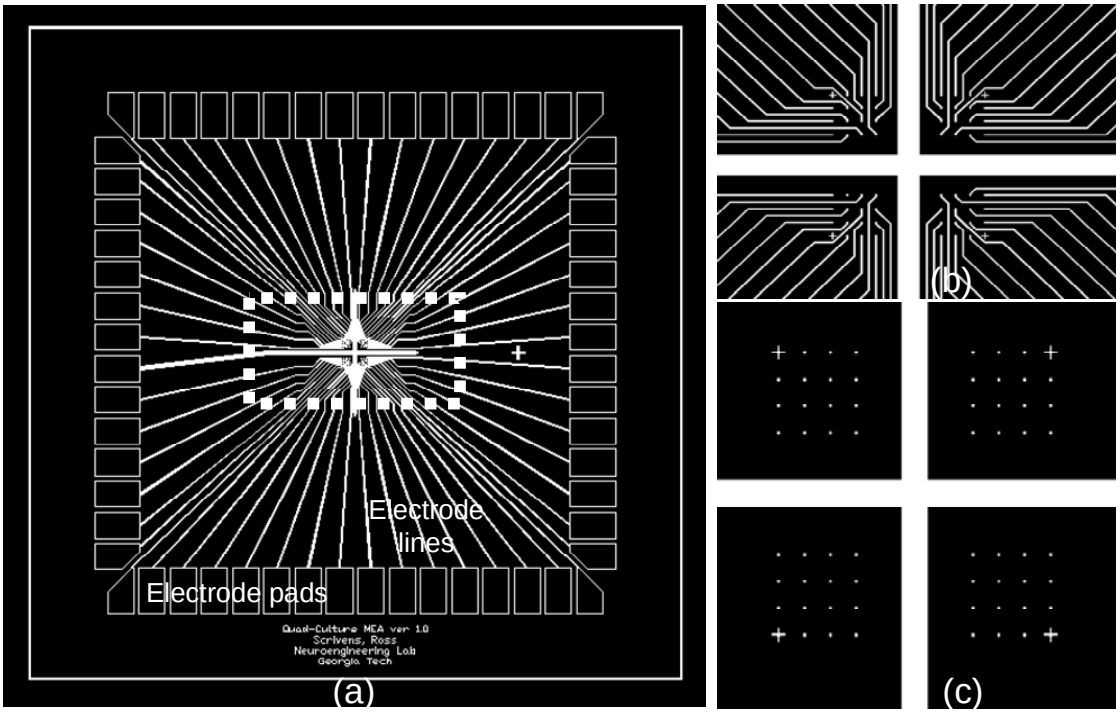

Figure 2.15. Mask design of second MEA substrate in AUTOCAD. (a) Entire design of the substrate. The squares on the periphery are the electrode pads. (b) Zoomed-in area of dashed square in a. (c) Mask for nitride openings that become aligned to the mask in a.

2.14. Fabrication of the Multielectrode Array Substrate

The fabrication process for making the MEAs is shown in Figure 2.16. The multielectrode array (MEA) was fabricated on a glass substrate. A plain borosilicate glass slide was cut to 49mmX49mm. Then metal was patterned on the slide. A DC sputterer was used to deposit 450Å of titanium followed by 2500Å of gold. Then Shipley 1813 photoresist was spun at 2000rpm for 30s and prebaked for 90s in an oven at 95°C. The substrate was exposed for 4s under an OAI Optical Aligner. The resist was developed in MF 354 developer for 10s. The underlying gold was etched for 30s using a potassium iodide solution and the titanium was etched using a 1% hydrofluoric acid solution to pattern metal in the shape of the electrodes. The substrates were rinsed with DI water and silicon nitride was deposited on them using a Plasmatherm PECVD. The deposition parameters were 40W power, 3sccm of NH_3, 300sccm of SiH_4, 900sccm of N_2 with a chamber pressure of 900mTorr. Approximately 1µm of silicon nitride was deposited onto the substrate.

The nitride was then patterned using photoresist. If positive photoresist was used, Shipley 1813 photoresist was spun at 2000rpm for 30s and prebaked for 90s in an oven at 95°C. The substrate is then exposed for 4s after alignment using the OAI Optical Aligner. Finally, the resist is developed in MF 354 for 10s. If negative resist was used, Futurrex NR-3000P was spun at 2000rpm for 30s and prebaked for 45min on a hotplate with ramp down at 95°C. The optical aligner was then used to expose the photoresist for 8s. The substrate was postbaked for 60min at 100°C on a hotplate with ramp down. Finally, the photoresist was developed in RD6 developer for 40s. Once patterned, the nitride was etched using the PlasmaTherm reactive ion etcher (RIE). The etch parameters

were 140W power, 13.9sccm of SF_6 and a chamber pressure of 100mTorr. The substrate was etched for 20min in the RIE. Finally, the photoresist was removed in an acetone, isopropanol, and DI water soak and dried.

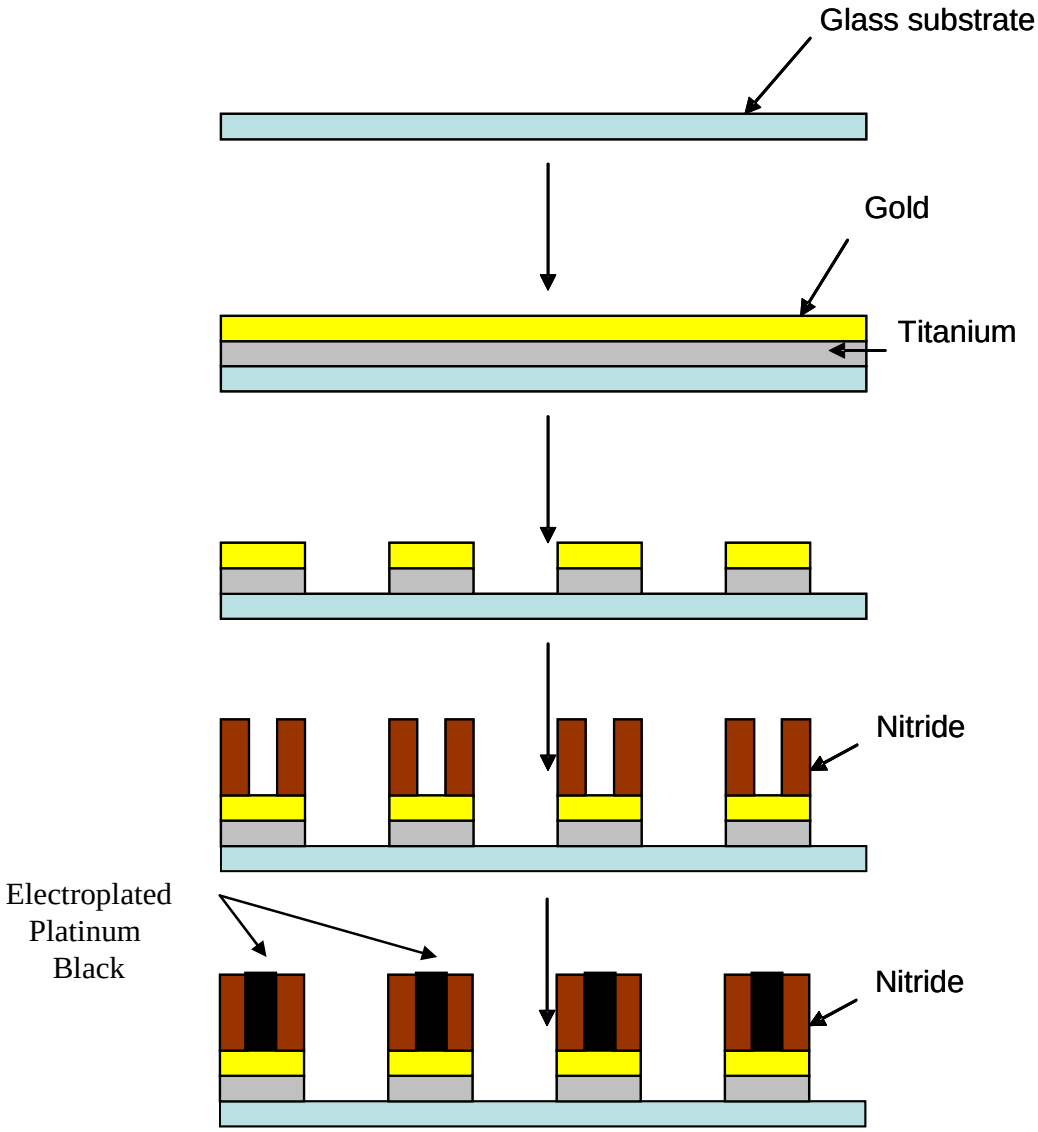

Figure 2.16. Process for making MEAs.

After this cleanroom process, a plastic ring was bonded to the substrate with PDMS. This plastic ring was approximately 25mm in diameter and was seated on the MEA substrate by inking the ring with uncured PDMS (Sylgard 184) and applying pressure to the system by placing a weight on it. The ring and weight remained on the MEA overnight as the PDMS cured. Finally, the weight was removed and the system was ready for electroplating with platinum black. The solution used for electroplating platinum black was 1% chloroplatinic acid (Sigma), 0.0025% hydrochloric acid, and 0.01% lead acetate in water. Platinum black was closen because it lowers the impedance of the electroplated electrodes, thereby increasing the signals recorded from the plated neurons. The impedance is lowered since platinum black increases the surface area of the electrodes by making the surface granular. Platinum black was electroplated using a multimeter to measure the voltage drop across the electrode as it was being plated. Electroplating was stopped once the voltage reached a minimum. This happened approximately 3-5 minutes after the plating was started for each electrode. A picture of the device used for controlling the electroplating is shown in Figure 2.17 and a picture of an electrode before and after electroplating is shown in Figure 2.18.

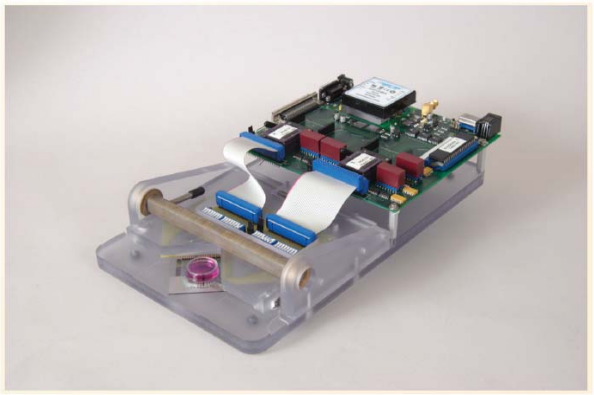

Figure 2.17. Device for electroplating platinum black onto multielectrode array.

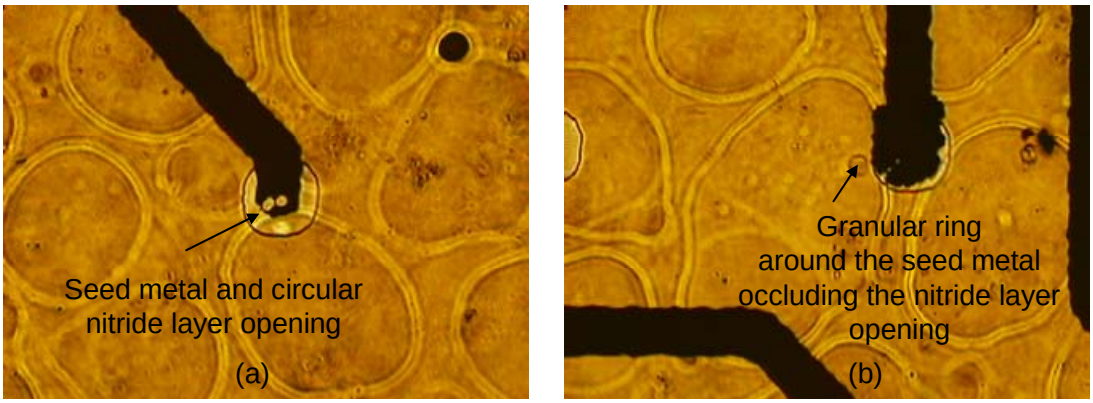

Figure 2.18. A single MEA electrode (a) before and (b) after electroplating with platinum black. Notice that the electrode on the right has a granular ring around the seed metal.

In the assembled system, the MEA substrate was hand aligned to the collagen patterning mold. Once patterned, this mold was removed and the compartment divider was hand aligned to it. Figure 2.19 shows the complete assembled system with one of the MEA designs. Figure 2.20 shows a close up view of an MEA with the design shown in Figure 2.15. Both substrates were used in the culture studies, but only the one shown in Figure 2.20 was used in the electrophysiology studies.

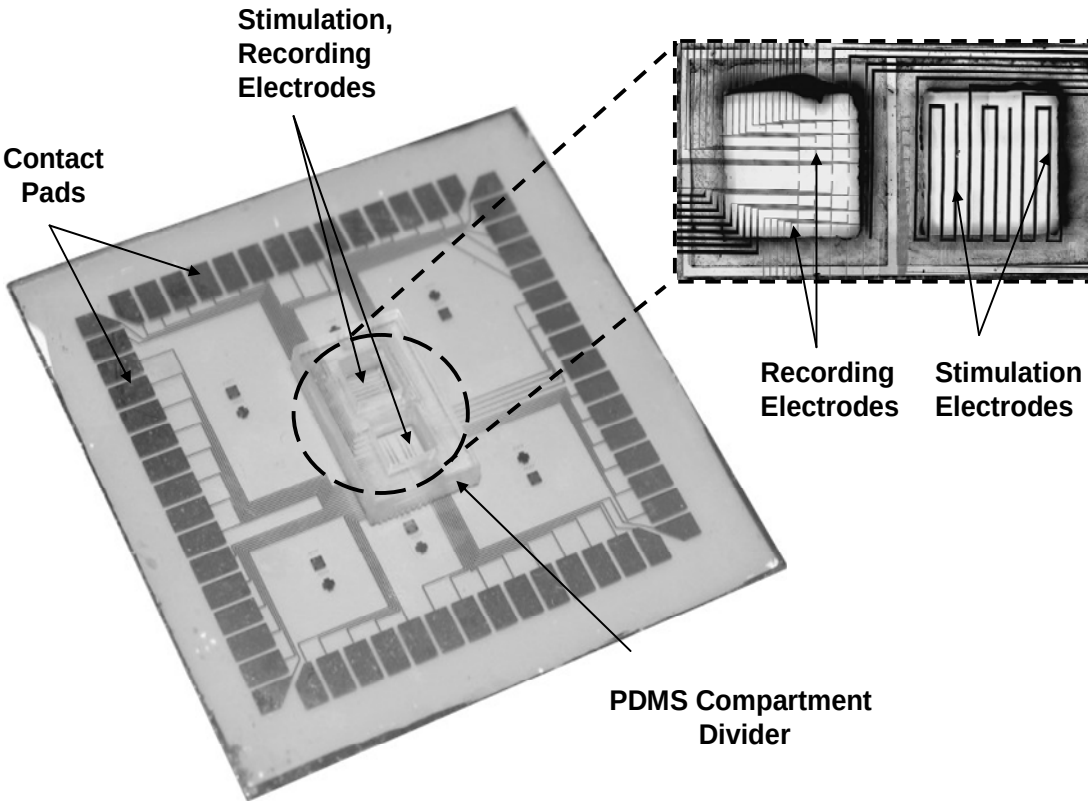

Figure 2.19. Assembled compartmented culture system. The microelectrode array (MEA) is fabricated using conventional semiconductor technology. The PDMS compartment divider is patterned with fluid barriers and aligned to the electrode design on the MEA substrate. Inset shows a close-up of the dashed area with all of the stimulation and recording points exposed in the nitride insulating layer.

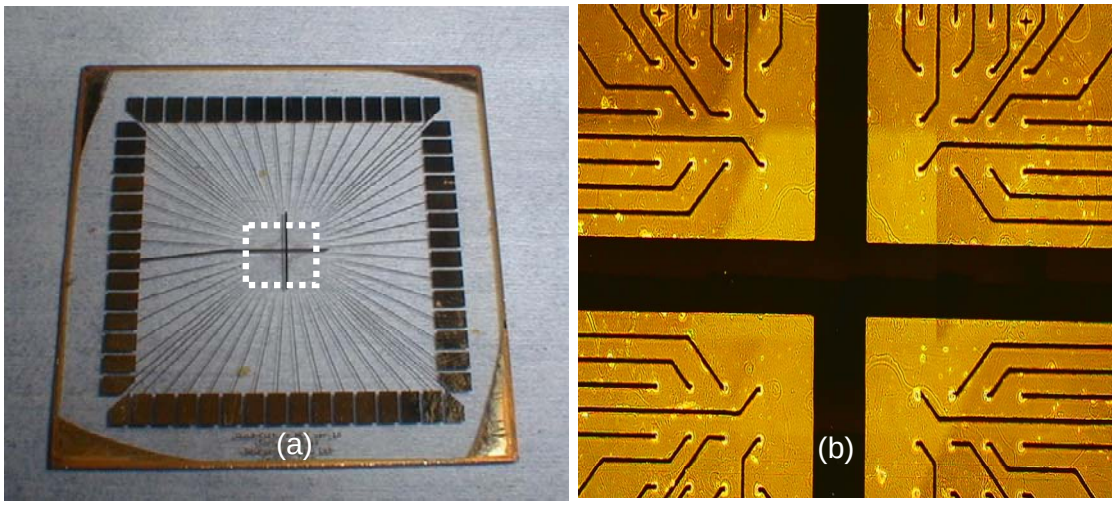

Figure 2.20. Alternate MEA design. (a) Fabricated electrode array with pads on the periphery. (b) Zoomed-in view of the dashed area shown in a. The thick electrode in the center is the ground electrode.

2.15. References

[1] E. Verpoorte and N. d. Rooij, "Microfluidics meets MEMs," *Proceedings of the IEEE*, vol. 91, pp. 930-953, 2003.

[2] X. Wu, Y. Zhao, Y. Yoon, S. Choi, J. Park, and M. G. Allen, "Wafer-scale micromolding of unitary polymeric microstructures with simultaneously formed functional metal surface," presented at Microtas, Boston, MA, 2005.

[3] P. C. Letourneau, "Cell-to-substratum adhesion and guidance of axonal elongation," *Developmental Biology*, vol. 44, pp. 92-101, 1975.

[4] J. A. Hammarback, J. B. McCarthy, S. L. Palm, L. T. Furcht, and P. C. Letourneau, "Growth cone guidance by substrate-bound laminin pathways is correlated with neuron-to-pathway adhesivity," *Developmental Biology*, vol. 126, pp. 29-39, 1988.

[5] J. M. Corey, B. C. Wheeler, and G. J. Brewer, "Compliance of hippocampal neurons to patterned substrate networks," *Journal of Neuroscience Research*, vol. 30, pp. 300-07, 1991.

[6] R. D. Fields, C. Yu, and P. G. Nelson, "Calcium, network activity, and the role of NMDA channels in synaptic plasticity *in vitro*," *Journal of Neuroscience*, vol. 11, pp. 134-46, 1991.

[7] A. S. Curtis and P. Clark, "The effect of topographic and mechanical properties of materials on cell behavior," *Critical Reviews of Biocomputing*, vol. 5, pp. 343-362, 1990.

[8] S. Britland, C. Perridge, M. Denyer, A. Curtis, and C. Wilkinson, "Morphogenetic guidance cues can interact synergestically and hierarchically in steering nerve cell growth," *Experimental Biology Online*, vol. 1, 1996.

[9] B. Lom, K. E. Healy, and P. E. Hockberger, "A versatile technique for patterning biomolecules onto glass coverslips," *Journal of Neuroscience Methods*, vol. 50, pp. 385-397, 1993.

[10] S. N. Bhatia, M. L. Yarmush, and M. Toner, "Controlling cell interactions by micropatterning in cocultures: hepatocytes and 3T3 fibroblasts," *Journal of Biomedical Materials Research*, vol. 34, pp. 189-199, 1997.

[11] G. P. Lopez, M. W. Albers, S. L. Schreiber, R. Carroll, E. Peralta, and G. M. Whitesides, "Convenient methods for patterning the adhesion of mammalian cells to surfaces using self-assembled monolayers of alkanethiolates on gold," *Journal of the American Chemical Society*, vol. 115, pp. 5877-5878, 1993.

[12] R. Singhvi, A. Kumar, G. P. Lopez, G. N. Stephanopolous, D. I. C. Wang, G. M. Whitesides, and D. E. Ingber, "Engineering cell shape and function," *Science*, vol. 264, pp. 696-698, 1994.

[13] J. C. Chang, G. J. Brewer, and B. C. Wheeler, "A modified microstamping technique enhances polylysine transfer and neuronal cell patterning," *Biomaterials*, vol. 24, pp. 2863-2870, 2003.

[14] J. Buitenweg, W. L. C. Rutten, E. Marani, S. K. L. Polman, and J. Ursum, "Extracellular detection of active membrane currents in the neuron-electrode interface," *Journal of Neuroscience Methods*, vol. 115, pp. 211-221, 2002.

[15] L. J. Breckenridge, R. J. A. Wilson, P. Connolly, A. S. G. Curtis, J. A. T. Dow, S. E. Blackshaw, and C. D. W. Wilkinson, "Advantages of using microfabricated

extracellular electrodes for in vitro neuronal recording," *Journal of Neuroscience Research*, vol. 42, pp. 266276, 1995.

CHAPTER 3

CHARACTERIZATION OF THE ENGINEERED SYSTEM

3.1. Chapter Outline

This chapter characterizes the system designed and fabricated in Chapter 2. Sections 3.2 and 3.3 characterize the collagen patterning mold. Sections 3.4 and 3.5 characterize the microfluidic compartment divider. Finally, section 3.6 characterizes the MEA substrate and section 3.7 outlines the different pilot studies that were performed with the system.

3.2. Characterization of the Collagen Patterning Mold

The collagen patterning mold was characterized both from the perspective of how it met design specifications and from the perspective of how it performed its function. Below is a discussion of each of these issues.

3.2.1. Characterization of Fabrication

As detailed in Chapter 2, the collagen patterning mold was developed using soft lithography. Critical features here were the channels and the spaces that were between them. As designed, the channels were 200μm wide and the spaces were 200μm wide. The total thickness of the SU 8 photoresist master was 100μm. At such thicknesses, it was very critical that the photoresist was completely developed. Otherwise, the channels and spaces would only be partially molded (see Figure 3.1). Therefore, it was very critical to use a stirbar when developing the photoresist for the full 20 minute develop

time. When this was done, the channels were molded to good precision, with their widths being between 190-210μm. Moreover, the ports that were ablated with the CO_2 laser easily went through the PDMS and generated very little debris. Some damage was made to the edges of the ablated ports; however, it was not significant enough to affect device performance (see Figure 3.2). Moreover, the PDMS mold was extremely resistant to wear through multiple iterations of washing with solvents like ethanol and water. However, the collagen that we used was extremely sticky and would clog the channels upon multiple uses (see Figure 3.3). Therefore, a detergent (Liquinox, Alconox, Inc.) was used to get as much of it off as possible after each use.

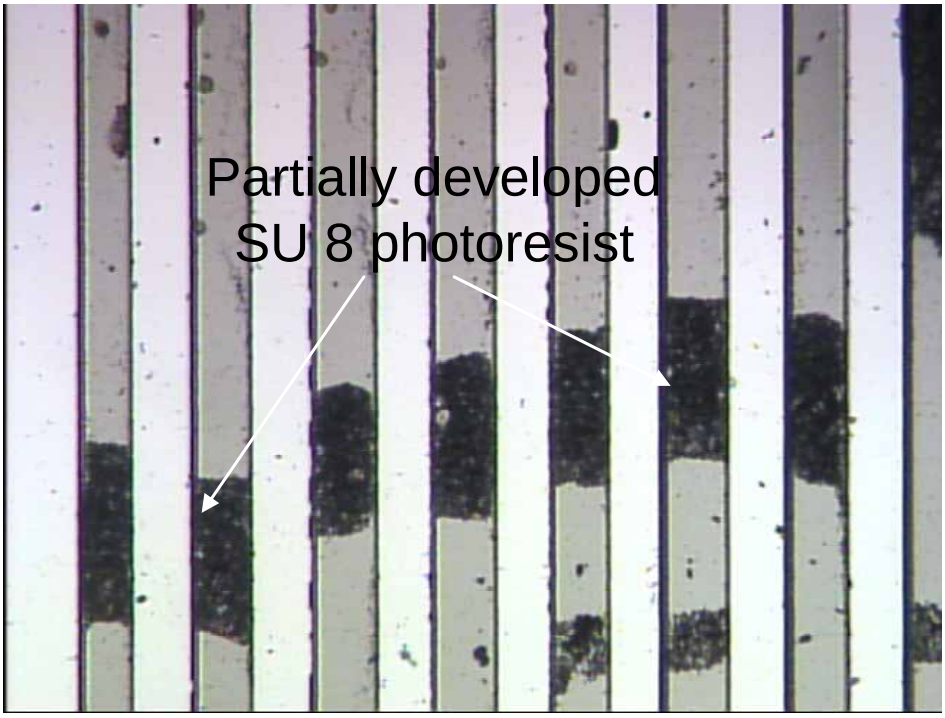

Figure 3.1. SU-8 in between channels due to incomplete develop.

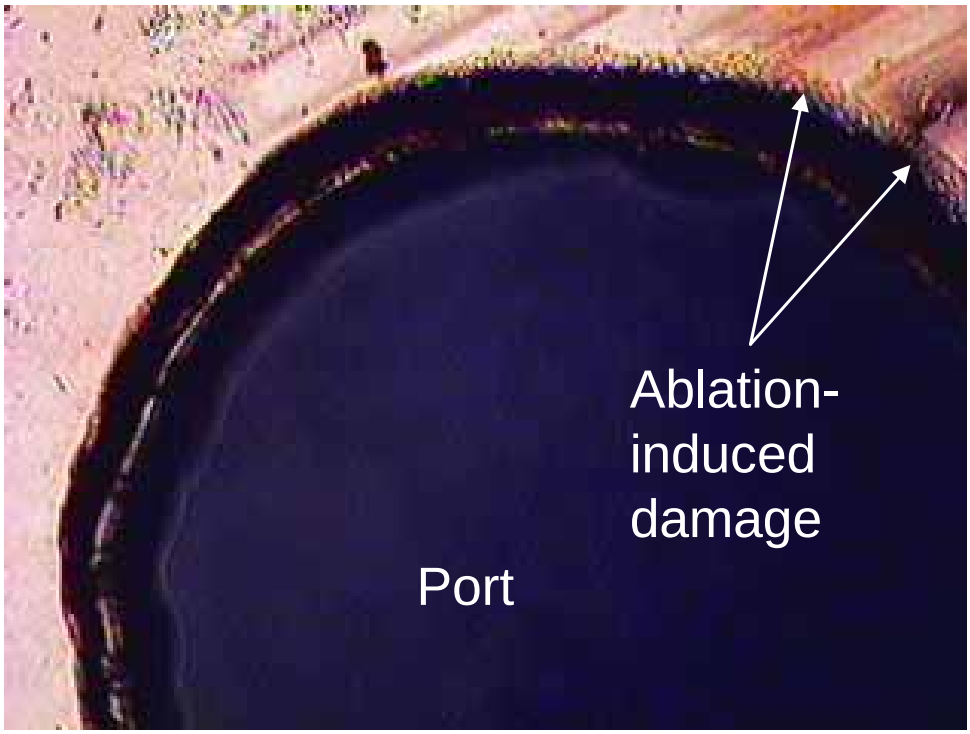

Figure 3.2. Damage around port for collagen patterning mold (not very significant to affect device performance).

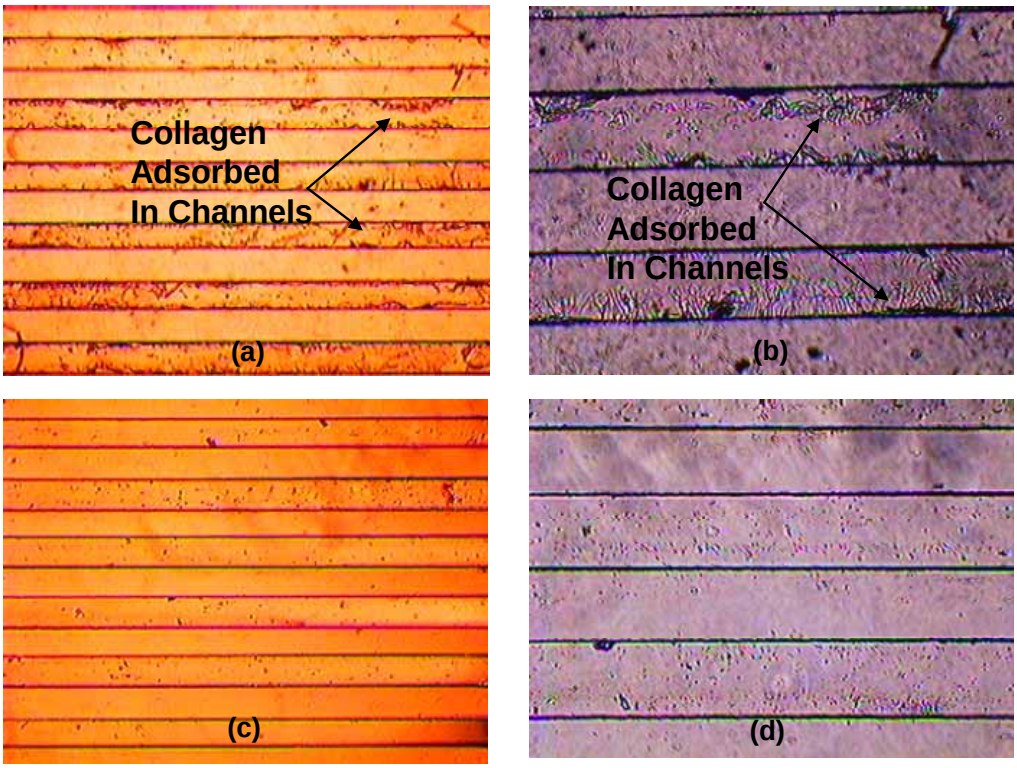

Figure 3.3. Collagen adsorbed onto the surface of the patterning mold. Notice how the channels in a and b have dried collagen residue. The pictures in c and d show a pristine unused patterning mold.

3.2.2. Characterization of Functionality

The collagen patterning mold was characterized for its ability to faithfully register patterned lines on a substrate. Three techniques were used to do this (see Figure 3.4). In the first technique the mold was seated on a plastic or glass substrate and pressure was applied to the mold to form a reversible spontaneous bond between the PDMS and the substrate. Then type 1 rat tail collagen (BD Biosciences) was injected with a conventional plastic syringe from the input port to the output port.

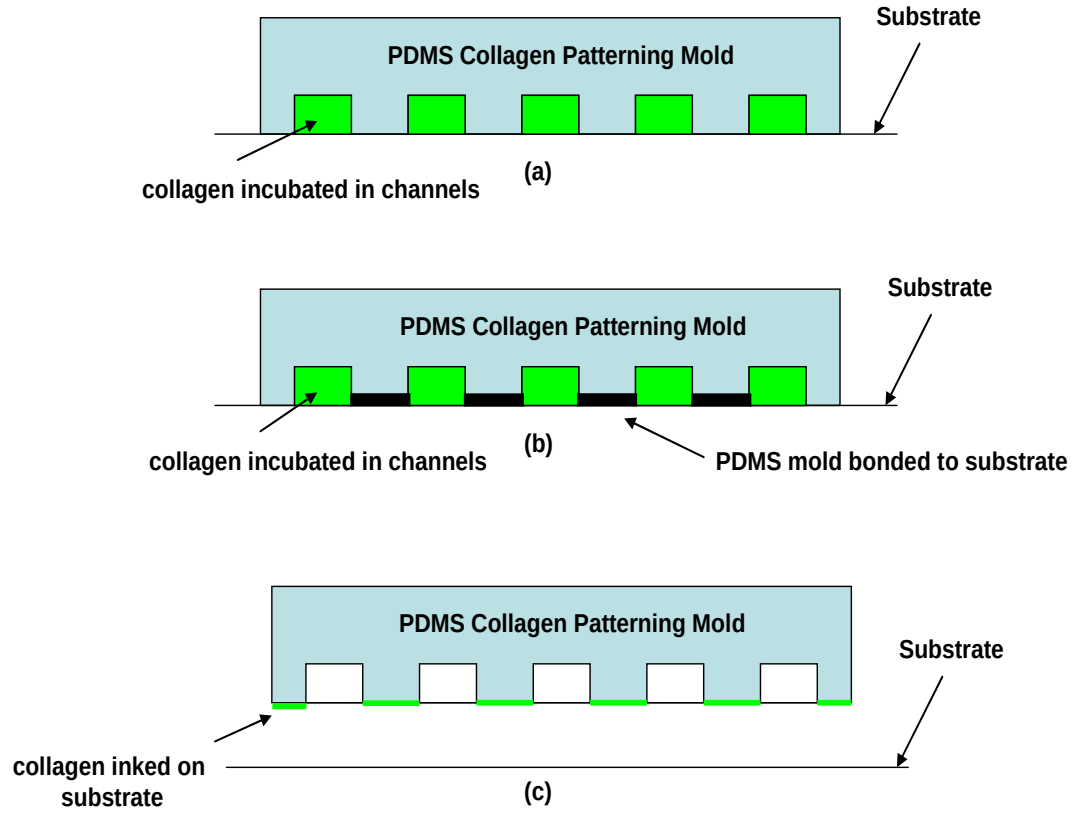

Figure 3.4. Three different techniques for patterning collagen on a glass/plastic substrate. (a) With the first technique, the mold is brought into contact with the substrate and pressed up against it. Collagen is then delivered in the channels. (b) With the second technique, the mold is bonded to the substrate by inking uncured PDMS. (c) With the third technique, a mold functionalized with collagen is brought into contact with the slide and clamped onto it.

The collagen was incubated in the channels for varying periods of time, anywhere from 10 min to overnight (12hrs). The incubation of the collagen was varied because incubation for too long a time resulted in flaking and peeling of the patterned lines due to too much surface adsorption. The time that produced consistent reliable patterns was 20mins in the channels, followed by removal of the mold and an air dry overnight in the incubator (see Figure 3.5).

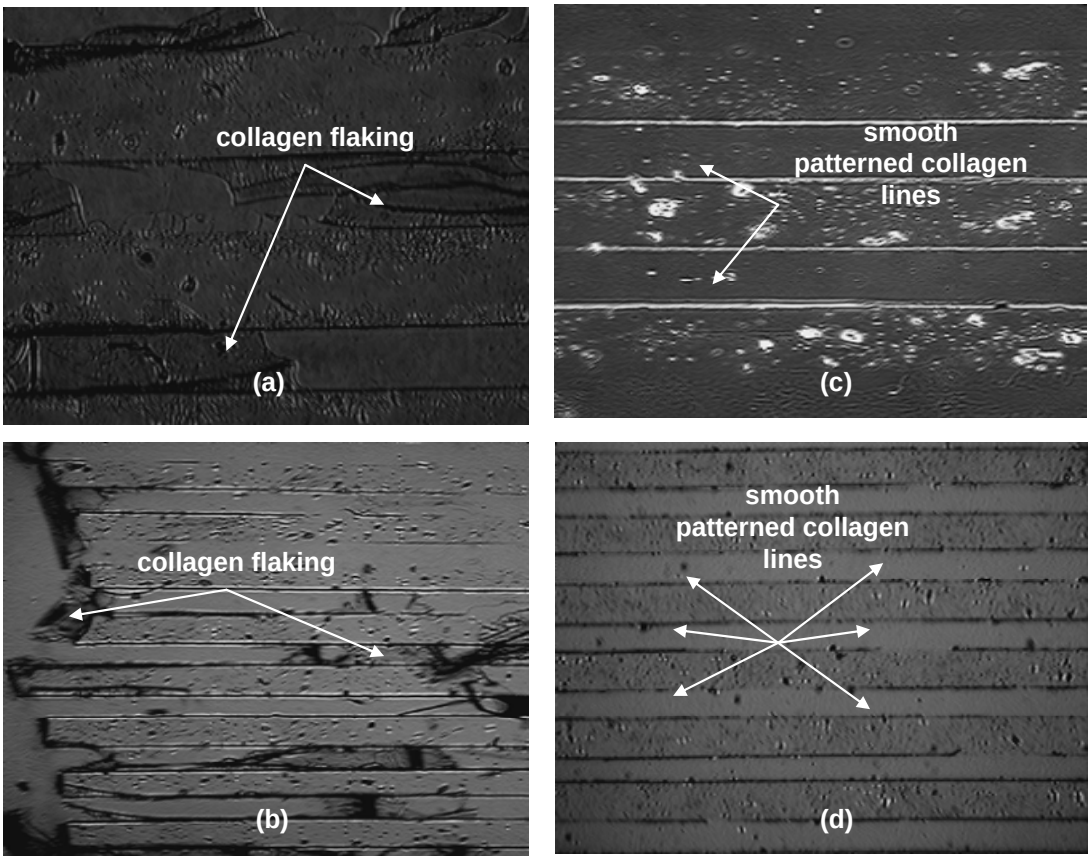

Figure 3.5. Examples of too much (a,b) and just the right amount (c,d) of collagen adsorbed onto a planar surface.

In the second technique, we bonded the collagen patterning mold to the substrate by inking a thin layer of uncured PDMS to the mold and seating the mold onto the substrate. The mold was ramped slowly from room temperature to 100°C on a hot plate

to ensure that the PDMS was fully cured. Then the collagen was injected into the channels in a manner similar to that in the first technique. This technique allowed us to more faithfully register the collagen pattern on the substrate, since there was less likelihood of the collagen seeping in between the channels.

In the third technique, a thin layer of collagen was spread across a sterile glass slide. The collagen patterning mold was then brought into contact with the slide and clamped onto it with a C-clamp. This configuration was held for 10 minutes. Then the clamp and mold were removed from the slide; the mold was then seated carefully onto a fresh glass or plastic substrate and clamped onto it. This configuration was again held for 10 minutes. During this time, the wet collagen that had adsorbed onto the mold during the first step was selectively adsorbed onto the second substrate. One of the problems associated with this technique was that when the mold was clamped onto the fresh substrate in the final step, some of the collagen would seep out of the mold and cause the pattern to not be as clean as we would have liked it to be. To minimize this effect, the mold was clamped to the substrate as lightly as possible.

3.3. Immunofluorescence of the Collagen Substrate

To better assess the collagen pattern adsorbed onto the substrate, we performed an immunofluorescenent stain of the protein. To do this, we had to fix the substrate with a 4% solution of paraformaldehyde in water for 15 minutes. Then the substrate was rinsed three times with PBS for 10 minutes. The substrate was then incubated in blocking buffer (5% goat serum, 1% bovine serum albumin (BSA), 0.05% TX100 in PBS) at room temperature for 60 minutes. Finally, it was washed with wash buffer (5% goat serum, 1%

BSA in PBS) two times for 10 minutes each. Then the primary antibody (at a diluton of 1:500) was placed in the blocking buffer overnight. After the overnight treatment, the sample was rinsed with PBS and was incubated with the secondary antibody (at a dilution of 1:1000) in blocking buffer at room temperature for 1hour. Finally, the sample was viewed under a fluorescent microscope.

Unfortunately, we were not able to obtain clear images of the fluorescently labeled collagen substrates. The collagen showed up only in those areas where it had readily accumulated (at the inlet and at the outlet ports). The staining in the channels was light and inconsistent. Increasing the concentration of the primary antibody in the blocking buffer did not seem to help. Therefore, we hypothesized that the adsorption of the collagen in the channels was not uniform and tended to vary greatly.

3.4. Characterization of the Microfluidic Compartment Divider Using Microstamping

The microfluidic compartment divider was characterized both from the perspective of how it met design specifications and from the perspective of how it performed its function. Below is a discussion of each of these issues.

3.4.1. Characterization of Fabrication

Issues similar to the ones that arose with the collagen patterning mold arose with the compartment divider. Here, the minimum feature sizes were 100μm microfluidic barriers. These barriers were again created with an SU 8 photoresist master (thickness=100μm). Again, use of a stirbar to ensure that these features were fully

developed was important in producing the barriers in the mold. The minimum feature sizes varied from 90µm to 110µm. As was the case with the SU 8 masters for some of the other components, repeated use of the master caused delamination from the substrate (see Figure 3.6). Moreover, the compartment divider was thicker than the collagen patterning mold (thickness of about 3-4mm). Therefore, higher power settings were needed on the CO_2 laser to ablate through the entire material (see Figure 3.7). As a result, there was more damage around the edges of the ablated areas. This part also stood up well to repeated washes with ethanol and water when preparing for cell culture. Cleaning it repeatedly did, however, reduce the optical transparency of the PDMS and resulted in pictures of neurons that were not as clear.

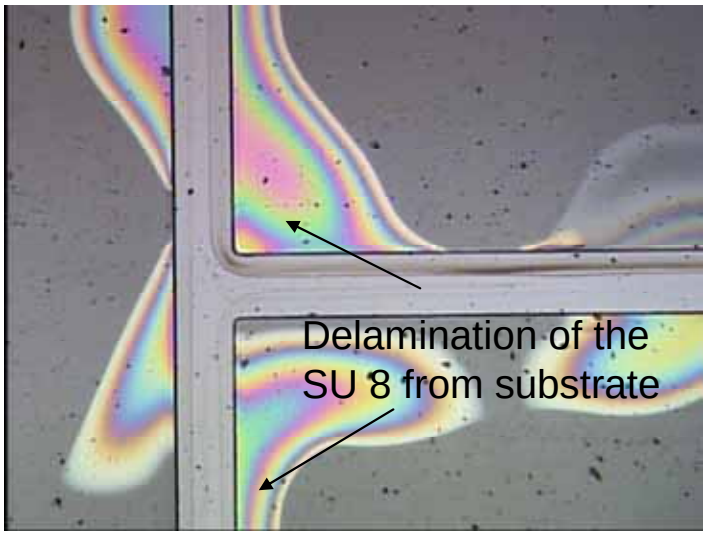

Figure 3.6. Delamination of the SU-8 master due to repetitive use.

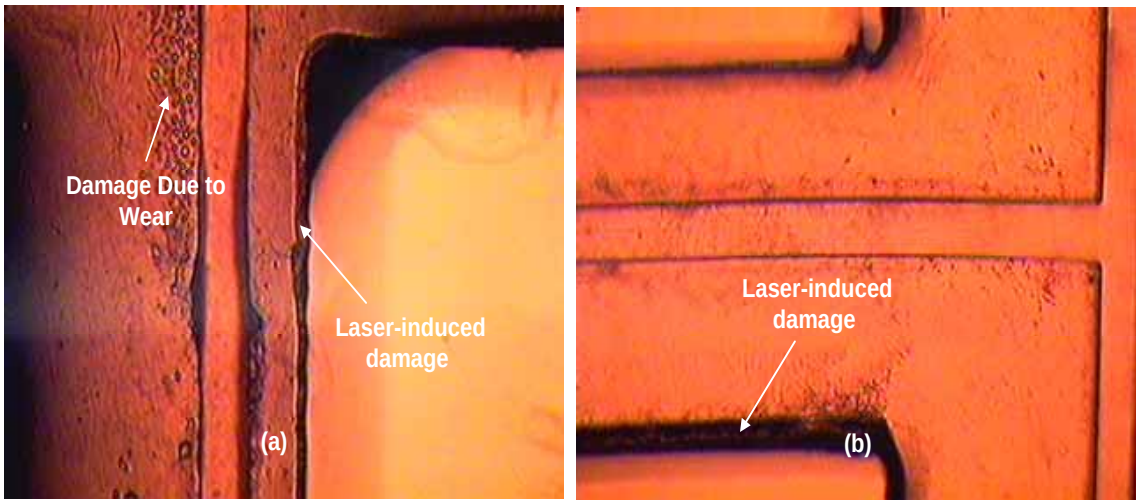

Figure 3.7. (a) Part of a compartment divider damaged due to wear and through the laser. (b) Part of a compartment divider before use.

On the devices that had topography only associated with the barrier between the compartments, leakage was a constant issue since more grease was stamped around the periphery of these dividers than in the center between compartments. To minimize this effect, we attempted to cut the mold around the periphery to make the distance between the edge of the compartment and the edge of the mold as small as possible. However, we were not able to cut the mold so precisely as to match the 200µm width of the barriers.

3.4.2. Characterization of Functionality

The compartment divider was examined for its ability to provide fluidic isolation over the many days of culture in an incubator. Given the small quantities of silicone grease being used, we examined the interface between adjacent compartments in a two compartment divider. First, the divider was stamped with silicone grease by bringing a glass slide that has been thinly coated with silicone grease into contact with the divider. The substrate, having been patterned with collagen and wetted with 10µL of 0.4%

Assembly Method 1: Traditional Compartmented Culture Assembly

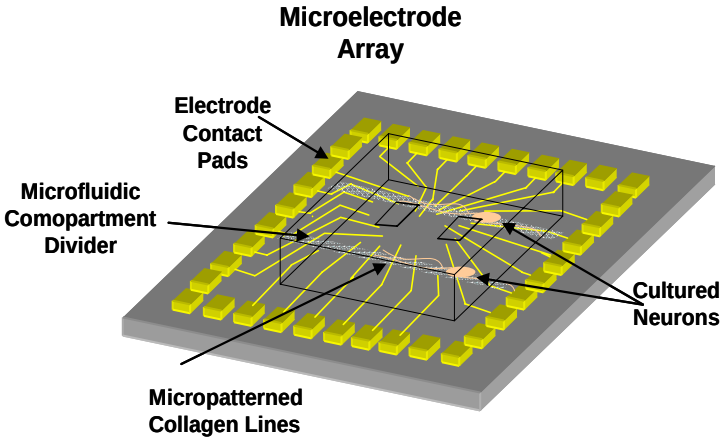

Assembly Method 2: Alignment of Divider After Neuronal Growth

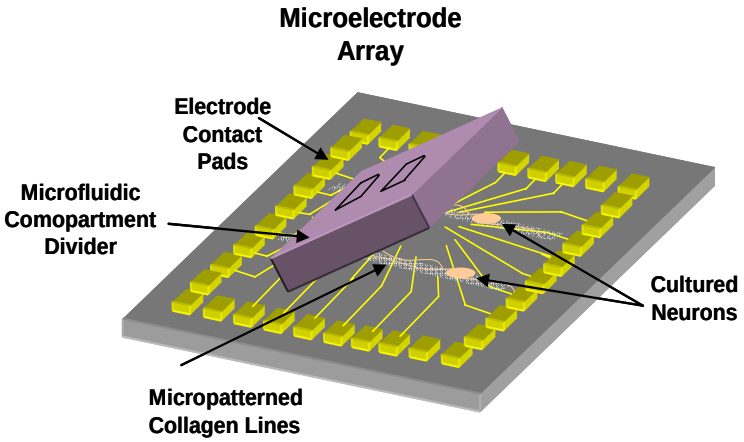

Figure 3.8. Two techniques for assembling the compartmented culture system.

methylcellulose dissolved in MEM media in the area between two adjacent compartments, was then brought into contact with the divider. Equal amounts of media were poured into the two compartments and food coloring was added to one of the compartments. The compartments would consistently fail after 2 to 3 days in the incubator due to the degradation of the grease over this time. Therefore, we examined different ways of overcoming this potential pitfall.

First, we tried to examine the interaction between the substrate and the grease. Bare glass or tissue culture plastic is hydrophobic; however, when they are coated with a thin layer of collagen, they become more hydrophilic. Therefore, over the many days that the compartment divider sits in the incubator, water accumulates at the barrier. This causes leakage between the compartments. To remedy this problem, we tried shortening the collagen lines so that the grease around the periphery of the compartment divider would not be in contact with a collagen floor. This helped to seat the divider properly on the substrate and to prevent the periphery of the divider from experiencing any leaks. We were able to consistently obtain leak-free compartments for 3 to 4 days using this technique.

As a further improvement, the compartment divider was seated on the neurons once they had grown on the substrate (see Figure 3.8). Here, neurons were plated on a sterile coverslip with a temporary barrier placed in the center. A compartment divider with no grease was placed on top of the coverslip. It provided a good enough seal with the coverslip such that when neurons were plated in one compartment, they did not leak into the other compartment. After allowing the neurons to attach to the substrate overnight, the divider was removed. Neurons were allowed to grow along the collagen

tracks for 4 to 5 days so that they had processes that were several millimeters in length. Then the culture media was aspirated out of the Petri dish containing the coverslip and the sides of the coverslip were coated with a thin layer of silicone grease using a sterile razor blade. The grease was spread as thin as possible and care was taken not to disturb the growing neurons. Then a sterile compartment divider was inked with silicone grease as described before and, using a dissection microscope, the divider was aligned to the growing neurons so that the somal bundles were in one compartment and their associated processes were in another.

Leakage between compartments was tested by adding dye to one of the compartments (see Figure 3.9). Initially, both compartments were filled with the same volume of media (50µl) and dye was added to one of the compartments (approximately 5µl). These dividers leaked on an average of 3 days after assembly. To help control leakage for a longer period of time, we added more fluid to one of the compartments

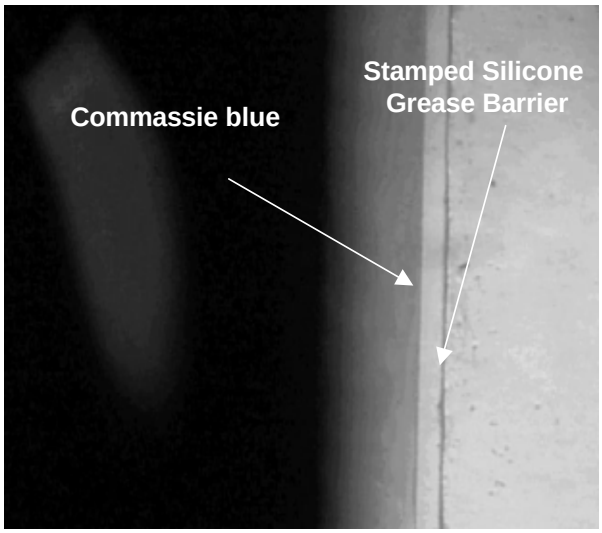

Figure 3.9. Technique for assessing leakage in the system. Compartment on the left has dye and compartment on the right has no dye. Microfluidic barrier separates the two compartments.

compared to the other ones. Here, approximately 10-15µl of dye (blue food coloring) was added to one of the compartments and 30µl of cell media was added to the other. Periodically adding cell media to the compartment that did not have any dye was useful in preventing further leakage.

Another option we explored was the use of materials other than silicone grease to contain drugs. We tried Vaseline instead of silicone grease and explored its ability to form an effective seal. Since Vaseline has a thinner consistency than the high vacuum grease (Dow Corning) that we used, it was easier to seat the divider on the substrate and cause it to form a seal with the substrate. However, this material was just as likely as silicone grease to eventually leak due to water accumulation at the interface between the two compartments.

3.5. Characterization of the Microfluidic Compartment Divider Using Microstenciling

3.5.1. Characterization of Fabrication

The fabricated microfluidic compartment divider using microstenciling had some of the same fabrication issues as the previous components of the system. Unique to this component was the stencil that was placed on top of the PDMS mold. As described in Chapter 2, this stencil was created using adhesive tape and was very sensitive to power fluctuations in the CO_2 laser (see Figure 3.10 and Figure 3.11). Only the lowest power settings for the tape were admissible since the tape was very thin. Too high a setting resulted in line widths that were greater than 400µm. One solution to this problem was

the use of the excimer laser. This laser allowed us to achieve line widths that were closer to 100µm; however, at this width, the sidewalls of the ablated area slanted inward, resulting in a width that was much smaller than 100µm at the bottom of the stencil. This produced uneven widths of stenciled grease and resulted in compartments that leaked continuously. Therefore, 200µm was the most effective ablated line width even with the excimer laser.

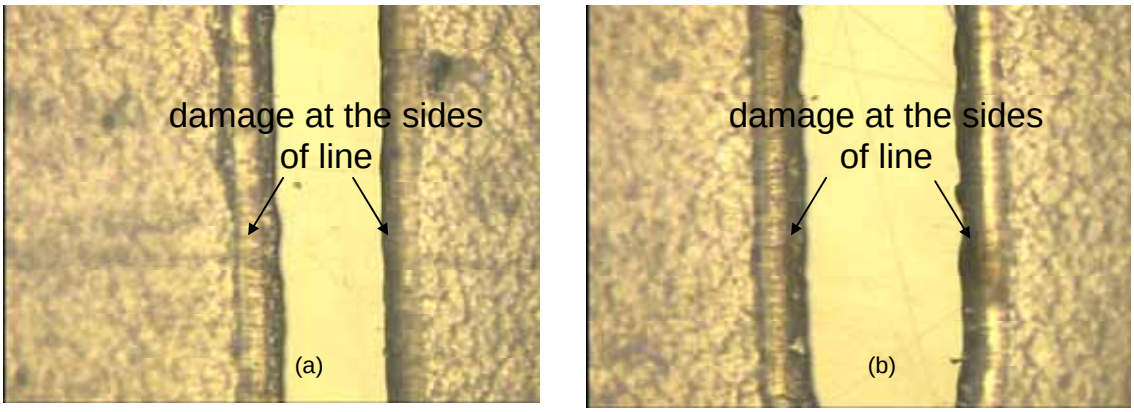

Figure 3.10. (a) Line in adhesive tape laser-ablated with the CO_2 laser at lowest power settings (325µm wide). (b) Line width almost doubles in size by doubling the power.

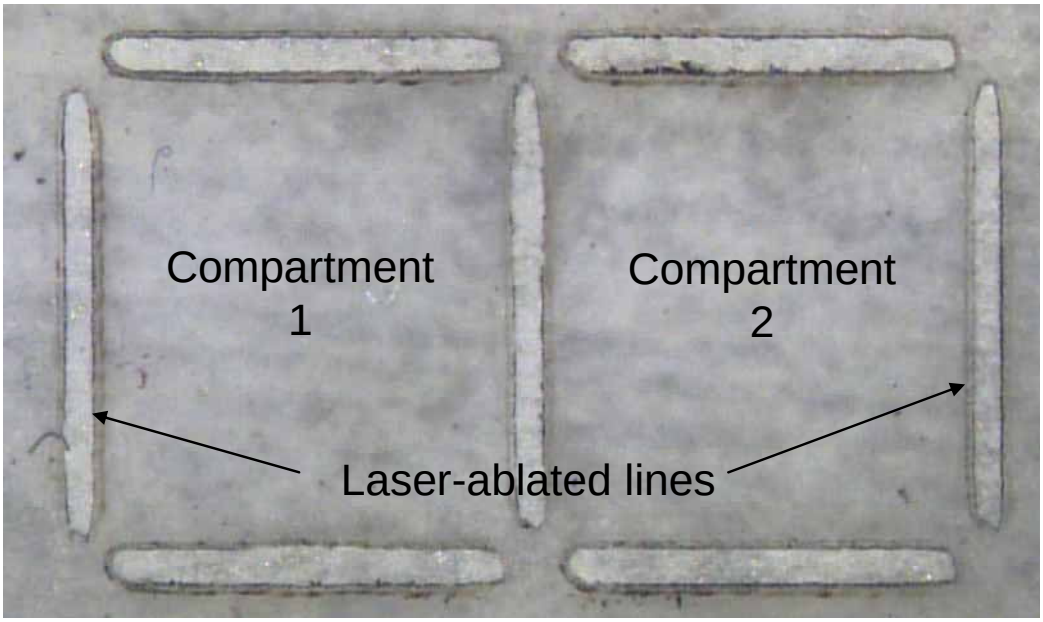

Figure 3.11. Full pattern of ablated tape showing compartment lines and spaces to create the stencil for a two-compartment divider. Even within a single power setting, there is some variability in line width.

3.5.2. Characterization of Functionality

Initially, with the laser ablated compartment dividers, the microstencil was aligned and taped to the divider and silicone grease was spread across it with a razor blade angled at 45°. Only a thin layer of silicone grease was spread across the divider. A second stroke was made after the initial one to firmly lodge the grease in the stencil. Then the stencil was removed in one stroke, leaving behind the grease pattern on the compartment divider.

Once the grease had been stenciled on the divider, it was assembled onto a glass or plastic substrate in the same way as it had been assembled using the previous approach for patterning grease. One problem encountered here was that the grease was not uniformily stenciled on the divider. The laser used to cut the stencil pattern had fluctuations in the power so we were not able to get a uniform silicone grease pattern; some areas of the stencil had thicker amounts of grease and others were thinner. Therefore, when the divider was seated on the substrate, some areas of the divider were seated more readily than others with the substrate. This caused the divider to be leak-prone at a very early stage (several hours after assembly).

3.6. Characterization of the MEA substrate

The MEA substrate was characterized for its ability to faithfully register extracellular neuronal signals. The impedance of the electrodes was characterized using a test apparatus connected to a PC (shown in Chapter 2). The apparatus had the ability to sequence through each electrode on the substrate. The electrodes started out with an

impedance of 300kΩ and after two minutes of plating at 1μA per electrode (16 electrodes at a time), were reduced to 30kΩ.

3.6.1. Characterization of Fabrication

The fabricated MEA met design specifications. The electrode line widths necked down from 200μm to 10μm openings. The critical step for producing these line widths was the amount of time the electrodes were placed in the gold and titanium etchants. Too short a time resulted in incomplete removal of the metal from unwanted areas. Too long a time resulted in severe undercutting of the metal, producing line widths much shorter than the designed values.

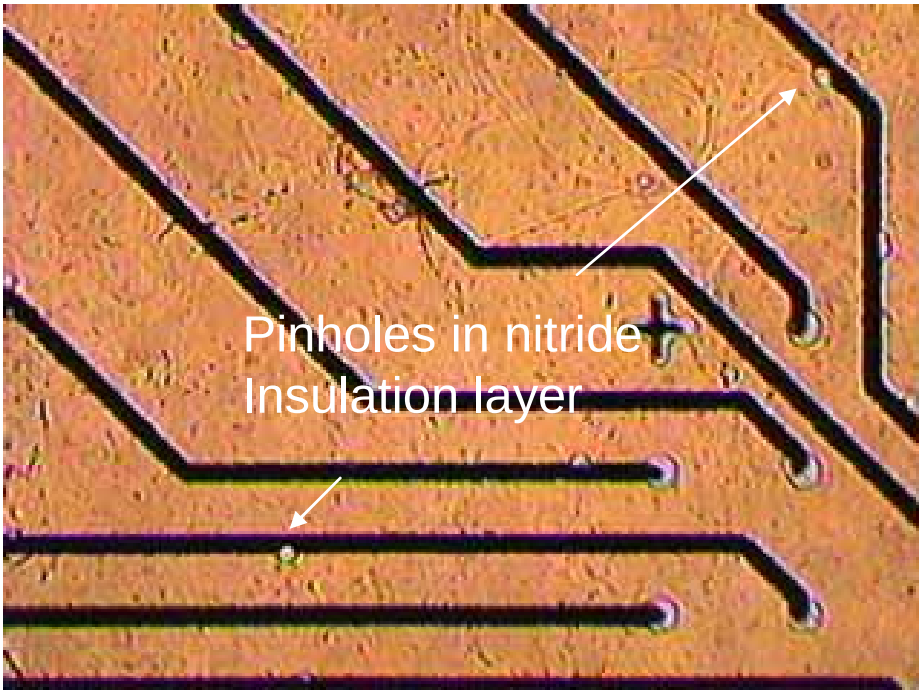

Figure 3.12. Pinholes in the nitride layer of the MEA.

One of the issues with respect to the electrodes was the insertion of pinholes into the nitride layer (see Figure 3.12). Pinholes are due to nonuniformities in the PECVD

deposition process of the silicon nitride. Others have reported several ways of mitigating this problem. One solution reported in the literature has been the incorporation of a silicon nitride and silicon dioxide sandwich. We opted for a somewhat nontraditional approach. The epoxy-based photoresist SU 8 (Microchem Corp.) was used to replace the nitride. A 1μm layer of SU 8 was easily spun-cast on the electrode substrate. SU 8 2 was spun cast by spinning at 2200rpm for 30s. It was then cured on a hotplate for 30min at 90°C. An OAI Optical Aligner was then used to align and expose the photoresist at 100mJ/cm^2. The substrate was then postbaked for 30min at 100°C. Finally, the film was developed using SU 8 developer for 10s. SU 8 produces a film that is very uniform and pinhole-free. We noticed a significant difference between the electrode impedance of the substrates insulated with SU 8 and those that were insulated with a similar thickness of silicon nitride. The electrode substrates insulated with SU 8 dropped from an impedance of 360kΩ to 12kΩ whereas those insulated with silicon nitride dropped from an impedance of 30kΩ to 9kΩ.

Another approach used to deal with the issue of pinholes was the use of the STS PECVD instead of the PlasmaTherm PECVD. The STS PECVD deposits higher quality nitride than the PlasmaTherm PECVD by alternating the frequency of the coils that power the system. Low stress nitride is continuously stacked on top of high stress nitride to produce a high quality film. With either PECVD deposition system, the thicker the nitride deposited, the more stress created in the thin film and the greater the variability in the thickness in different areas of the substrate. For our purposes, we determined that a 1μm thick film was enough to produce an effective insulation layer.

The alignment step for patterning the nitride was the most difficult step in the whole process. The alignment step was critical in opening up the appropriate areas for recording. Here, the openings had to be exposed for the right amount of time to UV light to ensure that the nitride openings were the same size as in the design. After alignment and exposure/development of the photoresist, the samples were placed in an SF_6 plasma. The process was optimized to certain gas flow pressures and duration. If the samples were not placed for long enough in the plasma, the nitride would not be fully removed in

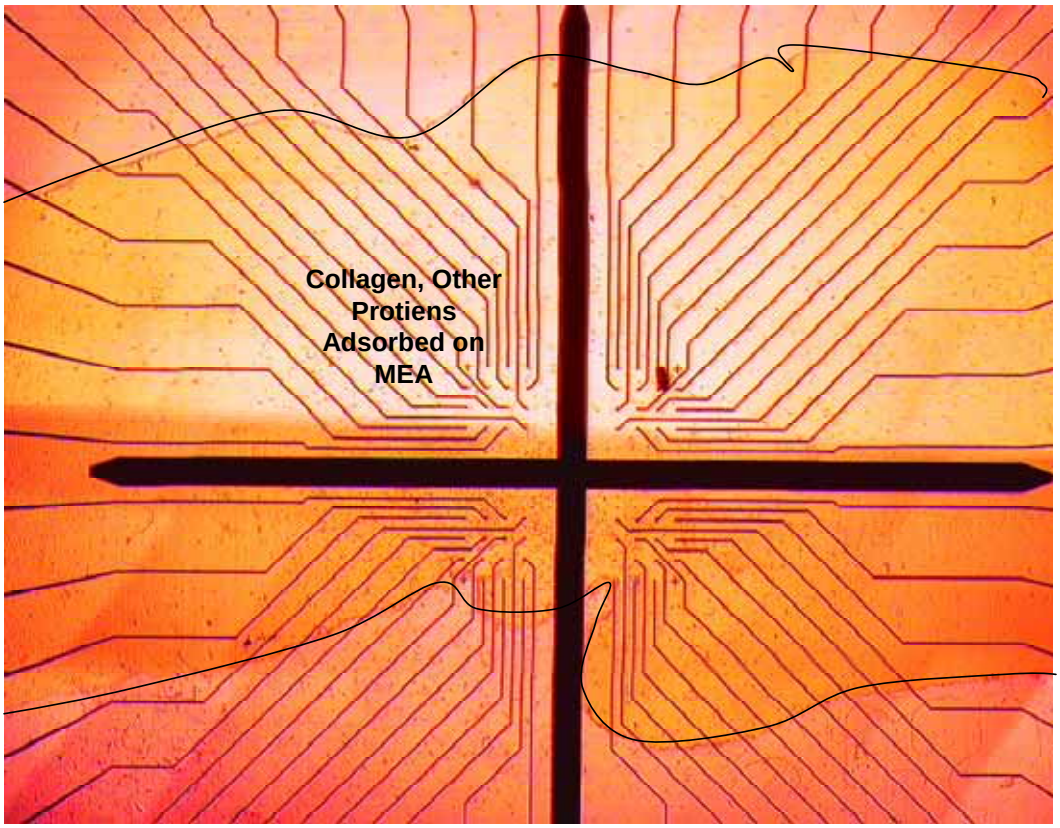

Figure 3.13. Deposition of collagen and other proteins from the culture media and neurons on the MEA substrate through repeated use.

the desired areas. On the other hand, if the nitride was placed for too long a time, the photoresist would be removed and the nitride underneath the photoresist would also be removed in unwanted areas.

Platinum black electrodeposition was important to ensure that their impedance was lowered. As indicated above, it was important to get either high quality nitride deposition or a good SU 8 insulation layer to ensure that there were no pinholes in the insulating layer. This allowed the electrodes to be plated only at the openings.

Of all the parts created, the substrates themselves were the toughest to clean for reusability. Once they were fabricated the substrates were soaked in ethanol and isopropanol. However, during the length of a culture (approximately 2 weeks), the patterned collagen and other biomolecules from the culture media and those secreted by neurons tended to deposit on the MEAs. To remove these depositions, the substrates were gently scrubbed with a foam applicator before soaking in ethanol and water for 1 hour. Care was taken to apply as little pressure as possible to the applicator. However, this method did not remove all of the accumulations and, after a dozen platings, depositions tended to invariably accumulate (see Figure 3.13).

When placed in the MEA recording setup with no cells and just culture media, the substrate was characterized for baseline noise levels. On each substrate there were invariably some channels that produced more baseline noise than desirable. The increase in noise levels was due to several imperfections in the fabrication process. For instance, variability in the etch rates of the metal lines sometimes produced breaks in the lines. Also, as mentioned earlier, pinholes in the nitride layer produced lines that had electro-deposited platinum black in undesirable locations. However, for the most part, all the channels had baseline noise levels that hovered around $\pm 10 \mu V_{peak\text{-}to\text{-}peak}$.

3.6.2. Culture Protocol for Cortical Neurons

Dissociated cortical cell cultures were prepared by papain digestion of embryonic-day-18 rat whole cortices. Timed-pregnant Wistar rats were euthanized by CO_2 inhalation, according to NIH-approved protocols for the care and use of lab animals. Embryos were removed, chilled on ice, and the cortex was microdissected under sterile conditions. Papain solution was quick frozen by immersion in liquid nitrogen in 2ml aliquots, stored at -15°C, and thawed at 35°C just before use. One millimeter cortex pieces were digested in 2ml papain solution for 30min at 35°C with gentle inversion every 5min. The papain solution was aspirated and the pieces were triturated three times, three passes each with 1mL of medium, using a P-1000 Pipetman. 50000 cells were plated in a 20µl droplet covering the 1.5mm electrode region of the MEAs, forming a dense monolayer. The dishes were flooded with 1ml of medium after the cells had adhered to the substrate for >15min and stored with FEP membrane lids in a 65% RH incubator at 35°C, 5% CO_2, 9% O_2. The medium was Dulbecco's modified Eagle's medium with 10% equine serum (Hyclone).

3.6.3. Culture Protocol for DRGs

The surgery involved several steps. Media was prepared with Eagle's MEM supplemented with 1% N_2 supplement and 7S NGF (Alomone Labs, Jerusalem, Israel) at 100ng/ml. The animal procured was an embryonic day 15 (Jackson Labs, Maine) Sprague-Dawley rat. First, the animal was anesthesized with a 0.4% solution of chloral hydrate. After 10 minutes, the pregnant female was laid on her back with the belly exposed. The belly was then soaked with alcohol and wiped with sterile gauze. Then the

abdomen was exposed by cutting and opening the skin. The uterus was then cut from the mother and the pups were plated into a 150mm Petri dish containing 5ml of MEM media. The pups were then separated from their placental sacs and placed in a 100mm Petri dish containing 2ml MEM media.

The head and tail were cut off with scissors. Then the pup was laid on their back and its organs were removed. To expose the spinal cord, the vertebral column was then cut away with fine forceps. The spinal cord was then pulled off of the body. Finally, the DRGs were plucked from the cord and placed in a 35mm Petri dish containing culture media. If dissociated cultures were used, the explants were incubated in 100µl of 10X trypsin for 30min. Afterwards, the cells were centrifuged and washed twice with cell media. After the second rinse, 200µl of cell media were added to the cells and they were mechanically triturated to complete the dissociation process. After counting the cells on a haemocytometer, they were plated at the appropriate density in each culture compartment. Pictures of outgrowth were taken each day for several days in culture using a light microscope.

3.6.4. Preliminary Electrophysiological Recordings from Cultured Neurons

To characterize the MEA substrate for its ability to record from neuronal signals, we initially studied how well the system could capture signals generated by cortical neurons. These neurons were used because they were well-characterized in one of our collaborators' labs (S. Potter, Georgia Tech). Moreover, they produce synaptically activated networks in culture and, therefore, fire spontaneously. Hence, we were able to avoid all of the issues with stimulation artifacts.

To perform this experiment, we prepared our MEAs using a standard cleaning protocol. First, a 3% BM cleaning solution (recommended by Multichannel Systems) was used to rinse the MEAs. Then they were soaked in ultrapure water overnight, sterilized in pure ethanol, and allowed to dry. On the day of use, a 100µl drop of 0.05% (w/v) polyethylene imine solution in borate buffer was applied to the center of the dish

Figure 3.14. MEA preamplifier recording setup with microfluidic compartment divider seated in the center of the MEA.

for 1hr, rinsed 4 times with sterile water, and allowed to dry. Twenty microliters of 1mg/ml laminin (Sigma) was diluted in 1mL of medium, and a 10µL droplet was applied to the center of the MEA, covering the electrode region. Dishes were covered and allowed to sit at room temperature for at least 30min to allow the laminin to attach to the substrate. Most of the droplet was aspirated just before adding the cell suspension to the dish.

Recordings were made using a Multichannel Systems (Reutlingen, Germany) preamplifier system (see Figure 3.14). After 1200X amplification, signals were sampled at 25kHz using a MultiChannel Systems data acquisition card, controlled through Meabench software. Meabench's digital filtering system for reducing stimulus artifacts allowed for detecting action potentials as early as 2ms after stimulation (except on the electrode used for stimulation, which remains saturated by stimulation artifacts for 50-150ms). Spikes were detected online by thresholding at 5X rms noise.

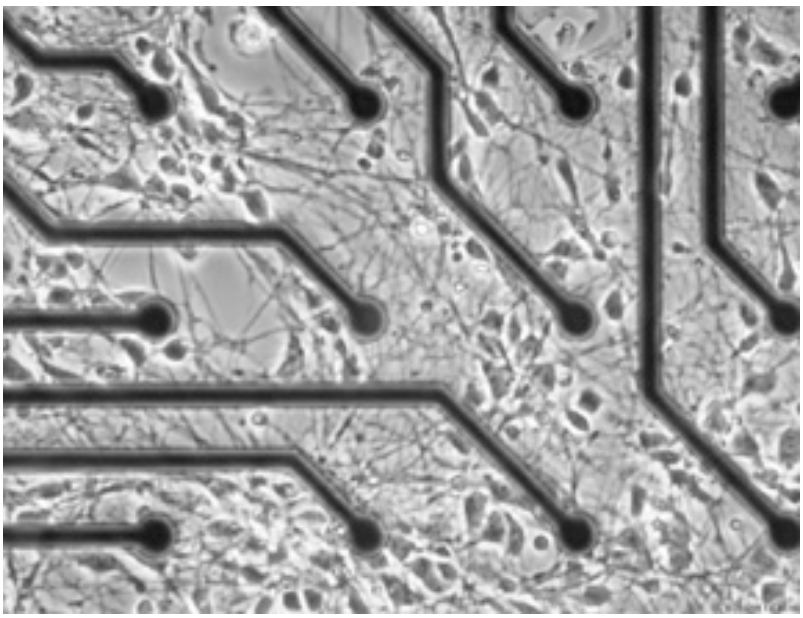

Figure 3.15. Cortical neurons on an MEA substrate.

After 9DIV, the cultures were placed in the preamplifier system and neuronal signals were recorded for 10s (see Figure 3.15). Baseline noise readings hovered between $\pm 10\mu V_{peak\text{-}to\text{-}peak}$. Several of the channels (approximately 1/5) exhibited neuronal activity and periodic bursts of activity. Neuronal activity (i.e., action potentials) ranged from 50μV to 100μV in amplitude and lasted anywhere from 2ms for single action potentials to 10ms for bursts.

Moreover, the ability to record action potentials from DRGs was confirmed on the MEA apparatus (see Figure 3.16). Dissociated cultures of DRGs were prepared as described in the previous section. Here the recording software was Multichannel Systems commercial software known as MC_Rack. Here also, spikes were recorded based on being 5X above RMS noise. DRGs do not fire spontaneously, so their acitivity needed to be stimulated. For this purpose, we chose a 2.5M solution of KCl in cell media. Upon addition of the KCl buffer, we were able to record extracellular action

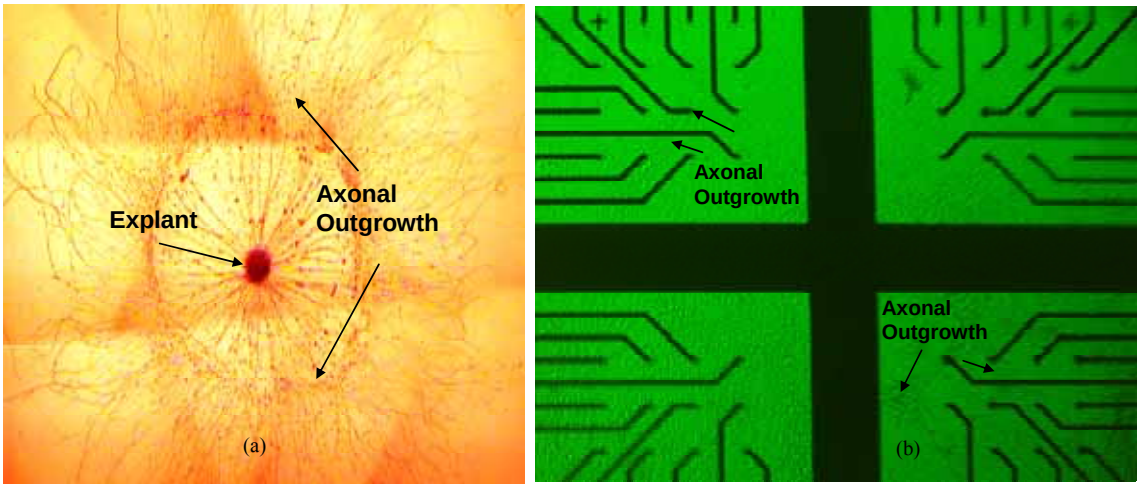

Figure 3.16. (a) DRG explant on a petri dish. Notice the lush outgrowth of axons from the somal bundle. (b) Dissociated cultures of DRGs on a MEA substrate (10DIV). Cells were initially plated near the crosshairs and their extensions can be seen growing away from them.

potentials from DRGs. Their amplitudes varied widely from run to run but ranged from tens to hundreds of microvolts. Also, during a 1 minute recording, we were able to record several hundred action potentials from the dish. A summary of this data is shown in Table 3.1. When compared with the level of activity for cortical neurons above, the number of action potentials generated is far less since most of the activity recorded in cortical neuronal cultures is due to network wide bursts. Looking at the data in Table 3.1, it seems that addition of cell culture media 1 minute after the KCl buffer solution causes

the activity to die down; however, there are still some aftereffects of the KCl buffer. Addition of the KCl buffer for a second time causes the neurons to fire again, leading us to believe that they are still alive.

Table 3.1. Summary of Data for Extracellular Action Potentials from DRGs

	Run 1		Run 2		Run 3	
	# of spikes	Amplitude (μV)	# of spikes	Amplitude (μV)	# of spikes	Amplitude (μV)
Cell Media	6	35.3916	15	23.038	6	59.524
25mM KCl	21	27.938	21	23.272	1	71.667
250mM KCl	6	26.56	40	26.574	6	180.686
2.5M KCl	141	35.38	113	27.588	345	956.369
Cell Media	83	35.38	40	44.8055	14	108
2.5M KCl	81	33.183	159	54.81	78	44.81

3.7. Pilot Studies with Cell Culture

The entire system was used to culture cells for biocompatibility. The system was assembled as described in the previous sections with the electrode substrate. Several different methods were investigated for biocompatibility of the materials. These methods were an ethanol rinse, UV overnight treatment, dry heat treatment, and an autoclave step. Of all the treatments, the autoclave step provided the most robust neurite outgrowth and was, therefore, adopted. While the ethanol rinse and the UV overnight treatment seemed to produce some good results, the dry heat treatment did not produce healthy growth.

Initially, we studied the growth of DRGs on a glass slide with the aid of a pin rake. The pin rake would provide small paths for the guidance of neurons. While some neurons were able to be guided effectively, the pin-raked lines were not uniform so neuronal growth was not uniform. However, as we became better at growing both DRG explants and dissociated DRG cultures, we began to grow DRGs on plastic substrates with pin raked grooves and on chemically modified substrates.

CHAPTER 4

NEURONAL GROWTH IN COMPARTMENTED CULTURES

4.1. Chapter Outline

This chapter outlines the neuronal growth in compartmented cultures. Sections 4.2-4.5 give the background information for neuronal cell culture. Finally, sections 4.6-4.8 detail the parameters of growing explants and dissociated dorsal root ganglia cells in compartmented cultures.

4.2. Background on Neuronal Cell Culture

The techniques of cell culture have developed over the last thirty years. Ever since the seminal discovery of R.G. Harrison, researchers have tried to take advantage of the ability to grow living tissue and cells outside of the body. Since that time, two means of neuronal cell culture have developed. One is the primary cell culture and the other is the cell line. Primary cultures are those obtained directly from animals. When cells from the embryonic brain are dissociated and cultured, neurons that have completed division will extend processes and become electrically active. Meanwhile, cell lines are originally obtained from tumor cells. With these cells, it is possible to "passage" them by removing them from the substrate and allowing them to divide again. However, the properties of the cultured cells change gradually with passaging, as more rapidly dividing cell populations dominate and more differentiated cells are lost. Though there are cell lines that express many of the individual characteristics of differentiated neurons, they are not always good candidates for the neuronal phenotype [1].

4.3. Background on Primary Cultures

A dissociated cell culture is one that is prepared from suspensions of individual cells obtained by dissociation of neural tissue. When plated onto a substrate, the neurons begin to extend processes within several hours and form a dense network. Under certain conditions, it is possible to maintain these cultures for months. These cultures develop axons and dendrites, form synapses, and express the receptors and ion channels characteristic of neurons. When certain types of neurons are cocultured with Schwann cells or oligodendrocytes, axons become myelinated. During the first few days in culture, before the neural network becomes too complicated, individual neurons can be seen. This allows direct observation of growing axons as they continue to branch. This specificity allows for many experiments to be performed. Primary dissociated neuronal cultures are thus suitable to morphological and physiological investigation.

However, a limitation of primary cell culture is that they are not as well-suited for traditional biochemical approaches because the quantity of material obtainable from these cultures is usually limited. Another limitation is that they often contain mixtures of different types of cells. Hence, the development of approaches to deal with the mixtures of cell types is essential to the successful use of primary cultures. Finally, a last obstacle in using primary cultures is that optimizing the conditions that permit good culture involves lots of work [1].

4.4. Background on Explant Cultures

Explant cultures are thin slices of tissue that are allowed to attach to an appropriate substrate and cultured in a nutrient medium. The need for nutrients and

oxygen to diffuse to the center of the tissue limits their thickness to approximately one millimeter. As with dissociated cell cultures, embryonic and neonatal tissue grows best. One advantage of using explant cultures is that they have extensive fiber outgrowth [1].

4.5. Background on Protocols for Cell Culture

At all stages, tissues and cells must be maintained in an osmotically balanced solution at physiological pH. A balanced salt solution consists of the right mixture of salts at concentrations approximating those of extracellular fluid and glucose. In addition to the salts, media contain nutrients like amino acids and vitamins needed for long-term growth of cells. There are several variations of balanced salt solutions that differ primarily in the buffers they contain [1].

The first step in the preparation of any primary culture is the dissection. Of primary importance is the fact that the tissue must not develop an infection. Normally, work is done either at room temperature or the tissue is kept on ice. For obtaining individual cells, the tissue must be dissociated to give a suspension of single cells. Dissociation is helped by the removal of divalent cations (such as calcium and magnesium). Usually, an enzyme like trypsin is used to perform the dissociation. The tissue fragments are then dissociated mechanically with the Pasteur pipette. Finally, they are plated on an appropriate substratum in cell media [1].

A complete medium for culturing cells consists of a basal medium, such as minimal essential medium, supplemented either with serum or with a defined set of hormones and growth factors. In all these media, glutamine is present at much higher concentrations than are other amino acids; this is because of its instability and its use as a

carbon source by many cells in culture. To provide the nutrients and growth factors necessary for growth and maintenance of certain cell types, basal media are frequently augmented by the addition of serum at concentrations ranging from 5% to 20%. In 1979, with the introduction of chemically defined media, neuronal cells were able to be cultured without the need for serum. One can either allow cultured cells to produce their own trophic factors or add purified growth factors to the medium. For several decades, the only factor that was available for use in tissue culture was nerve growth factor (NGF), and this was a limitation in the type of cells that could be cultured. During the last 10 years, however, many new growth factors have become widely available.

Many types of peripheral nervous system (PNS) neurons exhibit simple trophic requirements in vitro. For example, rat sympathetic and dorsal root sensory neurons require only NGF for their survival and can grow for several months with it. However, there are complications involved. For instance, rat dorsal root ganglia contain several cell populations. The small cell population is responsive to NGF, but the large cell population responds to different neurotrophins [1].

4.6. Growing Explants in Microfabricated Compartmented Cultures

4.6.1. Neuronal Growth in Pre-Assembled Systems

Explants were grown in the system because they are easy to culture. DRGs grow axonal halos that are approximately 5mm in length after 10 days in culture. The DRGs were placed into the chamber one of two ways. Either they were placed physically by grabbing them with fine forceps or they were injected into the chambers with a pippetter.

Usually, cultures worked best when 2 or 3 explants were plated in one compartment. Care was taken not to allow the DRG explants to float away from the barrier when

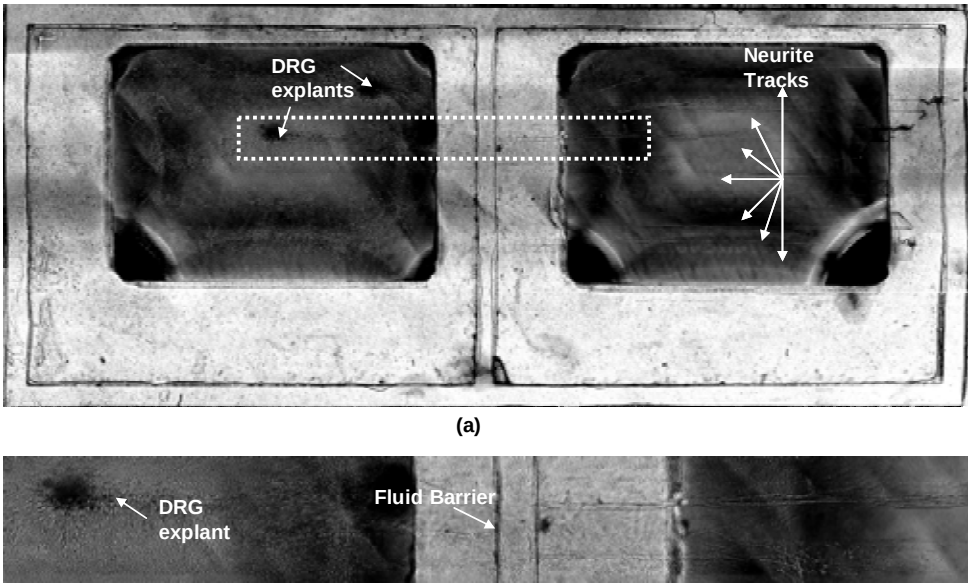

Figure 4.1. Culturing of DRG explants in a two compartment system for 15DIV. (a) an 8-track neurite system. Explants were plated in the left compartment and grew extensions along pre-patterned collagen tracks into the adjacent compartment after several days in vitro. (b) close-up of dashed box showing 2 of the 8 tracks.

moving the culture in and out of the incubator. The explant generally adhered to the collagen floor and began extending small processes after 12h in vitro. If the explant did not adhere to the substrate, it would not form any processes and would float in the media. To increase the likelihood of an explant not floating in the media, the tissue was placed as close to the surface of the substrate as possible.

A photomontage of growing axonal halos in a two compartment culture is shown in Figure 4.1. Here, 2 halos can be seen in one of the compartments and their extensions have grown into the adjacent compartment. Notice how the extensions are only loosely associated with the chemical pattern on the substrate in the compartment on the left but have more well-oriented growth cones in the compartment on the right. This was true of many of the explant cultures that we observed. We hypothesize that the extremely high

density of neuronal processes at the DRG center prevents the chemical pattern from being as effective. As the halo becomes larger over the course of several days, the density of projections thins out, allowing the individual processes to feel the effects of a chemically patterned substrate.

4.6.2. Neuronal Growth in Post-Growth Assembled Systems

The second approach used was assembling the divider after neuronal growth in the compartmented culture system. With this approach, the compartment divider was gently placed on the DRG after it had developed an axonal halo approximately with 3mm radius. To accomplish this, media was aspirated surrounding the DRG so that there was only a small puddle with the cell in the center. Silicone grease was spread very thinly

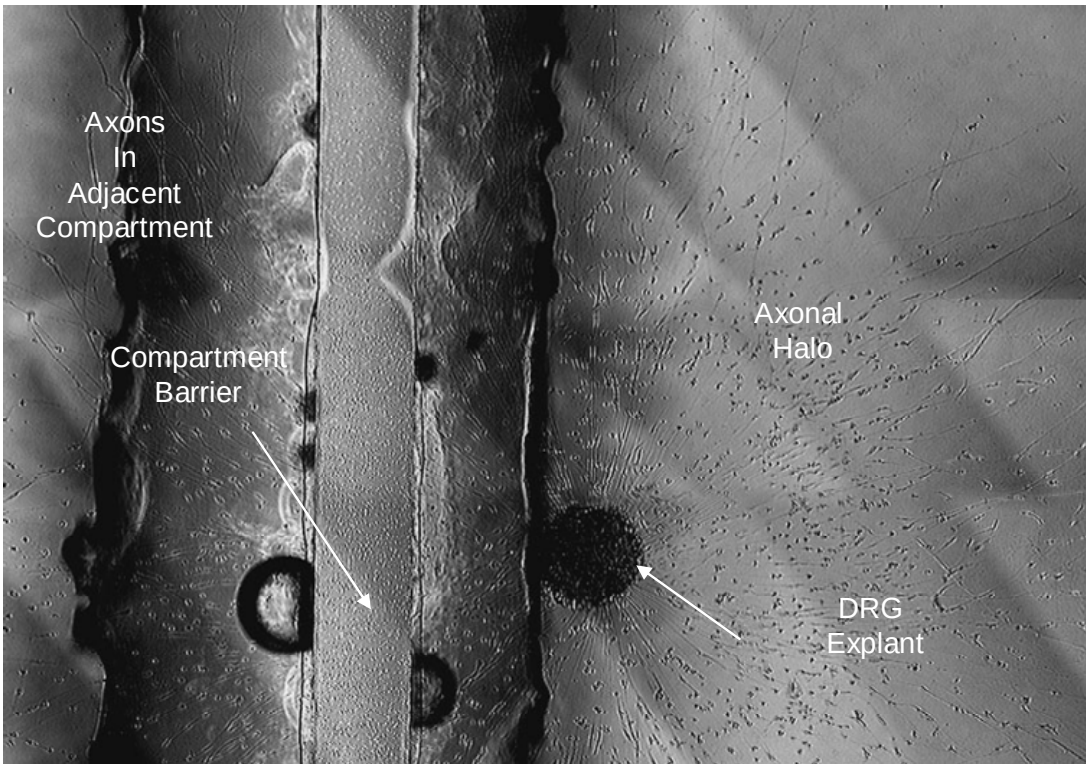

Figure 4.2. A two compartment divider placed on a DRG axonal halo after 5 DIV

using a razor blade to surround the cell. Then a compartment divider microstamped with grease was hand aligned to the explant under a dissection microscope. A picture of assembling the divider in this way are shown in Figure 4.2.

4.7. Growing Dissociated Cells in Microfabricated Compartmented Cultures

4.7.1. Neuronal Growth Before in Pre-Assembled Systems

Dissociated cells were grown in the system to allow yet another cell model to be studied. Explants were dissociated with trypsin incubation for half an hour in the

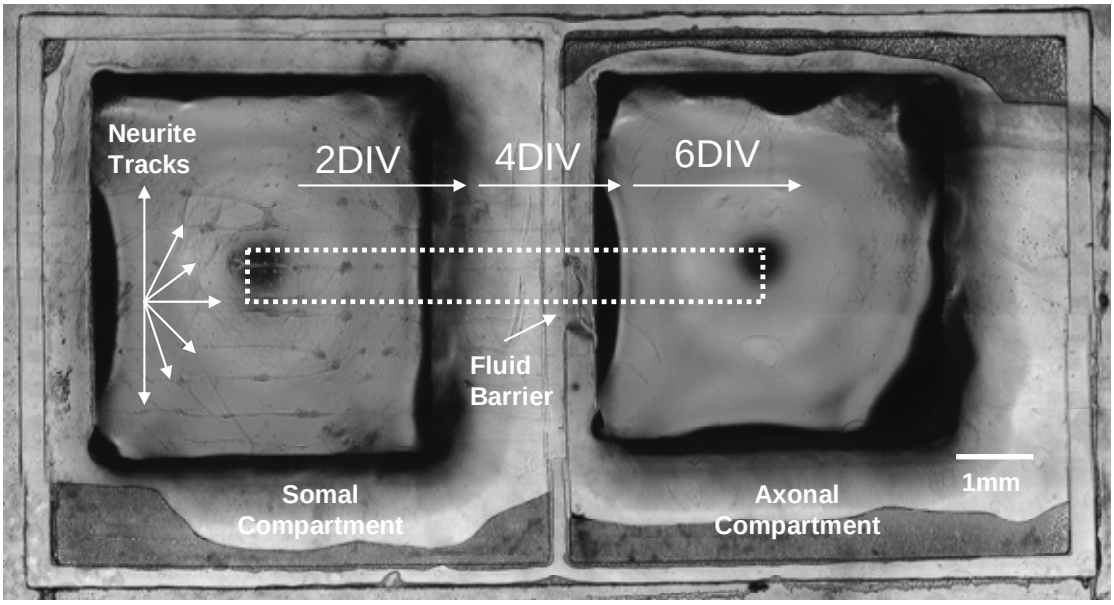

Figure 4.3. Culturing of dissociated DRG neurons in a two compartment system. (a) an 8-track neurite system. Neurons were plated in the left compartment and grew extensions along pre-patterned collagen tracks into the adjacent compartment after several days in vitro. Usually, after several hours in vitro, neurons initially plated in a random arrangement begin to group together along the collagen tracks and after 1 DIV, have already begun to grow processes in these tracks. Several of the neurons have "jumped" tracks and formed connections with the neurons in adjacent tracks. (b) close-up of dashed box showing 2 of the 8 tracks.

incubator. Approximately 100000 cells were plated in one of the two compartments and their growth was observed over the course of two weeks in the system. In the preassembled system, neurons traversed small silicone grease barriers (200μm wide) approximately after 6 DIV. Neurons grew an average of 1mm every 2days. A photo of the growing axons and their time course is shown in Figure 4.3. Clearly, bundles of cells of cell bodies can be seen in the somal compartment. Although some of the neurites have "jumped tracks", most of them have been confined to a single track.

Varying the plating density had differing effects on the culture. Plating densities were varied from 20000 cells all the way up to 200000. Too low a plating density caused poor growth, resulting in death only several days after plating. Plating too many neurons in one of the compartments resulted in poor pattern formation. Here, many neurons crossed from one track to another. An optimal number of neurons in a 4mmX4mm port was between 50000 and 100000 neurons. Within this range, cell densities closer to the lower bound resulted in cultures that had less bundle formation and fewer numbers of processes. The upper bound resulted in poorer pattern formation but more robust process outgrowth.

Finally, in the system where neurons were allowed to grow before they were compartmentalized, the compartment divider was assembled on top of the growing neurons after growing the neurons for 1 week in the incubator. If too much pressure was applied to the divider when seated over the axons, the distal portions of the axons would die, presumably due to too much pressure being placed on them. So, care was taken to seat the divider on the neurons gently. The grease-patterned divider was aligned to the neurons under a dissection microscope and, if it was allowed to sit long enough, the

grease would settle and the divider would settle along with it. Once assembled, the chamber device was placed in a 35mm Petri dish and viewed under an inverted microscope. If the divider was seated properly, the phase contrast would show the grease around the periphery to be darker than that of the grease in the center.

Compared to neurons cultured on unpatterned collagen substrates, there was a clear directionality associated with the growth. Neurons cultured on bare collagen with no patterning seemed to develop randomly oriented networks and meandered on the substrate.

4.7.2. Neuronal Growth in Post-Growth Assembled Systems

If the divider is assembled after neuronal growth, the divider was placed carefully on the growing neurons after 4-5 days of growth. This period of growth allowed the axons to grow to a sufficient length to be able to position the divider properly over the growing neurons. As described previously, a glass substrate was patterned with collagen, the neurons were grown in one of the compartments of a temporarily attached compartment divider, which was removed once the neurons attached. After five days of neuronal growth, all of the media was aspirated out of the 35mm Petri dish with the neurons and brought under a dissection microscope as described in the previous section for explants. Silicone grease was spread across the edges of the slide and the new grease-stamped compartment divider was placed on top of the neurons under a dissection microscope. In this scenario, we had to make sure to place the compartment divider on the neurons very gently, as too much pressure caused axonal injury. To accomplish this, we applied virtually no pressure in seating the compartment divider on the growing

neurites. The divider was brought into contact with the substrate very gently and placed on top of it.

4.8. Temporal Changes in Neurons Cultured on a Collagen-Patterned Substrate

Chemically patterned substrates were analyzed for their ability to guide neuronal growth. Neurons were plated in one compartment in a random arrangement and they reoriented themselves to fit the patterned substrates after several days in vitro (see Figure 4.4). Clearly, those neurons that did not adhere to the pattern had died after 1DIV. At 2DIV, bundles of neurons can be seen in one of the compartments and their processes are seen extending out into the compartment along tracks. In this experiment, 100000 DRG cells were plated in the somal compartment. Increasing or decreasing the cell density initially at plating did not significantly alter the general result; however, with lower cell densities, thinner lines of neurons were seen "hugging" the tracks.

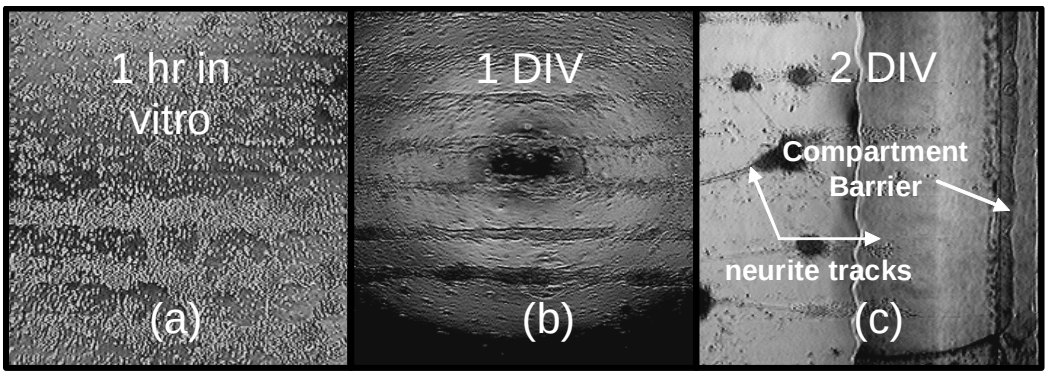

Figure 4.4. Photo montage showing the development of a neuronal pattern due to collagen tracks on a glass substrate. Notice how plating occurs in a random orientation at the beginning and after just 1DIV, neurons have already begun to cluster preferentially on the collagen tracks. Moreover, by 2DIV they have developed processes and are approaching the grease barrier at the right as shown in Figure 4.4c.

When an explant landed directly on a patterned line of collagen, sometimes all the extensions grew along that line and might branch to an adjacent line. This highly directional growth occurred throughout the entire time of culture. When it landed outside of the patterned area, it would grow in random orientations initially; however, the processes would grow along the patterned tracks when they reached this area. If the explants became lodged in the area right next to the grease barrier, the likelihood of growth was slim since the explant has a finite thickness associated with it. In this scenario, it became difficult to deliver nutrients and remove wastes to the explant. Therefore, there was a tradeoff in getting the explant close to the barrier to minimize the amount of growth it had to experience before its processes crossed the barrier and in being too close so that nutrients and waste products could not be effectively circulated.

4.9. References

[1] G. Banker and K. Goslin, *Culturing nerve cells*. Cambridge, MA: MIT Press, 1998.

CHAPTER 5

PHARMACOLOGICAL AND ELECTROPHYSIOLOGICAL STUDIES

5.1. Chapter Outline

This chapter outlines the pharmacological and electrophysiological studies that were conducted with the compartmented culture system. Section 5.2 gives an overview of axonal degeneration due to toxins applied in vitro. Sections 5.3 talks about the neurotoxin vincristine. Section 5.4 gives a brief overview of some types of electrophysiological responses obtained from DRGs and section 5.5 discusses some background information on the different electrophysiological responses obtained with vincristine. Sections 5.6 and 5.7 discuss the experiments conducted in a two compartment chamber; the first one deals with the toxicology of vincristine and the second section talks about how the electrophysiology correlates to the toxicological observations.

5.2. Neurotoxicant-Induced Axonal Degeneration

Axonal degeneration is the pathological substrate leading to loss of neurological function in a wide variety of acute and chronic disorders of the CNS and PNS. Diseases as different as stroke, spinocerebellar degenerations, and peripheral neuropathies share the common pathological substrate of axonal degeneration. Even in primary demyleinating disorders such as multiple sclerosis and HMSN, axonal degeneration is the pathological finding that is most highly correlated with the clinical symptoms. However,

the mechanisms underlying axonal degeneration in all of these disorders are unknown [1].

As mentioned in Chapter 1, several neurotoxicants have been used to induce axonal degeneration. Ultrastructural analysis of neurons after exposure to these neurotoxicants has revealed various impairments in the neuron; for instance some of these studies have shown neurofilament and microtubule impairment and others have shown direct toxic effects on the distal axon. These experimental model systems have become an invaluable tool for studying the molecular mechanisms behind neurodegenerative disease. More specifically, by examining the morphology and physiology of the neurons exposed to such experimental models of axonal degeneration, we have been able to better target pharmacological interventions for diseases exhibiting this phenotype.

5.3. Vincristine

Vincristine is a chemotherapeutic agent used to treat leukemias and other types of human cancer. However, patients treated with vincristine develop neuropathic symptoms and signs, some of which include distal-extremity paresthesias, sensory loss, and reduction of deep tendon reflexes. Pathologically, vincristine causes length-dependent axonal degeneration that is typical of many other drug-induced peripheral neuropathies [2]. While vincristine has been used since the 1960s, research on vincristine has been rudimentary. Vincristine is a naturally occurring alkaloid, and it is present in small quantities in the leaves of the periwinkle plant *Catharanthus roseus*. It has been known

for its medicinal properties since the seventeenth century, and its extracts were used to treat hemorrhage, scurvy, toothaches, wounds and diabetic ulcers. [2].

Neurotoxicity is the dose-limiting side effect of vincristine.. The neuropathy is particularly evident in the distal extremities. Moreover, severe central nervous system toxicity has also been reported, especially in patients who were treated with high dosages. However, many of the neurotoxic symptoms and signs disappear weeks to months after vincristine therapy has been discontinued. Several factors influence the severity of neuropathy; two of these factors are dosage regimen and age of the patient [2].

The most well-understood mechanism by which vincristine inhibits tumor growth is its interference with the mitotic spindle microtubules resulting in inhibition of mitosis. In vitro, vincristine causes apoptosis in tumor cells. Vincristine has its effect on microtubules by binding to tubulin or microtubules. Binding to spindle microtubules damages spindle structure in a concentration-dependent relationship, resulting in microtubule disruption. At low concentrations, vincristine stabilizes the spindle apparatus resulting in failure of the chromosomes to segregate leading to metaphase arrest and inhibition of mitosis. However, at higher concentrations, disruption and significant depolymerization of microtubules may be observed. Several authors have also demonstrated the in vitro importance of apoptosis in mediating the cytotoxicity of vincristine. This might explain why cells can die in M-phase as well as in interphase. Drug-induced disruption of the normal cell cycle is the likely trigger initiating apoptosis [2]. Some ultrastructural studies of the saphenous nerve in rats have shown also that vincristine treatment alters the cytoskeleton in that there were more tangential microtubules and neurofilaments that appeared to be abnormally clustered in the central

portion of the axoplasm in vincristine-treated axons. This same study found that while vincristine does not decrease the total number of microtubules in unmyelinated sensory axons, it does increase the axonal cross-sectional area and the diameter of unmyelinated sensory axons [3].

As stated previously, vincristine-induced neurotoxicity is caused by interference with microtubule function resulting in blockage of axonal transport and thus in axonal degeneration. An increase in the numbers of neurofilaments and accumulation and degeneration of organelles at the proximal end of the node of Ranvier have also been demonstrated. Vincristine induced axonal degeneration is described as Wallerian-like and of the dying-back type with changes in the distal nerves similar to those occurring after dissection from the cell body starting distally and progressing proximally. Changes of the proximal part with or without changes of the perikaryon have also been described. Demyelinization is considered secondary to axonal degeneration. However, recently, a greater degree of Schwann cell and myelin damage than axonal damage has been described, suggesting demyelinization might be the primary event. Vincristine associated neuropathy is reversible unless the degeneration process has reached the perikaryon. Regeneration requires nerve sprouting. Growth factors are released by denervated muscles. After absorption by the distal axonal end, growth factors will be transported to the nucleus, resulting in nerve sprouting and regeneration. Since neuronal microtubules have a function in nerve sprouting, it is probable that vincristine interferes with the process of regeneration [2].

Initially, uptake of vincristine into cells in vitro was thought to depend on a temperature-dependent and saturable carrier-mediated transport mechanism. Later, a

temperature-independent and non-saturable mechanism was found to be primarily responsible for vincristine uptake. Uptake into human hepatocytes is rapid. Once vincristine is taken up into normal or malignant cells, it is slowly released, even when vincristine is washed out of the culture medium. After vincristine injection, several other peaks other than that of vincristine have been identified by HPLC. Up to 13 peaks have been found in plasma, bile, and urine after vincristine injection in vivo or incubation in vitro. It is still controversial whether peaks are degradation products or metabolites of vincristine. The relationship between vincristine plasma pharmacokinetics and the oncolytic and neurotoxic features are poorly understood. Both in vitro and animal model studies have demonstrated a positive correlation between the oncolytic effect of vincristine and the degree of vincristine retention in tumor cells and tumor tissue [2].

The use of neuroprotective agents may decrease certain clinical consequences of vincristine neuropathy. The potential for these agents to interfere with the cytotoxicity of vincristine requires further study before these agents can be used outside experimental settings. Folinic acid, vitamins B1, B6, and B12 and gangliosides were promising in animal models but did not protect against vincristine-induced neuropathy in humans. Moreover, (L-)Glutamic acid was found to protect against vincristine-induced neuropathy in animal models as well as in patients. Potential protective agents against vincristine induced neuropathy studied more recently are insulin-like growth factor (IGF-I) and nerve growth factor (NGF). IGF-I, a polypeptide hormone, showed protection against vincristine induced neuropathy in mice. The mechanism of neuroprotection here might be stimulation of nerve regeneration or protection against apoptosis [2].

5.4 Current Clamping of DRGs

DRGs generate action potentials in a variety of ways. Many research groups have tried to stimulate and record from DRGs using conventional patch clamp techniques. DRGs respond to different types of stimulation parameters and in different ways to these protocols. One group has also tried to stimulate and record from DRGs using MEAs. This group found that signal processing was necessary after stimulation to obtain an extracellularly recorded signal. Also, a stimulation window was observed for evoking a response [4].

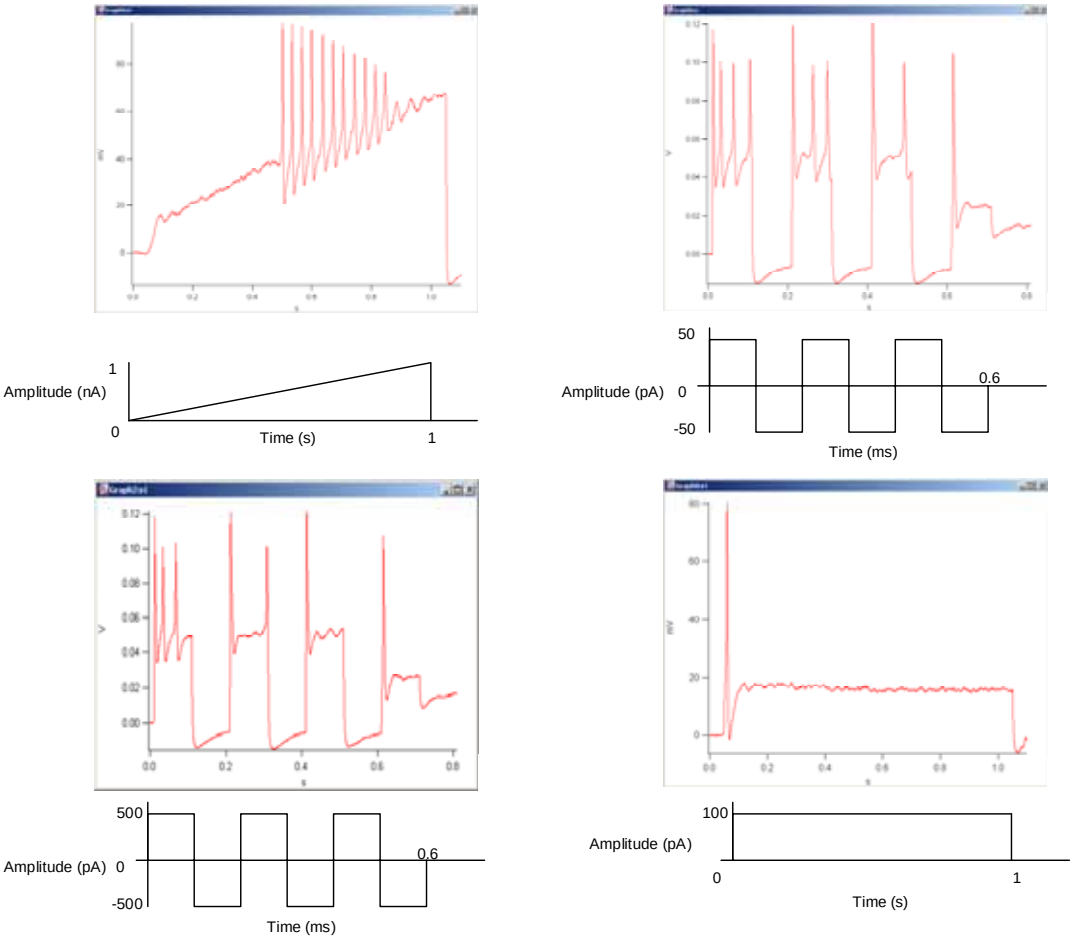

Figure 5.1. Various responses from current-clamp recordings of dissociated cultures of DRGs after 5DIV. Top figures in the four sets show responses and bottom graphs show the stimulation protocol used to obtain them.

To obtain a basic idea for the shapes and protocols needed for stimulation of our DRGs, we tried to obtain recordings from dissociated cultures that had been in the incubator for 5 days. The basic protocol for current clamping is as follows. The extracellular recording media consisted of a solution of 150mM NaCl, 5mM KCl, 1mM $MgCl_2$, 2.5mM $CaCl_2$, 10mM HEPES, and 10mM glucose, all in deionized water. The intracellular recording media consisted of 140mM KCl, 1mM $CaCl_2$, 2mM $MgCl_2$, 11mM EgTA, and 10mM of HEPES, all in deionized water. The pH was titrated to 7.4 with sodium hydroxide for the extracellular solution and with potassium hydroxide for the intracellular solution. The extracellular solution was targeted for 340mOsm and the intracellular solution was targeted for 310mOsm. Cells were placed under an inverted microscope with a platform for seating a 35mm Petri dish. A ground electrode was placed in the extracellular media using an Agar bridge filled with $CaCl_2$ solution. The patch electrodes were pulled to 2-5μm diameter and had a resistance of 5-10MΩ when placed in the extracellular media. Recordings were made with a HEKA EPC 9 preamplifier. DRGs were identified by their phase bright appearance in the microscope (to distinguish them from the phase dark appearance of Schwann cells).

Some of the protocols that were tried and the recordings obtained from them are shown in Figure 5.1. Notice that an action potential in DRGs was obtained for the four protocols that were tried. The maximum observed response lasted for 2-5ms and had an amplitude of 80mV, consistent with previous published literature on action potentials generated in DRGs [5]. Ramp functions and square waves were more effective in generating trains of action potentials than a simple step response.

5.5. Electrophysiological Effects in Vincristine Neuropathy

Neurophysiological studies have shown little or no change in nerve conduction velocities following vincristine treatment. An increase in distal latencies and a progressive decrease in the amplitudes of compound nerve action potentials have been demonstrated during treatment. These changes are consistent with axonal degeneration, which might be complicated by secondary demyelination. The mechanism responsible for increased latencies is uncertain and could be attributed to a reduction in the number of terminal nerve fibers prior to death. Previously, the pathogenesis was attributed to distal nerve involvement; however, recently, mainly proximal involvement was shown. These neurophysiological features are consistent with the clinical picture and pathophysiology of vincristine-induced neuropathy [2].

Also, the effect of vincristine to prevent any alteration in the excitability of dorsal horn neurons following peripheral nerve injury was investigated in rats. With injury, vincristine-treated rats had significantly lower levels of excitability than those that did not have the drug treatment. Without the injury, both the drug-treated and untreated groups exhibited normal values of excitability [6]. In another animal study, vincristine sulfate was administered intravenously to rats at doses of 0.25, 0.5, and 0.75 mg/kg. During the first week following treatment, extensor digitorum longus (EDL) muscle contraction strength and fiber electrophysiologic parameters were measured. At all doses tested, vincristine strongly reduced twitch and titanic tension [7]. Moreover, weekly injections of vincristine produced a dose-dependent delay in regeneration following sciatic nerve crush in rats. With 50 and 100μg/kg/wk, electrophysiological evidence of reinnervation of the foot muscles was significantly delayed and muscle action potential amplitude

increased at a slower rate compared to controls [8]. In cats, vincristine sulfate (50μg/kg intravenously every four days) was administered and studied after 7-29 injections when neurological deficits became evident. The conduction velocity spectrum of individual afferent nerves from soleus muscles was shifted toward slower velocities. Here, the average conduction velocity of soleus motor axons was reduced 30% but no deficit was detected in motor nerve terminal function [9]. Daily intraperitoneal injections of vincristine in rats (0.1mg/kg/day) for 5 days produced mechanical allodynia and hyperalgesia. Moreover, electrophysiological recording from wide dynamic range (WDR) neurons in the lumbar (L4-L5) spinal dorsal horn in hyperalgesic rats demonstrated significantly increased spontaneous activity and after-discharges to noxious mechanical stimuli [10]. Another rat study showed that systemic administration of vincristine (100μg/kg) caused approximately half of the C-fiber nociceptors to become markedly hyperresponsive to mechanical stimulation. Instantaneous frequency plots showed that vincristine induced an irregular pattern of action-potential firing in hyperresponsive C-fibers, characterized by interspersed occurrences of high- and low-frequency firing. This pattern was associated with an increase in the percentage of interspike intervals 100-199ms in duration compared with that in C-fibers from control rats and vincristine-treated C-fibers that did not become hyperresponsive. Analysis revealed that vincristine altered the pattern of action-potential timing, so that combinations of higher firing frequency and higher variability occurred that were not observed in control fibers [11].

Clinically, in humans, evidence of denervation was detected in weak muscles, but there was little fall in motor conduction velocity. Fall in sensory action potential

amplitude was closely related to dose and duration of therapy and occurred before clinical abnormalities were apparent. Sensory action potential amplitude remained abnormal despite clinical improvement or recovery. The electrophysiological studies suggest that the neuropathy is of the dying back type [12]. In another study, somatosensory evoked potentials were measured prospectively in 38 children with acute lymphoblastic leukemia to evaluate the side effects of vincristine therapy on conduction velocities in peripheral nerves. Patients that had been administered the drug showed a prolongation in the conduction time of the posterior tibial nerve [13].

5.6. Pharmacological Studies

We used vincristine as the test vehicle in our devices. After culturing dissociated cultures of DRGs for 5 to 6 days in our devices, we applied vincristine to both the somal compartment and the axonal compartment at varying concentrations. Vincristine has deleterious effects on neurons at all concentrations; however, at certain concentrations, the effects are more severe than at others. A picture of vincristine neuropathy is shown in Figure 5.2. Axonal degeneration was observed at concentrations of 0.01µM. We

Figure 5.2. Axonal degeneration caused by exposure to vincristine for 1 day. The axons at the far left have begun to break down compared to more proximal portions of the axons at the far right. Vincristine neuropathy results in a gradual dying away of axons from the distal to proximal portions. The exact mechanism behind this degenerative process is not known; however, it is thought to be related to the way it alters the structure of axonal microtubules.

performed tests on the rates of axonal degeneration in vincristine neurotoxicity when the drug was applied to the axonal compartment and to the somal compartment. The length of the axon was measured either from the edge of the explant to the end of the axon or from the soma to the end of the axon, depending on the type of culture. Table 5.1 and Graph 5.1 summarize the data for this study. Notice that axonal degeneration was present at this concentration only when applied to the distal axon, indicating that the distal axon is primarily susceptible to chemotherapy-induced neurodegeneration.

Table 5.1. Axonal Degeneration Due to Vincristine-Induced Toxicity in a Two Compartment Culture (n=4)

	Day 0	Day 1	Day 2
Control	5.44±0.78mm	5.66±0.42mm	6.28±0.75mm
Vincristine to Axons	4.38±0.21mm	1.22±0.24mm	1.19±0.10mm

Values are mean ± SEM. $P<0.001$ when vincristine sample compared to control at day 2.

Graph 5.1. Axonal degeneration due to vincristine-induced toxicity in a two compartment culture

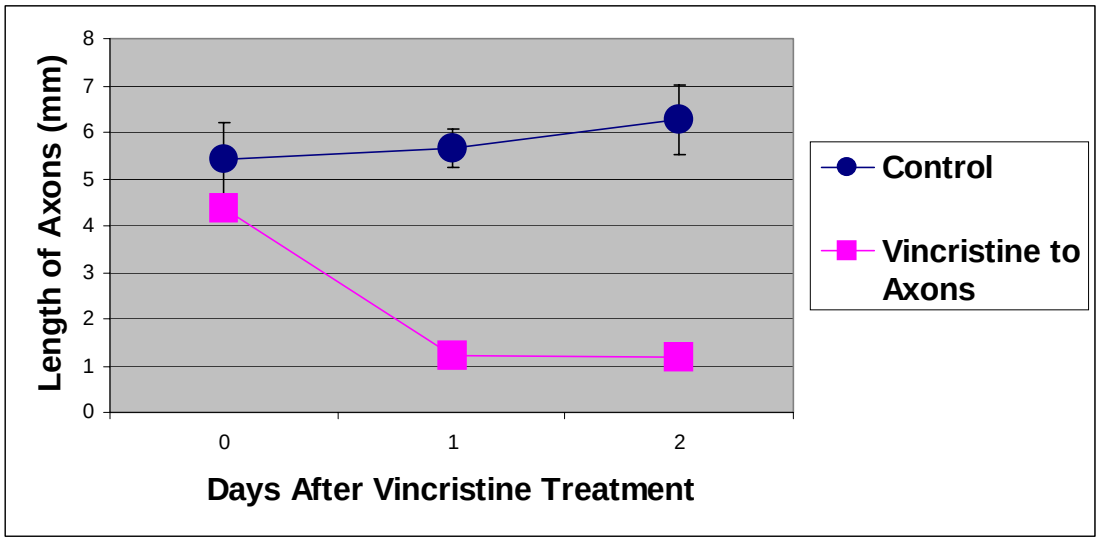

5.7. Electrophysiological Studies

5.7.1 Control Experiments with Tetrodotoxin

To gain more confidence in our electrode substrate, control experiments were performed with the sodium channel blocker tetrodotoxin. As described in Chapter 3, KCl (2.5M solution) was used to induce action potentials in the neurons. Tetrodotoxin was applied to the axonal compartment after KCl was applied to both of them. As expected, Table 5.2 shows that after application of the depolarizing chemical TTX, the neurites in the axonal compartment stopped generating action potentials.

Table 5.2. Summary of Data for Extracellular Action Potentials from DRGs In a Two Compartment Culture (n=4)

	KCL in Both Compartments		TTX Added to Axonal Compartment	
	Somal Compartment	Axonal Compartment	Somal Compartment	Axonal Compartment
Number Of Spikes	115±12	100±18	99±21	5±2

Values are mean ± SEM. $P<0.001$ when axonal compartments are compared. $P>0.05$ when somal compartments are compared.

5.7.2 Recordings with Vincristine

Electrophysiological recordings were then performed with the neurotoxin vincristine. After 10 days of culture, a 0.01μM solution of vincristine was applied to the

axonal compartment of the system. Then recordings were made on two systems every day for two days.

Table 5.3. Electrophysiological Evidence of Direct Axonal Effects in Vincristine-Induced Axonal Degeneration (n=4)

	No Vincristine (control)		Vincristine Added to Axonal Compartment	
	Somal Compartment	Axonal Compartment	Somal Compartment	Axonal Compartment
(Day 0) Number of Spikes	54±8	77±8	44±8	64±9
(Day 1) Number of Spikes	29±14	40±13	52±9	15±5
(Day 2) Number of Spikes	58±10	50±8	51±14	7±4

Values are mean ± SEM. $P<0.001$ when axonal compartments are compared at day 2. $P>0.05$ when somal compartments are compared at day 2.

Table 5.3 and Graphs 5.2 and 5.3 summarizes this data. Clearly, the data shows that over the course of a two day period, the number of action potentials generated by the axonal compartment decreases while the number of action potentials stays constant in the somal compartment. This finding adds more evidence that vincristine neuropathy is regulated by a mechanism local to the distal axon and that the soma is not involved in

Graph 5.2. Number of Action Potentials Recorded in the Somal Compartment during a One Minute Window.

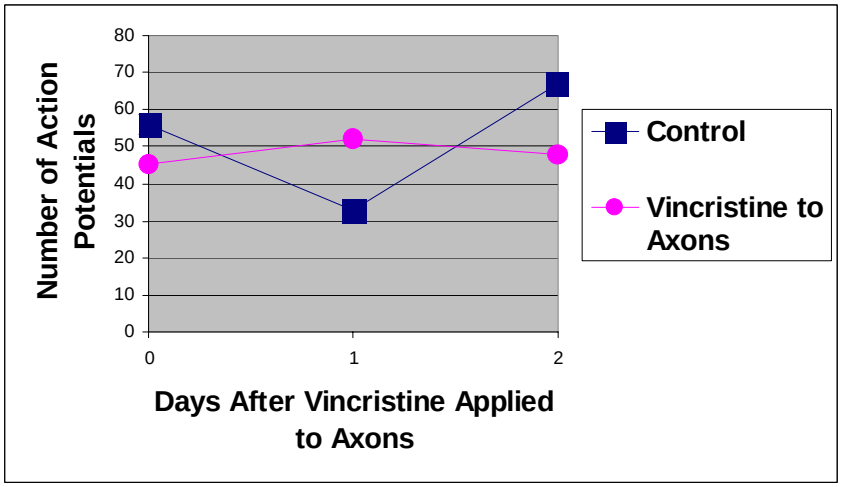

such a process.

Graph 5.3. Number of Action Potentials Recorded in the Axonal Compartment during a One Minute Window.

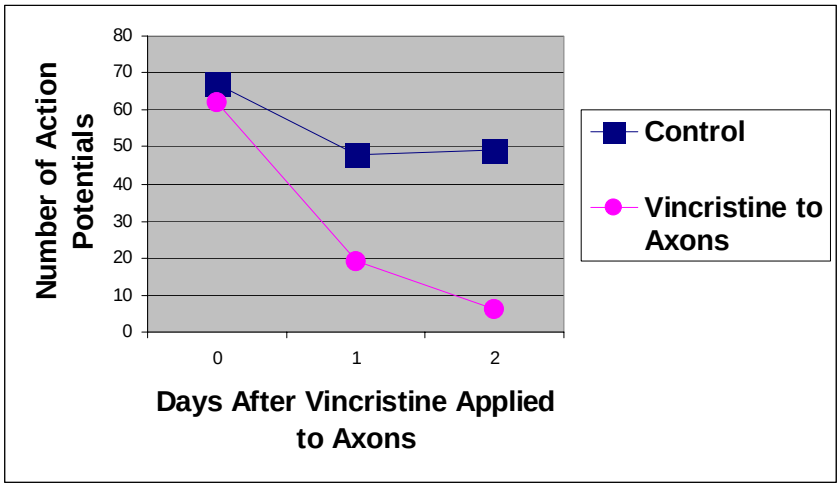

5.8. References

[1] M. S. Wang, Y. Wu, D. Culver, and J. D. Glass, "Pathogenesis of axonal degeneration: parallels between Wallerian degeneration and vincristine neuropathy," *Journal of Neuropathology and Experimental Neurology*, vol. 59, pp. 599-606, 2000.

[2] C. E. M. Gidding, S. J. Kellie, W. A. Kamps, and S. S. N. d. Graaf, "Vincristine revisited," *Critical Reviews in Oncology Hematology*, vol. 29, pp. 267-287, 1999.

[3] K. D. Tanner, J. D. Levine, and K. S. Topp, "Microtubule disorientation and axonal swelling in unmyelinated sensory axons during vincristine-induced painful neuropathy in rat," *Journal of Comparative Neurology*, vol. 395, pp. 481-492, 1998.

[4] J. Buitenweg, W. L. C. Rutten, E. Marani, S. K. L. Polman, and J. Ursum, "Extracellular detection of active membrane currents in the neuron-electrode interface," *Journal of Neuroscience Methods*, vol. 115, pp. 211-221, 2002.

[5] N. T. Blair and B. P. Bean, "Role of tetrodotoxin-resistant Na+ current slow inactivation in adaptation of action potential firing in small-diameter dorsal root ganglion neurons," *The Journal of Neuroscience*, vol. 23, pp. 10338-10350, 2003.

[6] M. L. Sotgiu, G. Biella, L. Firmi, and V. Pasqualucci, "Topical axonal transport blocker vincristine prevents nerve injury-induced spinal neuron sensitization in rats," *Journal of Neurotrauma*, vol. 15, pp. 1077-1082, 1998.

[7] F. D. Gregorio, G. Favaro, and M. G. Fiori, "Functional evaluation of acute vincristine toxicity in rat skeletal muscle," *Muscle Nerve*, vol. 12, pp. 1017-1023, 1989.

[8] S. Shiraishi, P. M. L. Quesne, and T. Gajree, "The effect of vincristine on nerve regeneration in the rat. An electrophysiological study," *Journal of Neurological Sciences*, vol. 71, pp. 9-17, 1985.

[9] B. D. Goldstein, H. E. Lowndes, and E. Cho, "Neurotoxicology of vincristine in the cat. Electrophysiological studies," *Archives of Toxicology*, vol. 48, pp. 253-264, 1981.

[10] H. R. Weng, J. V. Cordella, and P. M. Dougherty, "Changes in sensory processing in the spinal dorsal horn accompany vincristine-induced hyperalgesia and allodynia," *Pain*, vol. 103, pp. 131-138, 2003.

[11] K. D. Tanner, D. B. Reichling, R. W. Gear, S. M. Paul, and J. D. Levine, "Altered temporal pattern of evoked afferent activity in a rat model of vincristine-induced painful peripheral neuropathy," *Neuroscience*, vol. 118, pp. 809-817, 2003.

[12] E. B. Casey, A. M. Jellife, P. M. L. Quesne, and Y. L. Millett, "Vincristine neuropathy: clinical and electrophysiological observations," *Brain*, vol. 96, pp. 69-86, 1973.

[13] L. Vainionpaa, T. Kovala, U. Tolonen, and M. Lanning, "Vincristine therapy for children with acute lymphoblastic leukemia impairs conduction in the entire peripheral nerve," *Pediatric Neurology*, vol. 13, pp. 314-318, 1995.

CHAPTER 6

CONCLUSIONS AND FUTURE WORK

6.1. Conclusions

This work concentrated on the development of a microelectrofluidic compartmented culture system for interfacing with neurons. The neurons can be spatially divided into different drug compartments and their physiological response can be measured through microscopy and through substrate embedded electrodes. The system was designed, fabricated, and characterized using standard experimental techniques. The neurons used in this work were dorsal root ganglia, unipolar sensory neurons that are involved in transmitting sensory information from receptors in muscle and skin to the CNS. These neurons were shown to be cultured in the system and their growth rates were characterized. Moreover, the electrophysiological effects of vincristine, a chemotherapeutic drug and neurotoxin, was investigated in several experiments. The experiments showed that vincristine's neurotoxicological effects proceed by a mechanism local to the distal axon.

6.2. Modifications to the Compartment Divider

The work in this thesis concentrated on the development of a two compartment divider. Future work will concentrate on the development of compartment dividers with more compartments. For instance, by spatially dividing the neuron into more compartments, we can investigate how the promixal axons play a role in signaling between the distal axon and the neuronal soma. Moreover, we can take advantage of laminar flows in microchannels to provide a different means of compartmentalizing drugs

in channels. Use of flows in microchannels has the potential to circumvent some of the issues with leakage in channels that we have heretofore been experiencing; however, other issues with flow rates and the constant removal of autrocrine factors will present themselves. Also, interfacing the flow-based system with fluidic interconnect and a syringe pump will add complexity to the engineered system.

6.3. Modifications to the Multielectrode Substrate

The multielectrode substrate provides the ability to stimulate and record from neurons cultured on top of it. By varying the spacing between the electrodes to match the size of the compartment divider, new experiments can be designed that are tailored to answer specific neurobiological hypotheses. Also, we can investigate different, more robust insulating materials for the electrodes.

An interesting extension of this work might be the inclusion of substrate-embedded patch electrodes for stimulation and recording. If we are able to get neurons aligned to the patch electrodes, we can localize a recorded signal not only to a particular compartment but also to a particular point along the length of the neuron. To accomplish this task, the insulating layer must have topography micropatterned such that suction can be pulled on the neuron resting on top of the electrode. The materials and fabrication strategies for performing this task will be investigated.

6.4 Adding Complexity to the Biology

Arguably, the most exciting extension of this work lies in the complexity of the biological circuit that can be created with the engineered system. Neurons are cells that

communicate through a rich array of signaling mechanisms and the ability to image cells and sense their electrophysiological responses in multicompartment systems has the potential to answer some very interesting questions on physiological mechanisms in vivo. For instance, through synaptic interconnections, neurons can be co-cultured with other cell types, providing a more complete picture of the in vivo situation. Taken together, the platform developed has the potential to resolve questions in areas such as molecular trafficking, synaptic plasticity, and cellular apoptosis.

VITA

Surendra K. Ravula

Venkata Surendra Kumar Ravula was born in the town of Eluru, Andhra Pradesh, India. He moved with his parents to the US at the age of 5. He attended public schools in Greenville, South Carolina, and graduated from Duke University with a B.S.E.E. in Electrical Engineering in May of 2000. He then attended the Georgia Institute of Technology to pursue a doctorate in biomedical microelectromechanical systems.